

**DEVELOPMENT OF LIPOSOME NANOPARTICLES FOR  
DELIVERING RECOMBINANT HUMAN SECRETORY  
LEUKOCYTE PROTEASE INHIBITOR (rhSLPI) FOR  
ENHANCING OSTEOBLAST PROLIFERATION,  
ADHESION, AND DIFFERENTIATION**

**WANNAPAT CHOUYRATCHAKARN**

**MASTER OF ENGINEERING**

**IN BIOMEDICAL ENGINEERING**

**ลิขสิทธิ์มหาวิทยาลัยเชียงใหม่**  
Copyright © by Chiang Mai University  
All rights reserved

**GRADUATE SCHOOL  
CHIANG MAI UNIVERSITY**

**JUNE 2023**

**DEVELOPMENT OF LIPOSOME NANOPARTICLES FOR  
DELIVERING RECOMBINANT HUMAN SECRETORY  
LEUKOCYTE PROTEASE INHIBITOR (rhSLPI) FOR  
ENHANCING OSTEOBLAST PROLIFERATION,  
ADHESION, AND DIFFERENTIATION**

**WANNAPAT CHOUYRATCHAKARN**

**MASTER OF ENGINEERING**

**IN BIOMEDICAL ENGINEERING**

**ลิขสิทธิ์มหาวิทยาลัยเชียงใหม่**  
Copyright © by Chiang Mai University  
All rights reserved

**GRADUATE SCHOOL  
CHIANG MAI UNIVERSITY**

**JUNE 2023**

**DEVELOPMENT OF LIPOSOME NANOPARTICLES FOR  
DELIVERING RECOMBINANT HUMAN SECRETORY  
LEUKOCYTE PROTEASE INHIBITOR (rhSLPI) FOR  
ENHANCING OSTEOBLAST PROLIFERATION,  
ADHESION, AND DIFFERENTIATION**

**WANNAPAT CHOUYRATCHAKARN**

**A THESIS SUBMITTED TO CHIANG MAI UNIVERSITY IN PARTIAL  
FULFILLMENT OF THE REQUIREMENTS FOR THE DEGREE OF  
MASTER OF ENGINEERING  
IN BIOMEDICAL ENGINEERING**

**GRADUATE SCHOOL, CHIANG MAI UNIVERSITY**

**JUNE 2023**

**DEVELOPMENT OF LIPOSOME NANOPARTICLES FOR  
DELIVERING RECOMBINANT HUMAN SECRETORY  
LEUKOCYTE PROTEASE INHIBITOR (rhSLPI) FOR  
ENHANCING OSTEOBLAST PROLIFERATION,  
ADHESION, AND DIFFERENTIATION**

WANNAPAT CHOYRATCHAKARN

THIS THESIS HAS BEEN APPROVED TO BE A PARTIAL FULFILLMENT OF  
THE REQUIREMENTS FOR THE DEGREE OF  
MASTER OF ENGINEERING  
IN BIOMEDICAL ENGINEERING

**Examination Committee:**

*Ausanai Prapan*  
.....Chairperson

(Asst. Prof. Dr. Ausanai Prapan)

**Advisor:**

*S. Kum*  
.....

(Assoc. Prof. Dr. Sarawut Kumphune)

*S. Kum*  
.....Member

(Assoc. Prof. Dr. Sarawut Kumphune)

*CHAWAN MANASPON*  
.....Member

(Asst. Prof. Dr. Chawan Manaspon)

*Anirut Watcharawipha*  
.....Member

(Dr. Anirut Watcharawipha)

30 June 2023

Copyright © by Chiang Mai University

*This thesis is dedicated to my family for their love and supporting me and partnerships to my success.*



ลิขสิทธิ์มหาวิทยาลัยเชียงใหม่  
Copyright© by Chiang Mai University  
All rights reserved

## ACKNOWLEDGEMENT

First, I would like to express my sincere gratitude to my supervisor, Associate Professor Dr. Sarawut Kumphune for his invaluable guidance, support, compassion and expertise throughout the duration of my master's degree study. Moreover, I would like to appreciate Dr. Phornsawat Baipaywad, who has supported me with her experiences and brilliant ideas.

I would like to express my deepest gratitude to Assistant Professor Dr. Ausanai Prapan, Assistant Professor Dr. Chawan Manaspon, and Dr. Anirut Watcharawipha, the committee for this thesis examination.

I am grateful to the Biomedical Engineering Institution at Chiang Mai University for providing me with the resources and facilities necessary to conduct this research. In addition, I'd like to acknowledge the Faculty of Pharmacy, the Faculty of Science, Chiang Mai University, and Maejo University for their facilities.

This thesis, research, and innovation activity are supported by Chiang Mai University, and National Science, Research, and Innovation Fund (NSRF) and national research council of Thailand (NRCT). Furthermore, I would like to express our appreciation to Graduate School, Chiang Mai University whose financial support the TA&RA Scholarship for 2021 made this research possible.

Last but not least, I would like to express my heartfelt thanks to my families, friends especially SK LAB members, and loved ones for their never-ending support, understanding, and encouragement throughout this project. Their patience, motivation, and confidence in my abilities were indispensable in overcoming obstacles and attaining my goals.

Wannapat Chouyratchakarn

## หัวข้อปริญญานิพนธ์

การพัฒนาอนุภาคนาโนไลโปโซมเพื่อนำส่งโปรตีน  
ลูกผสมด้วยยั้งเอนไซม์ชนิดซีรีโทริลิวโคไซต์โปรตีเอส  
มนุษย์เพื่อเพิ่มการเพิ่มจำนวน การยึดเกาะและพัฒนาการ  
ของเซลล์สร้างกระดูกของมนุษย์

## ผู้เขียน

นายวรรณพรรณีย์ ช่วยราชการ

## ปริญญา

วิศวกรรมศาสตรมหาบัณฑิต (วิศวกรรมชีวการแพทย์)

## อาจารย์ที่ปรึกษา

รองศาสตราจารย์ ดร.สรารุช คำปวน

## บทคัดย่อ

ในปัจจุบันจำนวนผู้สูงอายุทั่วโลกนั้นได้เพิ่มสูงขึ้น และถือได้สังคมในตอนนี้เป็นสังคมผู้สูงอายุ โดยปัญหาสุขภาพที่มักเป็นปัญหาในสังคมผู้สูงอายุคือโรคเกี่ยวกับกล้ามเนื้อและกระดูก ซึ่งโรคกระดูกหักและกระดูกพรุนนั้นเป็นโรคที่พบบ่อยที่สุด สาเหตุเกิดจากการเสื่อมถอยของคุณภาพกระดูกในผู้สูงอายุนั้นเป็นข้อจำกัดในการรักษาและการฟื้นฟูกระดูกของผู้ป่วย มีรายงานการศึกษาเกี่ยวกับยาและสารชีวโมเลกุลหลายชนิดเพื่อใช้ในการเพิ่มความสามารและการพัฒนาของเซลล์กระดูกตัวอ่อน (Osteoblast) ไปเป็นกระดูก และได้มีรายงานว่าโปรตีนตัวยับยั้งเอนไซม์ชนิดซีรีโทริลิวโคไซต์โปรตีเอส (Secretory leukocyte protease inhibitor, SLPI) ซึ่งเป็นโปรตีนที่ยับยั้งซีรีนโปรตีเอส (Serine protease) มีความสามารถในการช่วยเพิ่มการยึดเกาะ การเพิ่มจำนวน และการสร้างความพัฒนาไปเป็นกระดูกของเซลล์กระดูกตัวอ่อน อย่างไรก็ตามการประยุกต์ใช้ SLPI ในทางคลินิกนั้นมีข้อจำกัด เนื่องจากครึ่งชีวิตสั้นในระบบหมุนเวียนเลือด และสามารถถูกทำลายได้โดยเอนไซม์โปรตีเอสในกระแสเลือด ดังนั้นการประยุกต์ใช้การห่อหุ้มของอนุภาคนาโนอาจเป็นประโยชน์สำหรับการนำส่ง SLPI การศึกษานี้มีวัตถุประสงค์เพื่อสร้างอนุภาคนาโนไลโปโซม (Liposome nanoparticles, LNPs) ที่ห่อหุ้มโปรตีนลูกผสมด้วยยั้งเอนไซม์ชนิดซีรีโทริลิวโคไซต์โปรตีเอสมนุษย์ (recombinant human SLPI, rhSLPI) (rhSLPI-LNPs) เพื่อเพิ่มครึ่งชีวิตและเพิ่มการพัฒนาของเซลล์กระดูกตัวอ่อน โดย LNPs ถูกสังเคราะห์ขึ้นด้วยวิธี Thin film

hydration และการห่อหุ้ม rhSLPI ดำเนินการโดยการเติม rhSLPI 0.33 ไมโครกรัม/มิลลิลิตร ใน น้ำบริสุทธิ์พิเศษ จากนั้นผสม rhSLPI กับฟิล์มของไขมัน จะทำให้ rhSLPI-LNPs จะก่อตัวเป็นถุง (Vesicles) โดยสังเคราะห์ของ LNPs ถูกตรวจสอบภายใต้กล้องจุลทรรศน์อิเล็กตรอนแบบส่องกราด (SEM) และกล้องจุลทรรศน์อิเล็กตรอนแบบส่องผ่าน (TEM) สังเคราะห์ของทั้ง blank-LNPs และ rhSLPI-LNPs มีรูปร่างเป็นทรงกลมและพื้นผิวขรุขระ และลักษณะของเปลือกของ rhSLPI-LNPs แสดงโครงสร้างคล้ายหัวหอม นอกจากนี้ขนาด, PDI และค่าศักย์ซีตาของอนุภาค (Zeta potential) ของ blank-LNPs หรือ rhSLPI-LNPs ถูกวัดโดยเครื่อง Zetasizer ผลการตรวจวิเคราะห์พบว่าขนาดของทั้ง blank-LNPs และ rhSLPI-LNPs มีค่าประมาณ 120 นาโนเมตร ค่า PDI เท่ากับ  $0.08 \pm 0.008$  และ  $0.075 \pm 0.006$  ตามลำดับ และค่าศักย์ซีตาเท่ากับ  $-64.47 \pm 1.12$  mV และ  $-51.98 \pm 0.90$  mV ตามลำดับ การห่อหุ้ม rhSLPI (Encapsulation efficiency) ได้รับการตรวจวัดโดยวิธี Enzyme-linked immunosorbent assay (ELISA) ผลการตรวจวัดพบว่า LNPs สามารถห่อหุ้ม rhSLPI ได้ สำหรับ %EE ของ rhSLPI-LNPs คือ  $18.313 \pm 0.24\%$  ในขั้นตอนต่อมาเปอร์เซ็นต์ของการปลดปล่อย (%releasing) ถูกตรวจวิเคราะห์โดย ELISA ผลปรากฏว่า rhSLPI ถูกปล่อยออกมาน้อยกว่า 1% นอกจากนี้ยังมีการตรวจสอบความสามารถในการยับยั้งโปรตีนเอสและผลการทดลองแสดงให้เห็นว่ายังคงมีความสามารถในการยับยั้งการทำงานของโปรตีนเอส นอกจากนี้ rhSLPI-LNPs สามารถเพิ่มการเพิ่มจำนวนเซลล์ที่ความเข้มข้น 1 และ 10 ไมโครกรัม/มิลลิลิตร สำหรับความเป็นพิษต่อเซลล์ พบว่า rhSLPI-LNPs ไม่ก่อให้เกิดความเป็นพิษใดๆ ต่อเซลล์สร้างกระดูกของมนุษย์ (hFOB 1.19) นอกจากนี้ การบ่มเซลล์ hFOB 1.19 ร่วมกับ rhSLPI-LNP นั้นสามารถเพิ่มการยึดเกาะของเซลล์สร้างกระดูก (Osteoblast cell adhesion) ได้ อย่างมีนัยสำคัญเมื่อเปรียบเทียบกับกลุ่มที่ไม่ได้รับการบ่มร่วมกัน ในขั้นตอนสุดท้าย qRT-PCR ใช้ในการตรวจสอบการพัฒนาของเซลล์สร้างกระดูก (Osteoblast cell differentiation) ผลลัพธ์แสดงให้เห็นว่า rhSLPI-LNPs นั้นสามารถเพิ่มการแสดงออกของ *Runx2*, *Colla1* และ *Ocn* โดยสรุปแล้ว นี่เป็นการศึกษาครั้งแรกที่แสดงให้เห็นว่าอนุภาคนาโนไลโปโซมที่ห่อหุ้ม rhSLPI (rhSLPI-LNPs) นั้นสามารถเข้ากันได้ทางชีวภาพกับเซลล์สร้างกระดูกของมนุษย์ และสามารถเพิ่มการยึดเกาะและการสร้างความแตกต่างของเซลล์สร้างกระดูกของมนุษย์



<b>Thesis Title</b>	Development of Liposome Nanoparticles for Delivering Recombinant Human Secretory Leukocyte Protease Inhibitor (rhSLPI) for Enhancing Osteoblast Proliferation, Adhesion, and Differentiation
<b>Author</b>	Mr. Wannapat Chouyratchakarn
<b>Degree</b>	Master of Engineering (Biomedical Engineering)
<b>Advisor</b>	Associate Professor Dr. Sarawut Kumphune

## **ABSTRACT**

The global number of elderly people has been increasing, and the world can now be considered an ageing society. One of the most concerning health problems in the elderly is a musculoskeletal disease, in which fractures and osteoporosis are the most common problems. The deteriorating bone quality in the elderly is a limitation for treatment and patient recovery. Several drugs and biomolecules have been studied for enhance osteoblast properties and differentiation. The secretory leukocyte protease inhibitor (SLPI), which is a serine protease inhibitory protein, has been reported to enhance osteoblast cell adhesion, proliferation, and differentiation. However, the application of SLPI in real clinical settings is limited due to its short half-life in circulation and the fact that it can be destroyed by circulating protease enzymes. Therefore, the application of nanoparticle encapsulation might beneficial for SLPI delivery. This study aims to fabricate liposome nanoparticles encapsulating recombinant human SLPI, or rhSLPI (rhSLPI-LNPs) for augmenting the half-life and enhancing human osteoblast differentiation. The liposome nanoparticles (LNPs) were fabricated by the thin film hydration method. Encapsulation of rhSLPI was performed by adding 0.33  $\mu\text{g}/\text{mL}$  rhSLPI in ultrapure water to the thin film lipid, and then rhSLPI-LNPs formed into vesicles. The morphology of LNPs was observed by scanning electron microscopy (SEM) and transmission electron microscopy (TEM). The morphology of both blank-LNPs and

rhSLPI-LNPs showed a spherical shape and a rough surface. The shell of rhSLPI-LNPs showed an onion-like structure. The size, PDI, and zeta potential of blank-LNPs or rhSLPI-LNPs were measured by the Zetasizer. The results showed that the size of both blank-LNPs and rhSLPI-LNPs was approximately 120 nm, the PDI was  $0.08 \pm 0.008$  and  $0.075 \pm 0.006$ , respectively and the zeta potentials were  $-64.47 \pm 1.12$  mV and  $-51.98 \pm 0.90$  mV, respectively. The rhSLPI encapsulation was confirmed by ELISA. The results showed that liposome nanoparticles could encapsulate rhSLPI. The %EE of rhSLPI-LNPs was  $18.313 \pm 0.24\%$ . The percentage of release was determined by ELISA. The result showed that rhSLPI was released at less than 1%. Additionally, proteinase inhibition activity was investigated, and the experimental results demonstrated that it still possesses the ability to inhibit protease activity. The rhSLPI-LNPs increased cell proliferation at concentrations of 1 and 10  $\mu\text{g}/\text{mL}$ . For cytotoxicity, rhSLPI-LNPs treatment did not cause any toxicity to the human osteoblast cell line (hFOB 1.19). In addition, pre-incubation of hFOB 1.19 with rhSLPI-LNPs could significantly enhance osteoblast adhesion when compared with the untreated group. Finally, osteoblast differentiation was observed by qRT-PCR. The results showed that rhSLPI-LNPs enhanced *Runx2*, *Colla1*, and *Ocn* mRNA expression. In conclusion, this is the first study showing that rhSLPI-encapsulated liposome nanoparticles (rhSLPI-LNPs) are biocompatible with human osteoblast cells and could enhance human osteoblast cell adhesion and differentiation.

ลิขสิทธิ์มหาวิทยาลัยเชียงใหม่  
Copyright© by Chiang Mai University  
All rights reserved

# CONTENTS

	Page
ACKNOWLEDGEMENT	d
ABSTRACT IN THAI	e
ABSTRACT IN ENGLISH	g
CONTENTS	i
LIST OF TABLES	l
LIST OF FIGURES	m
LIST OF ABBREVIATIONS	o
CHAPTER 1	1
Introduction	1
1.1. Background and problems	1
1.2. Objective	3
1.3. Hypothesis	3
1.4. Research scope	3
CHAPTER 2	4
Literature Review	4
2.1. Bone	4
2.2. The structure of bone	6

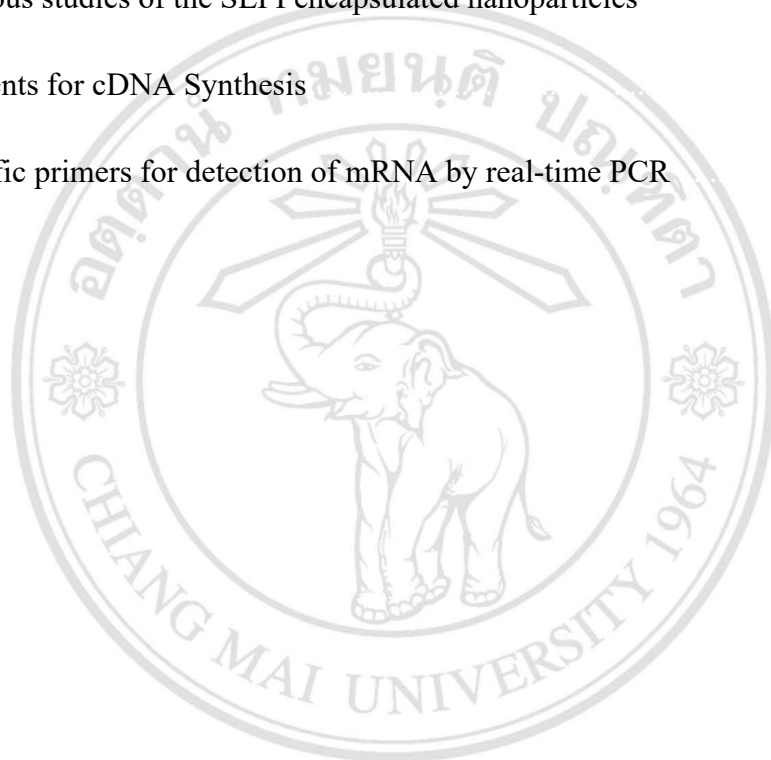
2.3.	Composition of bone	8
2.4.	Bone formation	12
2.6.	Bone remodelling	14
2.8.	Secretory leukocyte protease inhibitor (SLPI)	16
2.9.	The function of SLPI in normal physiology and Diseases	20
2.12.	Nanoparticles	25
2.13.	Classification of nanoparticles	25
2.14.	SLPI encapsulated nanoparticles	28
2.17.	Method for liposome nanoparticles fabrication	34
2.18.	Rationale of thesis	37
CHAPTER 3		39
Research Methodology		39
3.1.	Chemicals and Reagents	42
3.2.	Cell and cell culture	42
3.3.	Preparation of recombinant human secretory leukocyte protease inhibitor encapsulated liposome nanoparticles (rhSLPI-LNPs)	43
3.4.	Determination of physical characteristics of rhSLPI-LNPs	46
3.5.	Determination of rhSLPI by enzyme-linked immunosorbent assay	49
3.6.	Determination of encapsulated rhSLPI concentration	49
3.7.	Drug releasing assay	50
3.10.	Determination of cytotoxicity of LNPs	53
3.12.	Cell adhesion	53
3.13.	Determination of osteoblast cell differentiation	55
3.14.	Statistical analysis	59
CHAPTER 4		60
Results and Discussion		60

4.1.	Physical characteristics of liposome nanoparticles (LNPs)	60
4.2.	Determination of rhSLPI encapsulated concentration	66
4.3.	Drug releasing	69
4.4.	Anti-protease inhibition activity	72
4.5.	The cytotoxicity of LNPs	74
4.6.	Cell proliferation	76
4.8.	Osteoblast cell differentiation	82
	Limitations of study and suggestions	84
CHAPTER 5		87
Conclusion		87
REFERENCES		88
CURRICULUM VITAE		101

ลิขสิทธิ์มหาวิทยาลัยเชียงใหม่  
 Copyright© by Chiang Mai University  
 All rights reserved

## LIST OF TABLES

	Page
Table 1 Previous studies of the SLPI encapsulated nanoparticles	29
Table 2 Reagents for cDNA Synthesis	57
Table 3 Specific primers for detection of mRNA by real-time PCR	58



ลิขสิทธิ์มหาวิทยาลัยเชียงใหม่  
Copyright© by Chiang Mai University  
All rights reserved

## LIST OF FIGURES

	Page
Figure 1. Classification of bone by shape.	5
Figure 2. The general structure of bone.	7
Figure 3 The Osteogenesis Imperfecta.	11
Figure 4. The bone resorption by osteoclast cells.	13
Figure 5. The bone remodeling.	15
Figure 6. The structure of SLPI protein.	18
Figure 7. The amino acid sequence of SLPI.	19
Figure 8. The general structure of liposome nanoparticles.	31
Figure 9. The classification of liposome nanoparticles based on lamellarity.	33
Figure 10. The experimental design.	41
Figure 11. Schematic diagram demonstrating the fabrication of liposome nanoparticles.	45
Figure 12. The equipment of Zetasizer.	48
Figure 13. The conversion of MTT.	52
Figure 14. Morphology of nanoparticles by Scanning electron microscope (SEM).	61

Figure 15. Morphology of the nanoparticles shell was observed by transmission electron microscope (TEM).	62
Figure 16. Characterizations of nanoparticles.	63
Figure 17. The concentration of encapsulated rhSLPI.	67
Figure 18. Release profile of rhSLPI-LNPs.	71
Figure 19. The protease inhibition activity of rhSLPI-LNPs.	73
Figure 20. The cytotoxicity assay by the relative percentage of cell viability.	75
Figure 21. Osteoblast cell proliferation.	78
Figure 22. Cell adhesion assay.	81
Figure 23. The mRNA expression of cell differentiation.	86



## LIST OF ABBREVIATIONS

WHO	World Health Organization
CAD	Coronary artery disease
PAD	Peripheral artery disease
IHD	Ischaemic heart disease
MI	Myocardial infarction
I/R	Ischaemia/reperfusion
sI/R	Simulated ischaemia/reperfusion
ATP	Adenosine triphosphate
mPTP	Mitochondrial permeability transition pore
ER	Endoplasmic reticulum
SR	Sarcoplasmic reticulum
ROS	Reactive oxygen species
MPO	Myeloperoxidase
PMNs	Polymorphonuclear cells
WAP	Whey acidic protein
NE	Neutrophil elastase
TIMP	Tissue inhibitors of metalloproteinases
TLRs	Thymic stromal lymphopoietin
LPS	Lipopolysaccharides
TNF- $\alpha$	Tumour necrosis factor alpha
TSLP	Thymic stromal lymphopoietin
ECM	Extracellular matrix
NF- $\kappa$ B	Nuclear factor- $\kappa$ B
COPD	Chronic obstructive pulmonary disease
ECs	Endothelial cells
HAS	Human serum albumin
PBS	Phosphate-buffered saline

DOX	Doxorubicin
SLPI	Secretory Leukocyte Peptidase Inhibitor
rhSLPI	Recombinant Human Secretory Leukocyte Peptidase Inhibitor
LNPs	Liposome nanoparticles
rhSLPI-LNPs	Recombinant human Secretory Leukocyte Protease Inhibitor encapsulated liposome nanoparticles
SEM	Scanning electron microscope
TEM	Transmission electron microscope
FE-SEM	Field emission scanning electron microscopy
ELISA	Enzyme-linked immunosorbent assay
PDI	Polydispersity Index
DMEM	Dulbecco's Modified Eagle Medium
FBS	Foetal bovine serum
DI water	Deionized Water
EE%	Percentage of Encapsulation efficiency
HRP	Horseradish peroxidase
DMSO	Dimethyl sulfoxide

# CHAPTER 1

## Introduction

### 1.1. Background and problems

Currently, the world has entered an ageing society, the situation which is more than 10 percent of the population aged 60 years and older [1, 2]. Therefore, maintaining the health of the ageing population becomes the most important concern for the government to support. One of the leading causes of mortality and morbidity in older people is accidents. Falls cause 70 percent of accidental mortality in those 75 years of age and older, affecting sexes and all racial and ethnic groups [3]. The cause of the fall, particularly in elders, is a decline in vision and hearing and a loss of balance in the body. The most common problem encountered after falls is broken bones or fractures, which can lead to death or disability in elderly patients and also increase the cost of treatment [4]. It has been reported that the treatment cost of a fractured bone while hospitalised is approximately 10,075 USD, and one year of follow-up and health care is approximately 43,669 USD [5]. Another reason that fractures could easily occur in the elderly is the osteoporosis. Osteoporosis is a skeletal disease that occurs in the bones of the whole body and is a defect in maintaining bone mass and strength, increasing the risk of bone fracture [6]. The treatment of fractures can be treated by using a plaster cast to immobilise the bone or by surgically inserting metal rods or plates to keep the bone together while waiting for the bone healing process to be accomplished [7]. However, in the elderly, the bone healing process seems to be more difficult and slower than in healthy youth [6]. Therefore, any strategies to enhance the bone healing process are an interesting and challenging research question.

Bone healing is a recovery process that requires several material types, including bone cells, collagen, and matrix [2]. This process can be divided into four phases [8]: hematoma formation, fibrocartilaginous callus formation, bony callus formation, and bone remodelling. These processes take weeks or months to complete and may fail or take longer to heal [9]. Again, any strategies to enhance the bone healing process are an interesting and challenging research question. Intervention with new drugs or agents to treat bone cells and enhance bone cell activity seems to improve bone healing.

Secretory leukocyte protease inhibitor (SLPI) is an 11.7 kDa non-glycosylated protein. SLPI is mainly secreted from epithelial cells and immune cells as well [10]. The important function of SLPI is to inhibit serine proteases, including elastase and cathepsin G from the neutrophil, chymase, and tryptase [10]. Previous studies showed that SLPI can improve the differentiation and mineralization of osteoblast cells [11, 12] and enhance osteoblast cell adhesion on titanium surfaces [11]. Therefore, SLPI could have therapeutic potential for enhancing bone healing. One of the clinical limitations of using recombinant human SLPI as a therapeutic agent is its short half-life in circulation [10]. The pre-clinical study in animal models revealed that the half-life of recombinant human SLPI in circulation ranged from 10-60 min, while the half-life of recombinant human SLPI in humans ranged from 10-120 min [13]. Therefore, any strategies to improve the stability and extend the half-life of SLPI in the system could provide greater therapeutic benefit.

Several advantages of nanoparticles as peptide drug carriers have been listed, for example, reducing the enzymatic digestion and aggregation of peptide drugs and increasing transmembrane absorption. Nowadays, several types of nanoparticles have been studied [14]. In this study, liposome nanoparticles have been interesting. The liposome nanoparticle is a colloidal spherical structure form of the lipid molecule. The components of the liposome structure was mimicked the natural membrane of the human cell. In addition, the properties of the liposome are biocompatibility, biodegradability, and carrying a large drug payload [15]. Growing evidence of liposome nanoparticles suggests their benefits as drug delivery carriers. However, the efficiency of liposome

nanoparticles for rhSLPI delivery as a peptide drug, especially for osteoblast differentiation has never been investigated.

## **1.2. Objective**

1.2.1. To prepare rhSLPI encapsulated liposome nanoparticles (rhSLPI-LNPs) for rhSLPI delivery.

1.2.2. To determine an *in vitro* effect of rhSLPI encapsulated liposome nanoparticles on osteoblast adhesion, proliferation, and differentiation.

## **1.3. Hypothesis**

1.3.1. The liposome nanoparticles (LNPs) could encapsulate rhSLPI.

1.3.2. The rhSLPI-LNPs are able to induce osteoblast adhesion, proliferation, and differentiation.

## **1.4. Research scope**

The present study performs rhSLPI-nanoparticles by loading recombinant human secretory leukocyte protease inhibitor (rhSLPI) into liposome nanoparticles. Determine the cell adhesion, proliferation, and differentiation of human osteoblast cells line (hFOB 1.19).

ลิขสิทธิ์มหาวิทยาลัยเชียงใหม่  
Copyright© by Chiang Mai University  
All rights reserved

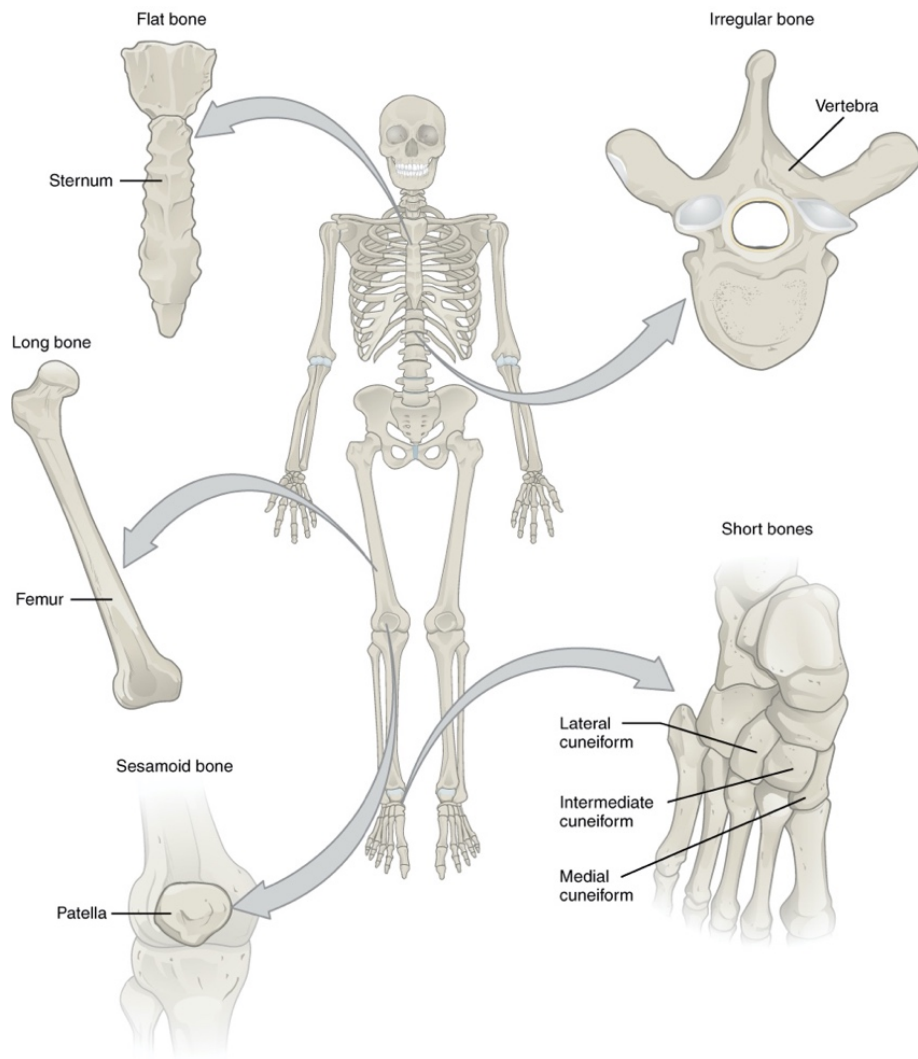
## CHAPTER 2

### Literature Review

#### 2.1. Bone

Bone is an active metabolic connective tissue [2], which is a framework for supporting and a place for the attachment of muscles to body movement, protection of vital internal organs and bone marrow, and accumulation of minerals or mineralization, especially calcium and phosphorus in the form of hydroxyapatite ( $[\text{Ca}_3(\text{PO}_4)_2]\text{Ca}(\text{OH})_2$ ) [16]. Bone can be classified in several ways, including shape, location, size, or density. For this study, bone was classified by shape: there are long bones, short bones, flat bones, Irregular bones, and sesamoid bones (Figure 1).

ลิขสิทธิ์มหาวิทยาลัยเชียงใหม่  
Copyright© by Chiang Mai University  
All rights reserved



ลิขสิทธิ์มหาวิทยาลัยเชียงใหม่  
 Figure 1. Classification of bone by shape [2].  
 Copyright© by Chiang Mai University  
 All rights reserved

## 2.2. The structure of bone

The general structure of bones can be divided into two types: cortical and cancellous bones [16]. Despite the fact that they have the same basic matrix composition, they differ in three keyways: density or porosity, three-dimensional structure, and metabolic activity. These three characteristics have a significant impact on their function and physiology [2]. Bones are made of a hard cortical component and a “spongy” cancellous or trabecular component. The main structural component that gives cortical bone strength is “the osteon”. Cancellous trabecular packets are arranged to maximise surface area for nutrient diffusion, exposure to circulating cytokines, and hormones, which are important in bone and mineral homeostasis. The periosteum is an important component covering the external surface of cortical bone, which provides attachments for ligaments, an additional vascular supply, and osteoprogenitor cells important in the initial stabilisation of the fracture callus [2, 16, 17] (Figure 2).



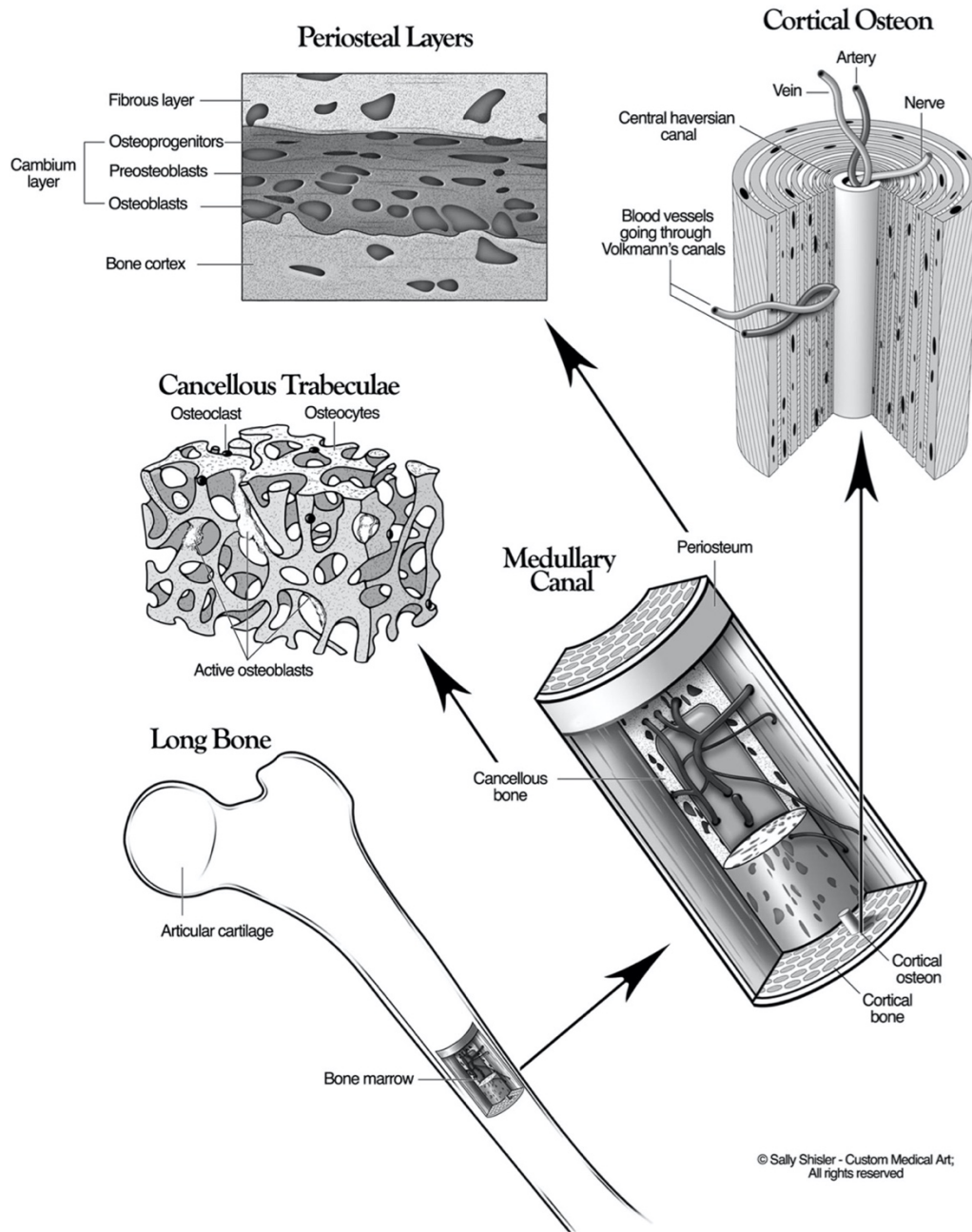


Figure 2. The general structure of bone [2].

## 2.3. Composition of bone

### 2.3.1. Matrix

The bone matrix is 90 percent of the component of the total bone volume. It is made up of four major components: an inorganic or mineral matrix (65 percent), an organic matrix (20 percent), and lipids and water (less than 15 percent). The inorganic bone matrix retains 99 percent of the calcium, 85 percent of the phosphorus, and 40 to 60 percent of the magnesium and salt in the body. The inorganic matrix, mostly hydroxyapatite, is responsible for the majority of bone strength, stiffness, and resistance to compressive stresses. Bone becomes soft, pliable, and spongy when the inorganic matrix is removed; an example is osteomalacia or rickets caused by a vitamin D deficiency. Collagen type I makes about 90 percent of the organic matrix released by osteoblasts, although it also contains proteoglycans, glycoproteins, and growth factors. Bone morphogenic proteins (BMP), additional transforming growth factor- $\beta$  (TGF- $\beta$ ) family factors, interleukin-1, interleukin-6, osteocalcin, osteonectin, and bone sialoprotein are among these growth factors. All of these elements have a role in bone formation, mineralization, and remodelling. The organic matrix gives bone its shape and offers tensile resistance. Osteogenesis imperfecta (Figure 3), which causes hard, brittle bones, is a well-known organic matrix abnormality [2, 17].

### 2.3.2. Cells

Bone cells represent 10% of total bone volume. They are made up of two types of stem cells: osteoprogenitor cells from the mesenchymal stem cell lineage that transform into osteoblasts and osteocytes, and osteoclasts from the hematopoietic stem cell [2, 17].

The osteoprogenitor is a stem cell of bone canals, endosteum, periosteum, and marrow that develops into bone-forming cells. Vascular pericytes may also supply them. Until they receive stimuli to migrate to a site, proliferate, and develop into osteoblasts, osteoprogenitor cells remain undifferentiated. [2, 17].

Osteoblasts line on surfaces of bones and are densely packed together. They consider the bone-forming cells, which produce and release organic bone matrix. The enzyme alkaline phosphatase (ALP), which is released by active osteoblasts, reveals their activity. They can become osteocytes, remain quiescent osteoblasts lining bone, or revert to the osteoprogenitor cell line once triggered. Bone morphogenic proteins (BMP) and other members of the transforming growth factor- $\beta$  (TGF- $\beta$ ) family are important mediators of osteoblast development and activation [2, 17].

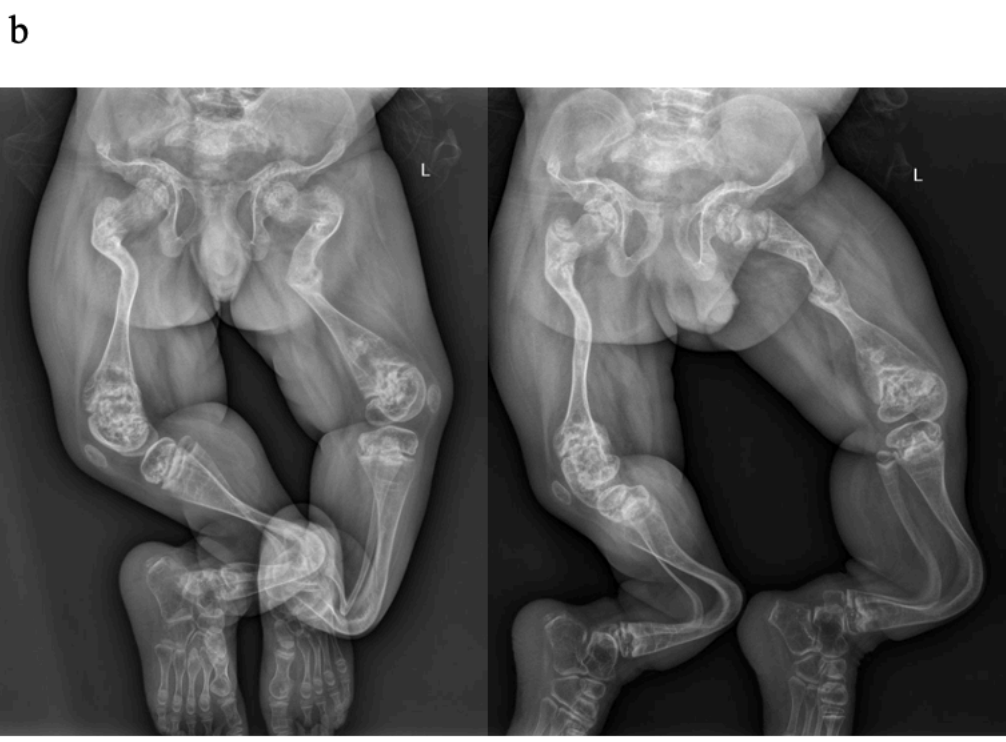
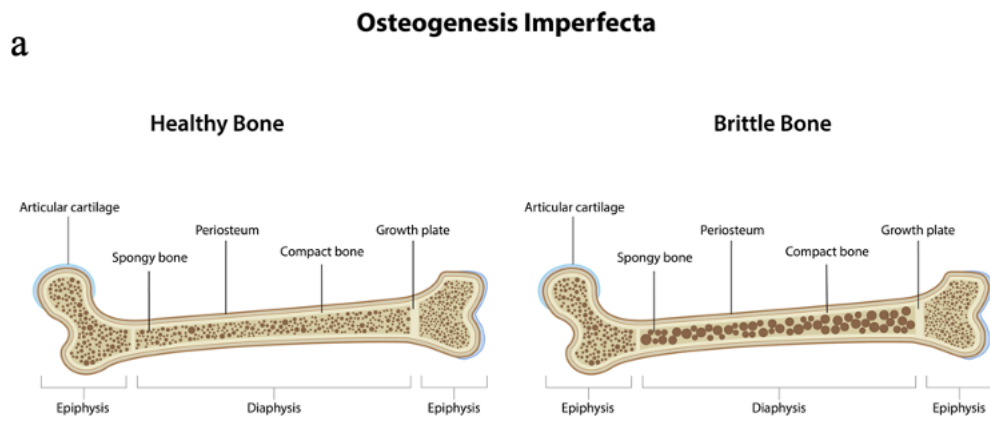
Osteocytes are 90 percent of bone cells. They are osteoblasts that dwell in vacuoles termed lacunae and are surrounded by an organic matrix. Once encased in a matrix, they generate cytoplasmic projections that go into the bone and contact adjacent osteocyte cell processes, allowing direct communication. Osteocytes regulate calcium homeostasis and preserve the bone matrix. The parathyroid hormone can also cause them to resorb bone directly [2, 17].

Osteoclasts are large multinucleated cells that reside in Howship's lacunae, which are shallow depressions on bone surfaces. They can also reside in deep resorption cavities called cutting cones throughout the remodelling and bone healing processes. Bone-resorbing cells are known as osteoclasts. They adhere to the bone matrix through a brush boundary and acidify it, facilitating matrix phagocytosis. Only mineralized bone can be resorbed by osteoclasts. The receptor activator of NF- $\kappa$ B ligand, osteoprotegerin, interleukin-1, interleukin-6, macrophage colony-stimulating factor, parathyroid hormone,

1,25-dihydroxy vitamin D, and calcitonin are only a few of the known agents and cytokines that regulate osteoclast development and activity [2, 17].



ลิขสิทธิ์มหาวิทยาลัยเชียงใหม่  
Copyright© by Chiang Mai University  
All rights reserved



Copyright © by Chiang Mai University  
All rights reserved

Figure 3 The Osteogenesis Imperfecta. a) Comparison of healthy bone and brittle bone [18]; b) X-ray films showed characteristics of bone abnormality caused by disease [19].

## **2.4. Bone formation**

Osteoprogenitor cells, also known as mesenchymal stem cells, develop into immature osteoblast cells and osteoblast cells to produce bones [2]. Osteoblast cells are important in the formation of bone matrix, the synthesis of bone matrix protein, the secretion of alkaline phosphatase (ALP) indicated to active osteoblasts, and the increasing of mineralization. whereas osteoclasts are responsible for bone resorption. Additionally, osteoblasts are physical and metabolic indicators [20]. Osteoblast differentiation enhances bone mass. Collagen type 1, runt-related transcription factor 2 (Runx2), osterix (OSX), osteopontin, and osteocalcin (OCN) are involved in the osteogenic genes and proteins that osteoblast cells express after cell differentiation. Runx2 is a transcription factor that regulates the differentiation of osteoblasts into bone production [21].

## **2.5. Bone resorption**

The bone matrix and the hydroxyapatite crystals contained within the sealing zone were acidified and proteolyzed by osteoclasts, resulting in bone resorption [22]. The mobilisation of hydroxyapatite crystals by digestion of their collagen connections is the initial step in bone matrix resorption [23]. The remaining collagen fibres are then degraded by cathepsins or active collagenases, with the residues being internalised or carried across the cell and discharged at the basolateral domain. Both locally acting cytokines and systemic hormones affect osteoclast activity. Calcitonin, androgens, thyroid hormone, insulin, PTH, IGF-1, interleukin (IL)-1, CSF-1, and PDGF37 osteoclastic receptors (RANK) have been discovered [16, 22, 23] (Figure 4).

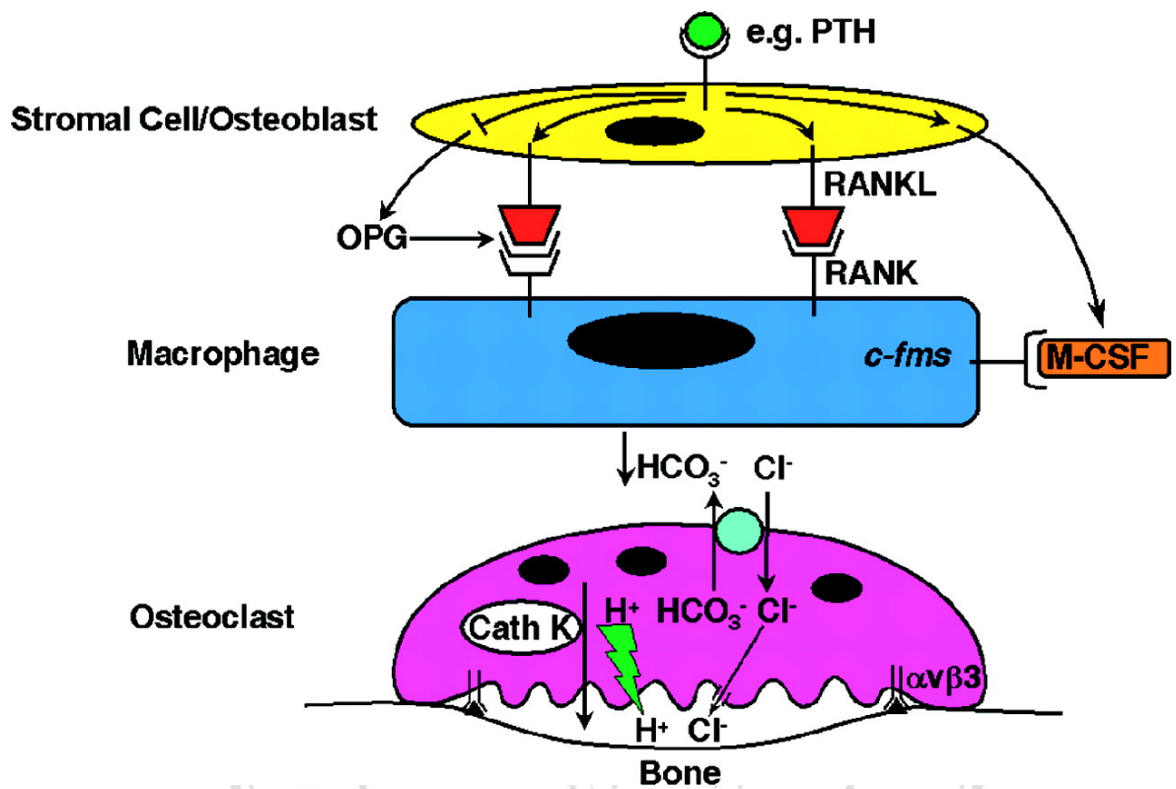


Figure 4. The bone resorption by osteoclast cells [22].

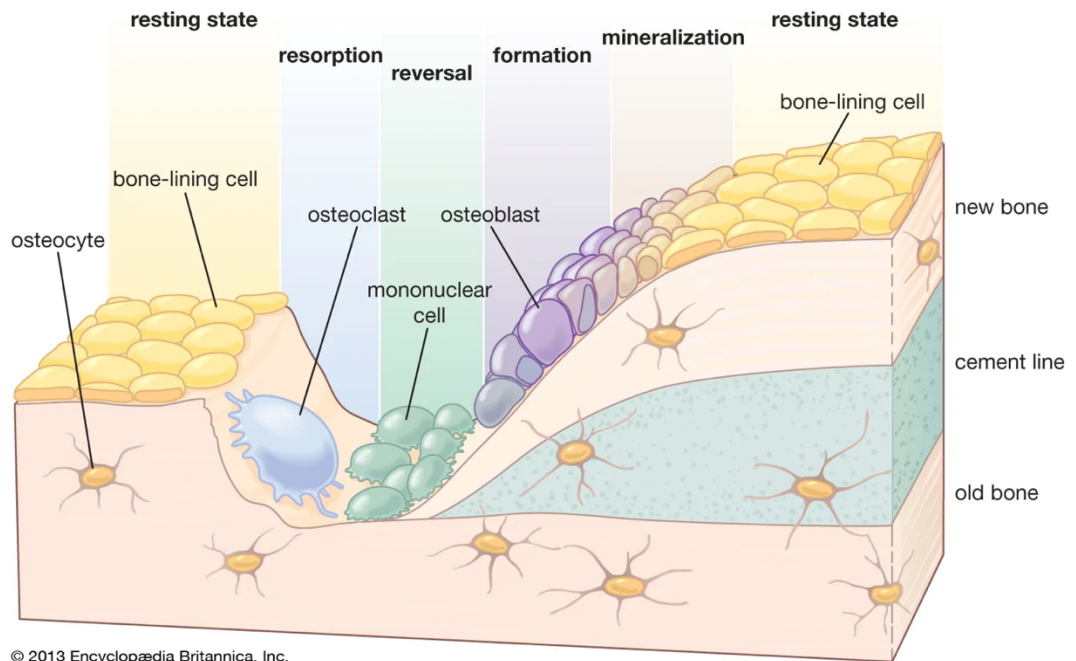
ลิขสิทธิ์มหาวิทยาลัยเชียงใหม่  
 Copyright© by Chiang Mai University  
 All rights reserved

## 2.6. Bone remodelling

Bone remodelling is the process by which osteoclasts and osteoblasts replace old bone with new bone [24] (Figure 5). Bone cells in normal adults maintain a balance between bone resorption and formation. There are many variables that influence bone remodelling, including cytokines, hormones such as calcitonin and calcitriol, growth hormone, glucocorticoids, parathyroid hormone, thyroid hormone, and the active form of vitamin D [23]. Quiescent, activation, resorption, reversal, creation, and mineralization are the six phases of bone remodelling. The first phase begins with the breakdown of existing bone by osteoclast cells, followed by the replacement of osteoblast cells with new bone. Finally, osteoblast cells accumulate calcium in the osteoid matrix, after which they transform into osteocytes and the bone enters the resting phase [2, 16].



### Bone remodeling



© 2013 Encyclopædia Britannica, Inc.

Figure 5. The bone remodeling [25].

ลิขสิทธิ์มหาวิทยาลัยเชียงใหม่  
Copyright© by Chiang Mai University  
All rights reserved

## **2.7. Imbalance of bone formation and bone resorption**

In adults, the mechanisms of bone cells, such as osteoblast cells and osteoclast cells, normally maintain a balance between bone creation and bone resorption. Nevertheless, bone mass is not stable in the human bone, resulting in decreased bone mass and decreased bone synthesis while increasing bone resorption [24]. The bone remodelling system is affected by an imbalance of osteoblast and osteoclast activity. Furthermore, the most powerful element affecting the imbalance of the bone mechanism is growing older [5]. As a result, the bone mass density (BMD) of elderly people may decrease, resulting in decreased bone strength and leading to bone fractures after a fall or other accident.

Osteoporosis is a skeletal disorder that occurs in elderly people [6], particularly those who are postmenopausal or senile. Furthermore, secondary osteoporosis results from a metabolic abnormality of the skeleton, which results in a lower peak of bone mass in patients. Chronic illness, medications, endocrine, idiopathic, diet, and cancer are all potential causes of secondary osteoporosis [24]. Osteoporosis is characterised by a loss in bone mass, a reduction in mechanical strength, and an increased risk of bone fracture [6]. Elderly people with less physical activity are more prevalent to bone fractures. As a result, osteoporosis is a serious disease that can cause mortality and morbidity in the elderly, as well as high medical costs for treatment and monitoring.

## **2.8. Secretory leukocyte protease inhibitor (SLPI)**

The secretory leukocyte protease inhibitor (SLPI) is an 11.7 kDa non-glycosylated protein that is a member of the whey-acidic protein (WAP) family, and the SLPI gene is on chromosome 20q12 13.2 [10, 26, 27]. SLPI is expressed in various types of cells, including epithelial cells and immune cells such as macrophages, neutrophils, and mast cells [28]. The SLPI protein has a boomerang-like structure and consists of two domains. 1: comparable structures; 2: four disulfide bridges connecting the polypeptide segments of each domain (Figure 6) [29]. Two domains of SLPI are WAP II (C-terminal), which

has the ability to inhibit protease enzyme, and the protease-inhibiting region localised between residues 67-74, and the antimicrobial ability is on the WAP I (N-terminal) domain (Figure 7) [10].



ลิขสิทธิ์มหาวิทยาลัยเชียงใหม่  
Copyright© by Chiang Mai University  
All rights reserved

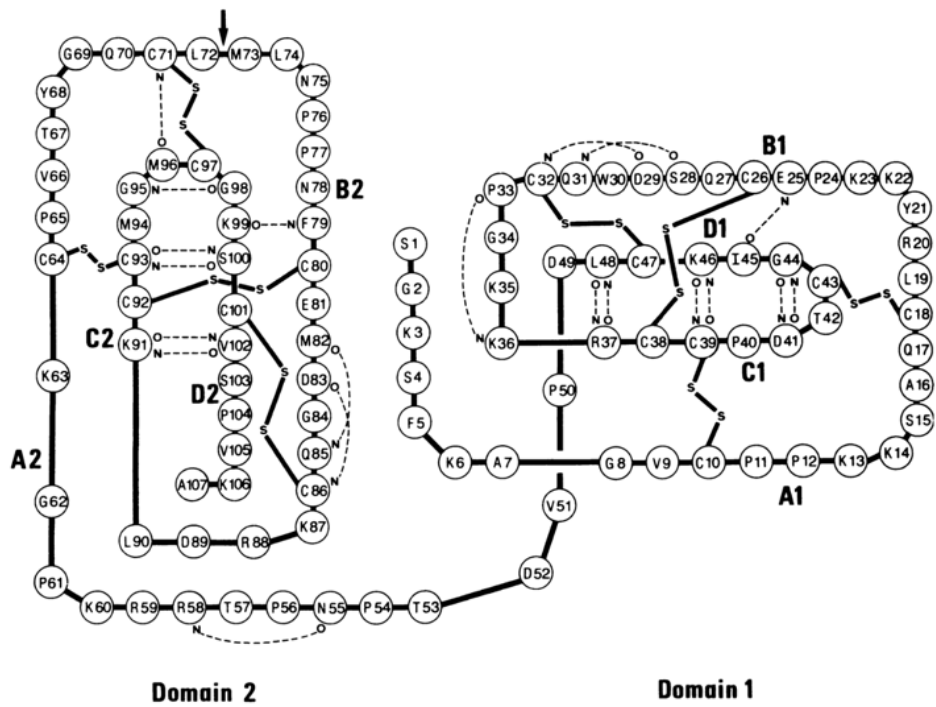


Figure 6. The structure of SLPI protein showed the polypeptide chain of human SLPI and its disulfide connection [29].

ลิขสิทธิ์มหาวิทยาลัยเชียงใหม่  
 Copyright© by Chiang Mai University  
 All rights reserved

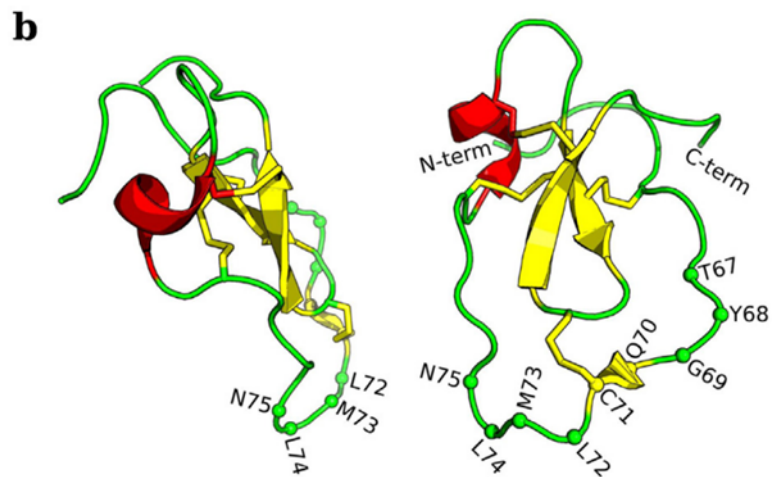
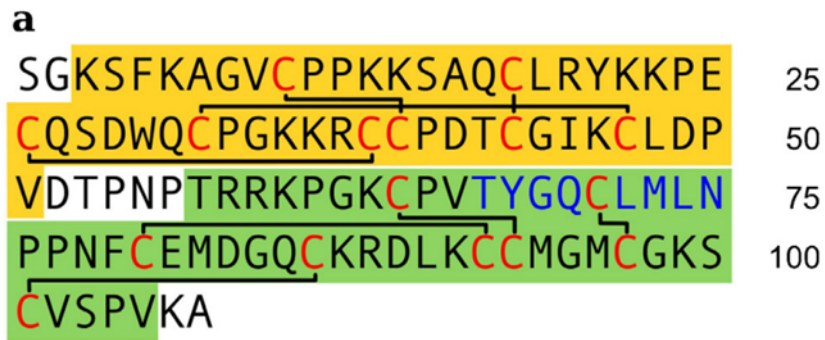


Figure 7. a) amino acid sequence of SLPI; b) 3D structure of SLPI that represent WAP I (N-terminal) and WAP (C-terminal) domains [10].

## 2.9. The function of SLPI in normal physiology and Diseases

### 2.9.1. Anti-inflammation

To counteract the effects of proteases secreted by innate immune cells, SLPI can decrease the creation of proinflammatory cytokines and the consequent recruitment of immune cells. Extracellular SLPI interferes with lipopolysaccharide (LPS) binding to soluble CD14 and the migration of LPS from CD14 into cell membranes; cytosolic SLPI suppresses degradation of the NF- $\kappa$ B inhibitor alpha (IB) to suppress TLR2 and TLR4 activation, and SLPI competes with p65 for NF- $\kappa$ B in the nucleus [27]. The ability of SLPI to inhibit NF- $\kappa$ B signalling is the independent anti-protease activity of the protein, as amino acid substitutions in the C-terminal domain disrupt the anti-protease function of SLPI and it did not affect LPS-induced nitric oxide and tumour necrosis factor-alpha (TNF- $\alpha$ ) production by macrophages [10]. SLPI alters the balance of cellular cytokine production by reducing the synthesis of proinflammatory cytokines by activated monocytes (TNF- $\alpha$ ; IL-8), dendritic cells (DCs; TNF- $\alpha$ ; IL12p70), macrophages (TNF- $\alpha$ ; nitric oxide), and epithelial cells by blocking NF- $\kappa$ B signalling (IL-8) [30].

An *in vivo* information suggests that SLPI regulates CD4<sup>+</sup> T cells indirectly via dendritic cells. SLPI expression in DCs reduces the production of microbiota-induced IL-12p70, monocyte chemoattractant protein 1 (MCP1), and IL-6 in lymph nodes draining the nasal mucosa, preserving T cell-mediated mucosal tolerance to innocuous proteins found at the highly colonised nasal mucosal surface [31]. Furthermore, by blocking NF- $\kappa$ B signalling, SLPI was generated by tonsillar epithelial cells decreases immunoglobulin class switching in activated B cells [32].

### 2.9.2. Antimicrobial activity

SLPI has antibacterial, antifungal, and antiviral activities against *Escherichia coli*, *Staphylococcus aureus*, *Pseudomonas aeruginosa*, *Staphylococcus epidermidis*, *Candida albicans*, and *Aspergillus fumigatus* are all susceptible to SLPI. SLPI is also the only salivary protein with action against the human immunodeficiency virus type 1 (HIV-1) at physiological concentrations [33].

The N-terminal domain has antibacterial and antifungal properties, whereas the C-terminus has less antibacterial activity [10]. As a result, SLPI's antibacterial action is most likely unrelated to its antiprotease activity. The processes by which SLPI kills bacteria, however, remain unknown. SLPI binds to bacterial mRNA and DNA in *Escherichia coli*, inhibiting translation and halting bacterial development. Furthermore, SLPI's cationic character may allow it to adhere to and disrupt bacteria's anionic cell membrane [34]. The result of amino acid changes that impair SLPI's protease inhibitor efficacy have no effect on its anti-HIV-1 action, SLPI can prevent HIV-1 transmission through a mechanism unrelated to its antiprotease activity. SLPI attaches to human macrophages through annexin II, a cofactor implicated in HIV-1 infection, and inhibits HIV-1-macrophage interactions. SLPI also prevents the host membrane proteins phospholipid scramblase 1 and 4 from interacting with CD4, the major HIV-1 receptor on T cells and macrophages [27].

### 2.9.3. Prevention of cell destruction

Serine proteases, particularly neutrophil elastase, are significantly inhibited by SLPI [10]. Proteases are secreted by leukocytes to help them move through the extracellular matrix of tissues and destroy phagocytosed bacteria. To reduce collateral tissue damage, endogenous protease inhibitors block the activity of these proteases. Some protease inhibitors ('systemic antiproteases')

are generated by the liver, whereas others ('alarm antiproteases') are created locally and activated by bacterial products and inflammatory cytokines [35]. Human alarm antiproteases SLPI and Elafin (also known as peptidase inhibitor 3 or skin-derived antileukoproteinase) have been widely studied [36]. The region responsible for the protease inhibitory activity of SLPI is located on its C-terminal domain. SLPI is the major inhibitor of neutrophil elastase in the cytoplasm of neutrophils and is the only elastase inhibitor that has been identified in saliva. SLPI retains its capacity to inhibit neutrophil elastase when cross-linked to fibronectin or elastin by tissue transglutaminase-2 and plasma factor XIIIa. In addition, SLPI inhibits the production of matrix metalloproteinases (MMPs) by monocytes [37] and can also prevent the formation of neutrophil extracellular traps (NET) [38].

## **2.10. Role of SLPI in different systems**

### **2.10.1. Skin**

SLPI is expressed and upregulated by human keratinocytes [34]. The main feature of SLPI in the skin is wound healing. There are reported that in the wounding skin of *slpi* knockout mice, wound healing is delayed due to increased elastase activity, neutrophil, and monocyte accumulation, and TGF- $\beta$  activation [27]. In addition, SLPI promotes wound healing by inhibiting neutrophil elastase from converting progranulin, which is an epithelial growth factor that prevents TNF- $\alpha$  from neutrophil activation to granulin peptides as well [27, 39]. The microbial activity in the skin was not unclear but SLPI has the ability to kill microorganisms including skin-associated bacteria such as *Staphylococcus aureus*, and *S. epidermidis* [10, 27].



### 2.10.2. Respiratory tract

SLPI protein in the lung is expressed by bronchial epithelial cells, alveolar neutrophils and macrophages [40]. In the upper respiratory tract, SLPI function in anti-elastase activity. However, in the peripheral airspaces,  $\alpha$ 1-antitrypsin (A1AT) is more prevalent and most SLPI protein is inactive. In comparison to the superficial epithelium, SLPI mRNA is expressed at 30-fold higher amounts in human airway submucosal glands. TGF- suppresses SLPI synthesis in airway epithelial cells, but neutrophil elastase and defensins promote it. In alveolar epithelial cells, IL-1 $\beta$  and TNF- $\alpha$  increase SLPI expression. SLPI is also found in lung connective tissue and is exclusively linked with elastin fibers, suggesting that SLPI shields these fibers against the elastase destruction [27].

### 2.10.3. Gastrointestinal tract

SLPI prevents intestinal tissues against protease destruction and excessive inflammation by reducing both intestinal epithelial cells and dendritic cells in mucosa-draining lymph nodes to microbial stimulation. Although SLPI has been shown to be against intestinal pathogens including *Salmonella typhimurium*. In addition, SLPI enhances oral mucosa tissue healing through processes similar to those found in the skin [41].

### 2.10.4. Cardiovascular system

The function of SLPI in the cardiovascular system involve in ischemia/reperfusion damage protection in cardiac transplantation has been documented. SLPI knockout hearts were transplanted immediately or incubated for 10 hours in a cold preservation solution, otherwise known as cold ischemia (CI). The findings revealed that SLPI deletion hearts exposed to CI had reduced myocardial contraction, which is linked to increased

cardiac protease enzyme production. At day 10, the inflammation, myocyte vacuolization, and cellular necrosis in SLPI<sup>-/-</sup> hearts were all considerably higher. When rhSLPI was introduced to the preservation solution, myocardial contraction in SLPI<sup>-/-</sup> hearts improved, protease enzyme expression dropped, and TGF-expression decreased as well [42]. In 2018, Nichawat Paiyabhroma reported that SLPI can protect cardiac fibroblasts in I/R injury conditions *in vitro*. Signal transduction is important in I/R damage and responses. Several protein kinases and cellular apoptotic regulatory proteins have been implicated in the etiology of I/R damage. The p38 MAPK, Bax, Bcl-2, and caspase cascades have all been identified as mediators of cellular death in the context of I/R damage. Overexpression of SLPI in cardiomyocytes or treatment of isolated hearts with SLPI could drastically reduce cell death, damage, and infarct size [43].

#### 2.10.5. Roles of SLPI in bone

The functions of SLPI in bone are enhanced cell viability, differentiation of mice preosteoblast cells, and mineralization by upregulated expression of alkaline phosphatase. In 2016 Baik-Dong Choi represented that SLPI can promote differentiation and mineralization of MC3Tc-E1 preosteoblast on titanium surfaces [12]. In addition, Soon-Jeong Jeong was studied about adhesion of osteoblast cells on titanium surfaces and the results showed that SLPI can enhance osteoblast adhesion and cell survival on titanium surfaces by stimulation of cytoskeleton modification and focal adhesion through focal adhesion kinase (FAK) pathway and ERK1/2 gene for promoting cell mitosis [11]. Therefore, previous studies showed that SLPI could have therapeutic potential for enhancing bone healing.

## **2.11. The clinical limitations of SLPI**

It has been shown that SLPI has a limited half-life in circulation as a therapeutic agent [13]. The half-life of recombinant human SLPI in circulation was studied by injection of 35 Sulphur-labelled secretory leukocyte protease inhibitor (SLPI) in four dogs, and the result showed that SLPI was cleared to urine in 10-60 min, whereas the half-life of human SLPI in humans was shown to be 10-120 min by intravenous injection of 125 Iodine-labelled SLPI in three human volunteers [13]. And one of the clinical limitations of SLPI was that it was digested by protease enzymes, including Cathepsins B, L, and S, which is cysteine proteases produced by macrophages, fibroblasts, and epithelial cells in the lung [44]. Therefore, any strategies to improve the stability, extend the half-life, and protect of SLPI against urine clearance or protease enzymes.

## **2.12. Nanoparticles**

Nanoparticles (NPs) are defined by the NNI (*National Nanotechnology Initiative*). The size of NPs ranges from 1 to 1000 nm in at least one dimension [45]. NPs are being investigated for potential medical applications. NPs can be used as carriers to deliver medication molecules to cells or tissues within the body. NPs can be engineered to have specific surface properties that enable them to selectively target cells, which are used to deliver drugs to kill cancer cells while avoiding healthy cells, thereby increasing drug efficacy and decreasing adverse effects [46].

## **2.13. Classification of nanoparticles**

classification of nanoparticles based on their composition

### **2.13.1. Polymeric-based nanoparticles**

Polymeric nanoparticles (NPs) can be synthesised from the monomers or polymers of natural or synthetic materials, allowing for a wide range of

conceivable structures and properties [47]. Polymeric NPs can be fabricated by various techniques, such as emulsification, nanoprecipitation, ionic gelation, and microfluidics [48-50]. The polymeric nanoparticles have variable drug-delivery capacities, the drug molecules can be encapsulated within the core of NPs, in the polymer matrix, chemically conjugated to the polymer, or bound to the surface of NPs [51]. This allows for the delivery of various types of molecules, including hydrophobic and hydrophilic compounds, as well as cargos with varying molecular weights, such as small molecules, biological macromolecules, proteins, and vaccines [51, 52].

#### 2.13.2. Inorganic nanoparticles

Inorganic nanoparticles were performed with inorganic materials such as dendrimers, and inorganic nanocarriers such as silica, magnetic, and gold nanocarriers can be used to encapsulate and deliver drugs to target sites [53]. Inorganic nanoparticles have been widely studied for their potential use in drug delivery systems due to their unique properties, such as their small size, biocompatibility, stability, and protection against drug degradation [54]. However, In addition, inorganic NPs, such as dendrimers, can stimulate the immune response and cause toxicity, which limits their use in certain applications [14].

ลิขสิทธิ์มหาวิทยาลัยเชียงใหม่  
Copyright© by Chiang Mai University  
All rights reserved

### 2.13.3. Peptide-based nanoparticles

Peptide-based nanoparticles were performed from fragments of naturally occurring proteins or peptides. Since the majority of proteins or peptides NPs are frequently used as targets for cell surface receptors or used as a shell to protect the drug molecule from degradation [14, 55]. The advantages of body protein or peptide NPs are low immunogenicity, biocompatibility, biodegradability, and mimicking of a body protein [56]. Peptides are a beneficial instrument for the development of drug delivery systems [57].

### 2.13.4. Lipid-based nanoparticles

Lipid-based nanoparticles (NPs) are most typically spherical structures comprising lipid bilayers surrounding internal aqueous compartments [58]. As a delivery system, lipid-based NPs have several advantages, including formulation simplicity, self-assembly, biocompatibility, the ability to deliver large cargoes, and a range of physicochemical properties that can be controlled to modulate their biological characteristics [57]. One of the subsets of lipid-based NPs that we are interested in is liposome nanoparticles.

## 2.14. SLPI encapsulated nanoparticles

Previous studies demonstrated the models and effects of SLPI-encapsulated nanoparticles (Table 1). In 2009, Gibbons A. et al. used SLPI-encapsulated liposome nanoparticles to protect against cathepsin L digestion [59]. In 2011, Gibbons A. *et al.* fabricated SLPI liposome nanoparticles in asthma models to reduce the rate of clearance into the blood circulation and increase lung residence time after post-inhalation [60]. In 2019, Hill M. et al. reported alginate/chitosan nanoparticles to deliver SLPI for pulmonary applications by using Tobramycin and SLPI to be antimicrobial and increasing the efficacy of drug delivery over prolonged periods [61]. In 2020, Tarhini M. et al. reported human serum albumin (HSA) nanoparticles encapsulating SLPI for antibacterial and anti-neutrophil elastase (Anti-NE) activity. It has been demonstrated that encapsulated SLPI still maintains its antibacterial and anti-NE properties [62].

Table 1 Previous studies of the SLPI encapsulated nanoparticles

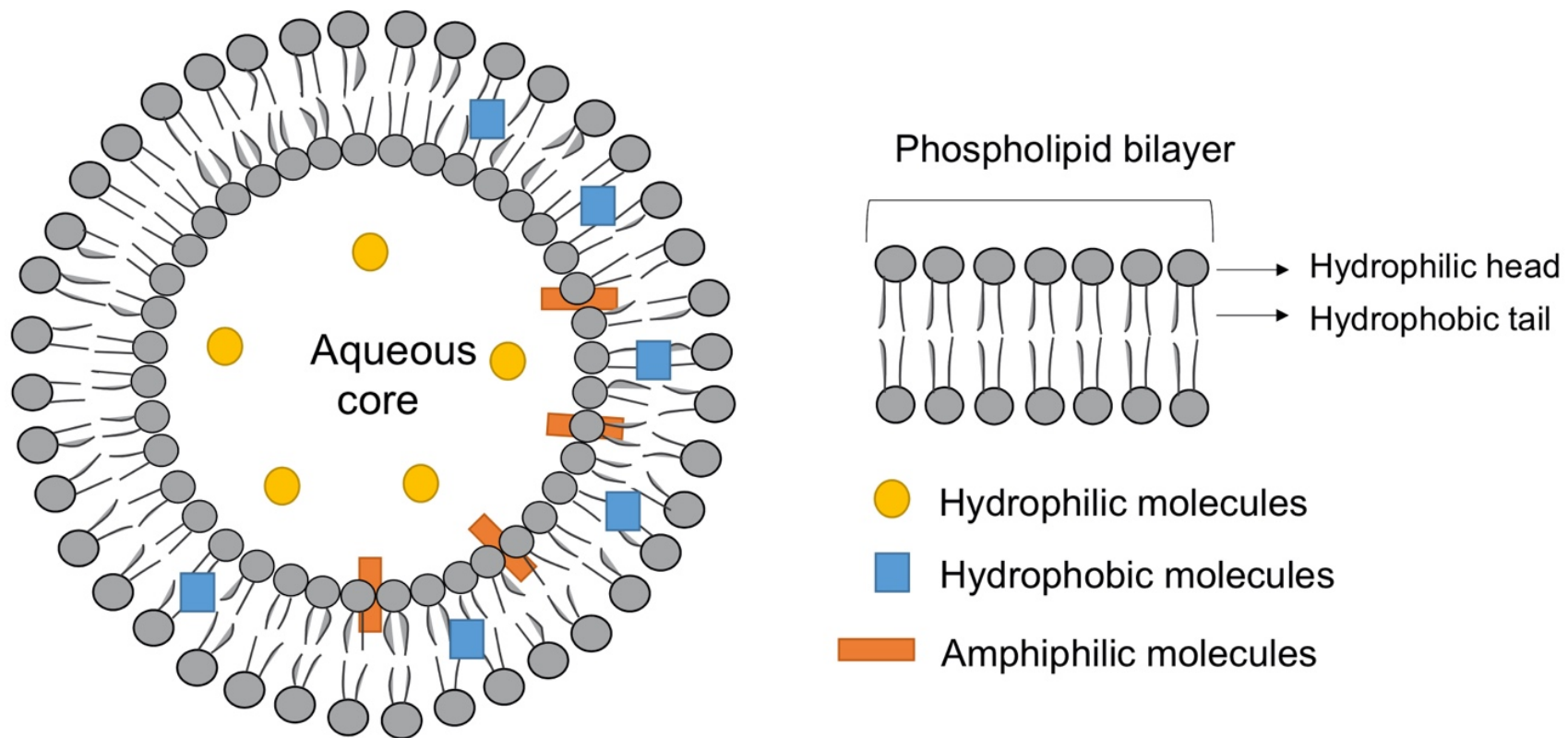
Nanoparticles	Conc. SLPI (mg/ml)	Size of NPs (nm)	Encapsulated efficiency (%)	Applications	References
Liposome	0.33	153.6	74.1±2.97	Asthma model	[60]
Liposome	0.001	153.6	74.1±2.97	Protection of SLPI from enzyme digestion	[59]
Alginate/Chitosan	25	437.5	-	Antibacterial and antiinflammation	[63]
HSA	1.5	127	-	Antibacterial activity	[55]

ลิขสิทธิ์มหาวิทยาลัยเชียงใหม่  
 Copyright© by Chiang Mai University  
 All rights reserved

## 2.15. Liposome nanoparticles

Liposomes are colloidal spherical structures synthesised by amphiphilic lipid molecules in solution, including phospholipids, self-assembling. One or more lipid bilayers (lamellae) arranged around an internal aqueous core, with the polar head groups oriented to the inner and outer aqueous phases, make up the liposomal membrane. Liposomes have the unique capacity to load and distribute compounds with varying solubilities due to their well-organised structure. Internal aqueous core with hydrophilic molecules, lipid bilayer with hydrophobic molecules, and water/lipid bilayer interface with amphiphilic molecules (Figure 8). The amphiphilic phospholipids mimic the natural cell membrane, which allows the nanoparticle to penetrate into the intracellular space and enhance cellular uptake [15]. The properties of liposome nanoparticles are biocompatibility, biodegradability, non-toxic molecules, and non-immunogenicity [64].





ลิขสิทธิ์มหาวิทยาลัยเชียงใหม่  
 Copyright © by Chiang Mai University  
 All rights reserved

Figure 8. The general structure of liposome nanoparticles [15].

## 2.16. Classification of liposome nanoparticles

Liposomes are classified by the number and size of lipid bilayers, or lamellae [15]. The liposomes can be classified as unilamellar vesicles (ULV), multilamellar vesicles (MLV), and multivesicle vesicles (MVV) (Figure 9). Unilamellar vesicle (ULV) is a liposomal nanoparticle that presents a single bilayer and is suitable for hydrophilic drug or peptide encapsulation. ULV can be divided into 2 types: small unilamellar vesicle (SUV), which is 20-100 nm, and large unilamellar vesicle (LUV), which is larger than 100 nm [65]. Multilamellar vesicles (MLV) are the liposomal nanoparticles; there are lamellae that are stacked in lamellar vesicles by an onion-like structure. In addition, MLV is suitable for lipophilic drug encapsulation, and the size of MLV is larger than 500 nm [15]. Multivesicular vesicles (MVV) consist of several small lamellar vesicles inside a single lipid bilayer. The size of MVV is larger than 1000 nm and is suitable for large volumes of hydrophilic drug loading [65].

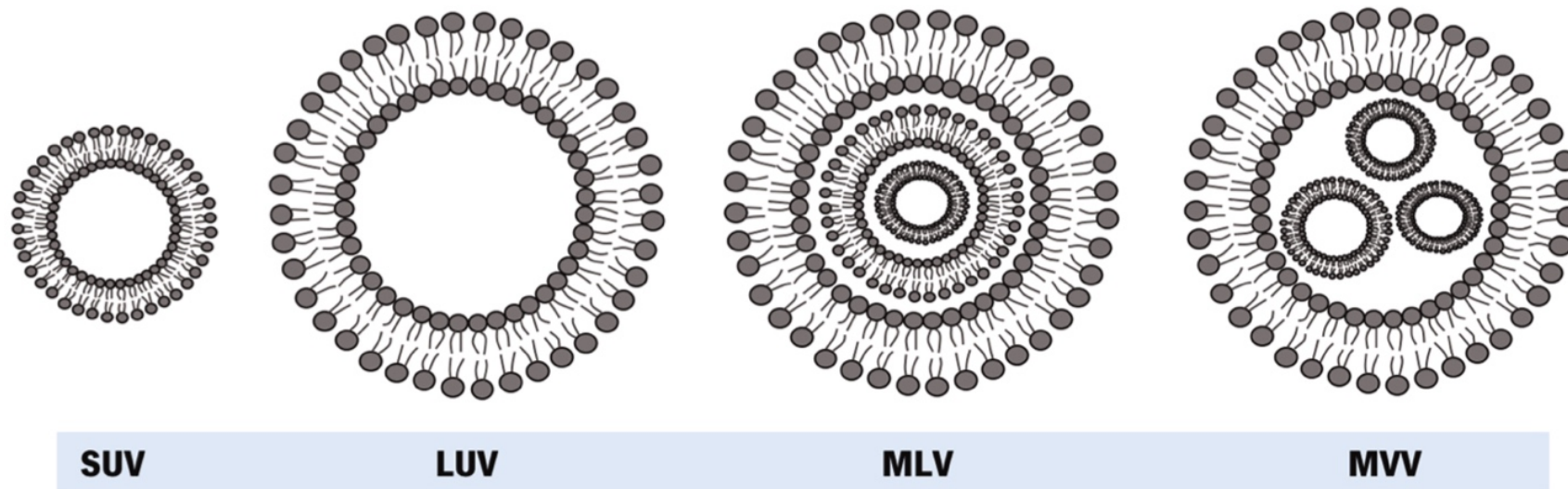


Figure 9. The classification of liposome nanoparticles based on lamellarity. SUV (Small unilamellar vesicles), LUV (Large unilamellar vesicles), MLV (Multilamellar vesicles), and MVV (Multi vesicular vesicles) [15].

ลิขสิทธิ์มหาวิทยาลัยเชียงใหม่  
Copyright© by Chiang Mai University  
All rights reserved

## 2.17. Method for liposome nanoparticles fabrication

There are numerous techniques for the fabrication of liposome nanoparticles. Size, lamellarity, and encapsulation efficiency (EE) are some of the ultimate properties of liposomes that can be influenced by various techniques. Methods to produce liposomal formulations can be classified as either conventional or advanced. In the following section, several of these techniques will be discussed.

### 2.17.1. Conventional methods

#### 2.17.1.1. Thin film hydration

The thin film hydration method was first reported by Bangham *et al.* in 1967 [66]. This is the first method that was initially used for liposome production. In this basic procedure, the mixture of lipids and cholesterol is dissolved in an organic solvent, typically chloroform, ether, or methanol, and then evaporated to produce a thin lipid film in a round-bottom flask. The obtained thin lipid film is hydrated using an aqueous solvent, resulting in the formation of liposomes. The advantages of this method are the production of larger and more heterogeneous liposomes, a high capacity for entrapment, biocompatibility, and simplicity. Despite its simplicity, the thin film hydration method can result in some batch-to-batch variability. Moreover, The thin film hydration method can occasionally result in liposome aggregation or fusion during the rehydration step [15, 67].

#### 2.17.1.2. Reverse phase evaporation

Reverse phase evaporation is an alternative technique for preparing liposomes. The initial procedure is similar to that of thin film hydration. Phospholipids are dissolved in an organic solvent to form a film, which is then evaporated to remove the solvent. Re-dissolving the film in an organic solvent, which is typically diethyl ether and/or isopropyl ether, and then adding

an aqueous phase results in the formation of an oil-in-water emulsion. Sonication is used to generate inverted micelles, resulting in a homogeneous emulsion. The final evaporation of the organic solvent under reduced pressure produces a viscous substance from which a liposomal suspension is produced [15, 67, 68]. The advantage of this method is its high encapsulation efficiency [69]. However, The compounds to be encapsulated are exposed to sonication conditions and even organic solvents, which are disadvantages [70]. Additionally, this method is reported as a time-consuming [15].

#### 2.17.1.3. Solvent injection technique

The liposomes can be fabricated using the solvent injection technique. This technique involves the rapid injection of lipids dissolved in an organic solvent, including ethanol or ether, into an aqueous medium, leading to the formation of liposomes [71]. The advantages of this method are reproducibility, rapid implementation, scalability, and the absence of lipid degradation or oxidative alterations [67]. However, there are some limitations to this method, including heterogeneity of liposomes, very low EE of hydrophilic compounds, and incomplete removal of ethanol from the liposomes, which is the most concerning point [15].

#### 2.17.1.4. Detergent removal

Detergent removal is an additional known method for fabricating liposomes. Liposomes are produced when detergent is used to dissolve lipids, resulting in the formation of defined mixed micelles. As the detergent is subsequently removed via column chromatography or dialysis bags, phospholipid molecules self-assemble into liposomes. Phospholipids form homogeneous unilamellar vesicles with an advantageously large encapsulated volume [15, 69]. The disadvantages of the detergent removal

method include the presence of detergent residues in the final liposomal formulation, the possibility of an interaction between the detergent and the encapsulated compound, and the fact that this technique is time-consuming [72].

#### 2.17.2. The advance methods

##### 2.17.2.1. Freeze drying method

Liu *et al.* developed the lyophilization monophasic solution method for preparing liposomes [73]. The lipid and substance are dissolved in tert-butyl alcohol at 45°C, while the lyo-protectant dissolves in water at 45°C. The two obtained solutions are combined to create a third identical monophasic solution, which is then filtered and freeze-dried to produce proliposomes. First, the sample is frozen at -40°C, and then it is desiccated at room temperature. Upon hydration, the sample produces liposomes with a mean dimension of 100–300 nm [58, 73]. The advantages of this method are increased stability, simplicity, and its used in commercial-scale production. However, the limitation is the time-consuming process [74].

##### 2.17.2.2. Supercritical anti-solvent (SAS) method

SAS is the optimal technique due to its simplicity, low solvent residue, and application to drugs with limited solubility in SCFs (antisolvents). Using an atomized nozzle, the drug solution is poured onto the supercritical fluid in the form of tiny droplets using this technique. Liposomes are obtained by hydrating an aqueous solution with water. Supercritical carbon dioxide functions as an antisolvent for the solute but is miscible with organic solvents. Compared to liposomes generated by conventional methods, the liposomes obtained are devoid of an organic solvent [74, 75].

### 2.17.2.3. Depressurization of an Expanded Liquid Organic Solution Suspension Method (DELOS)

In this method, phospholipids are dissolved in organic solvent at the required temperature and pressure, and then the solution is added to a cosolvent vessel containing supercritical CO<sub>2</sub>. In addition, a nozzle is used to depressurize this solution in order to generate liposomes. The advantage of this technique over the PGSS method is that thermosensitive materials can be used to produce liposomes, as this method does not require high temperatures and is carried out at low working pressures. The advantages of this method are simplicity and suitability for temperature-sensitive drug molecules. However, this method has the limitation that solution residues are frequently retained in the liposome nanoparticles [74, 76].

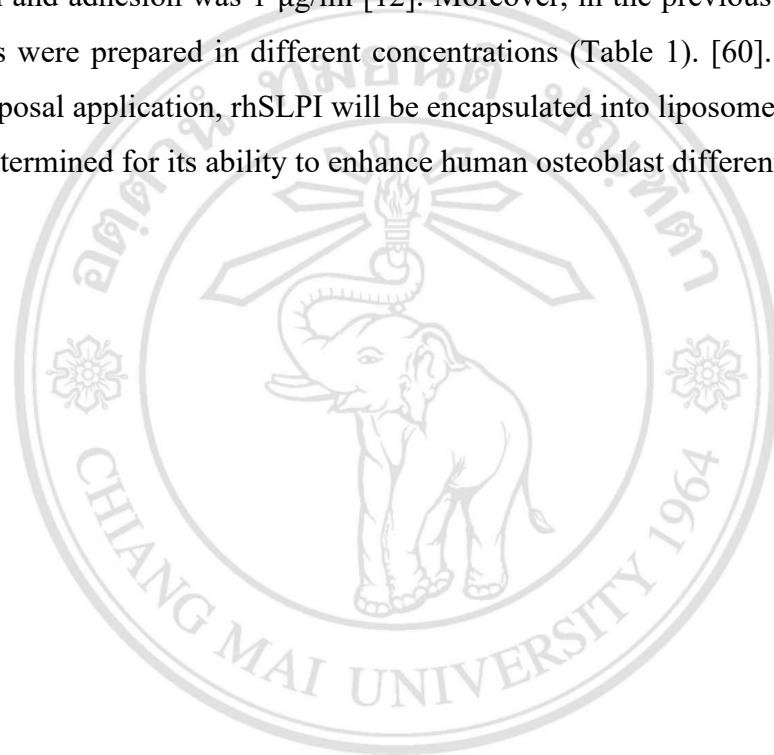
## 2.18. Rationale of thesis

The imbalance of bone formation and bone resorption in elderly people leads to decreased bone mass. Decreased bone mass in elderly people leads to fragility and fractures, which may result in disability or mortality. The treatment of a bone fracture can be treated by using a plaster cast to immobilise the bone or by surgically inserting metal rods or plates to keep the bone together while waiting for the bone healing process. However, an elderly patient has an imbalance of bone formation and resorption. As a result, an elderly patient takes longer or is more complicated to treat.

The secretory leukocyte inhibitor (SLPI) is a serine protease inhibitor. SLPI also enhances osteoblast cell differentiation and mineralization. However, the limitation in clinical usage of SLPI is due to its short half-life in blood circulation and can be digested by protease enzymes including cathepsin B, L, and S. Therefore, any strategies to improve the stability, extend the half-life, and protect SLPI against urine clearance or protease enzymes.

The nanoparticles were chosen to enhance SLPI stability. The nanoparticle is able to carry and release SLPI into osteoblast cells to improve cell differentiation and mineralization. In this thesis application, we aim to develop liposome nanoparticles to encapsulate rhSLPI and its effect on human osteoblast differentiation.

Previous studies showed that the optimum dose of SLPI that could enhance osteoblast differentiation and adhesion was 1  $\mu\text{g/ml}$  [12]. Moreover, in the previous studies, SLPI concentrations were prepared in different concentrations (Table 1). [60]. Therefore, in this thesis proposal application, rhSLPI will be encapsulated into liposome nanoparticles and will be determined for its ability to enhance human osteoblast differentiation.



ลิขสิทธิ์มหาวิทยาลัยเชียงใหม่  
Copyright© by Chiang Mai University  
All rights reserved



## CHAPTER 3

### Research Methodology

This chapter presents the methodology of this research, including materials and methods. The details of each topic are described below.

In this thesis, the conceptual framework of the study is presented in Figure 10. This study aims to fabricate liposome nanoparticles (LNPs) for delivering recombinant human secretory leukocyte protease inhibitor (rhSLPI) and determine an *in vitro* effect of rhSLPI-liposome nanoparticles (rhSLPI-LNPs) on human foetal osteoblast 1.19 (hFOB 1.19) cell line adhesion, proliferation, and differentiation. This study plan is divided into two different aims, including

#### **Aim 1. To prepare liposome nanoparticles to encapsulate rhSLPI (rhSLPI-LNPs)**

The rhSLPI-loaded liposome nanoparticles (rhSLPI-LNPs) were fabricated by the thin film hydration method (Figure 10a). Then, the physical characteristics of rhSLPI-LNPs were assessed, as shown in Figure 10b. The determination of morphology was performed by scanning electron microscopy (SEM) and transmission electron microscopy (TEM). The determination of particle size, zeta potential, and polydispersity index (PDI) was measured by a Zetasizer. The quantification of encapsulated rhSLPI protein in LNPs and released rhSLPI was measured by enzyme-linked immunosorbent assay (ELISA). The protease inhibitory activity was observed by the casein protease inhibition assay. The stability of rhSLPI was observed by Zetasizer.

#### **Aim 2. To determine an *in vitro* effect of rhSLPI-LNPs on osteoblast cell adhesion, proliferation, and differentiation**

The human foetal osteoblast 1.19 (hFOB 1.19) cell line was used as an *in vitro* model to determine the effect of rhSLPI-LNPs. The effect of rhSLPI-LNPs on osteoblast toxicity, proliferation, and adhesion was determined by the MTT cell viability assay. The effect of rhSLPI-LNPs on osteoblast cell differentiation was assessed through gene expression by quantitative reverse transcription polymerase chain reaction (q-RT-PCR), as shown in Figure 10c.



ลิขสิทธิ์มหาวิทยาลัยเชียงใหม่  
Copyright© by Chiang Mai University  
All rights reserved

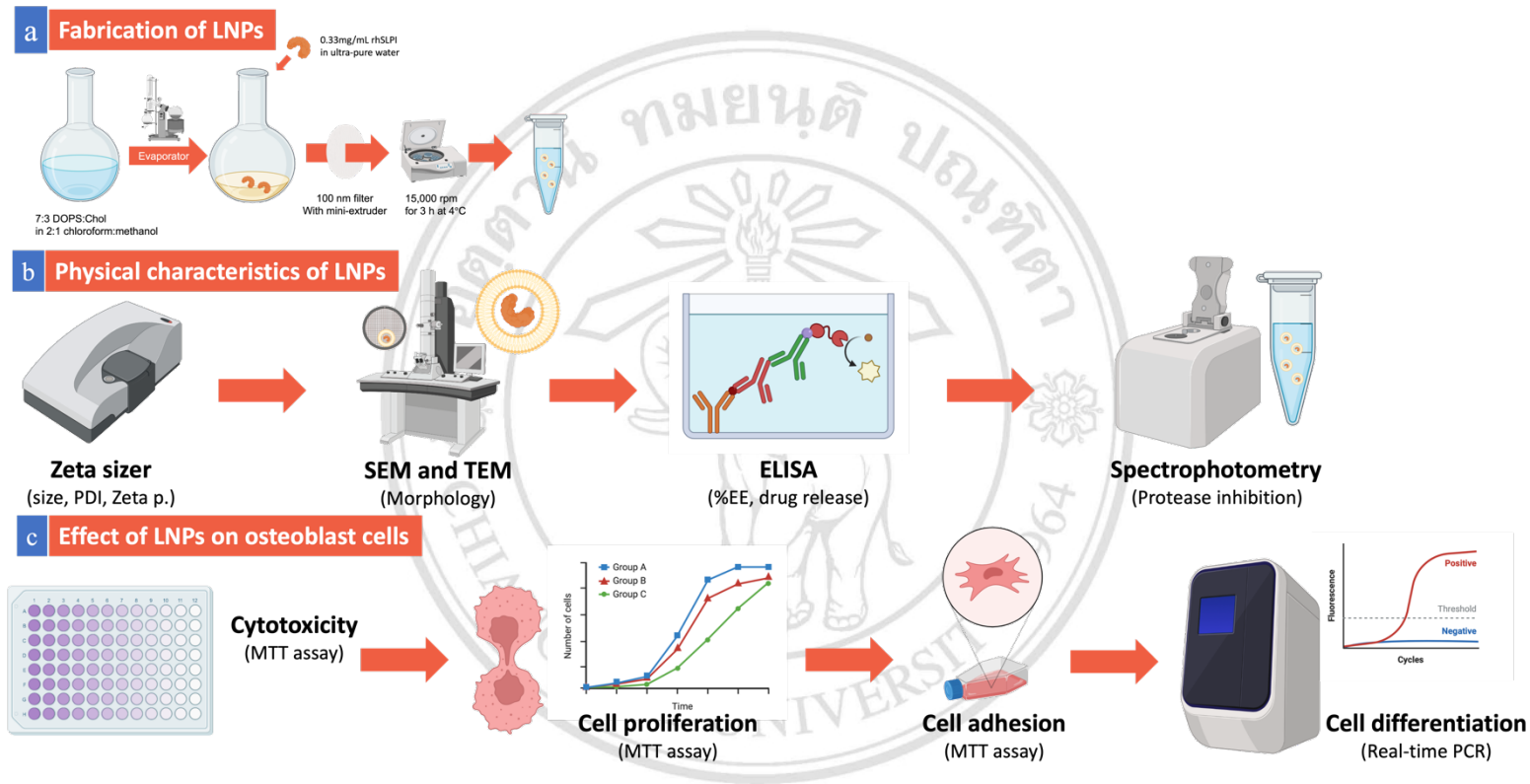


Figure 10. The experimental design will be divided into 3 parts: a and b) the experimental design for aim 1: liposome nanoparticle preparation and characterization, c) the experimental design for aim 2: *in vitro* effect of rhSLPI-LNPs on osteoblast cell differentiation.

### 3.1. Chemicals and Reagents

Recombinant human secretory leukocyte peptidase inhibitor (rhSLPI) was purchased from Sino Biology Inc. (Beijing, China), and Dulbecco's modified Eagle's medium (DMEM): Ham's F-12 media, foetal bovine serum (FBS), and trypsin-EDTA were purchased from Gibco BRL; Life Technologies Inc. (New York, USA). Dexamethasone, L-2-ascorbic acid, and  $\beta$ -glycerophosphate were purchased from Sigma-Aldrich (St. Louis, MO, USA). Fast 5-Bromo-4-color-3-indolyl and nitroblue (BCIP/NBT), alkaline phosphatase substrate (ALP), and phosphate buffer saline (PBS) tablets were purchased from Amresco (Ohio, USA). The 1,2-Dioleoyl-sn-Glycero-3-[Phospho-L-Serine] (DOPS) and Cholesterol (Chol) were purchased from Aventi Polar Lipid (Birmingham, AL, USA). Chloroform, methanol, and 3-(4,5-dimethylthiazol-2-yl)-2,5-diphenyltetrazolium bromide (MTT) were purchased from Sigma-Aldrich (St. Louis, MO, USA). (St. Louis, MO, USA).

### 3.2. Cell and cell culture

The human foetal osteoblast 1.19 (hFOB 1.19) cell line is an adherent osteoblast cell that was obtained by transfection of limb tissue with the temperature-sensitive expression vector pUCSVtsA58 and the neomycin resistance expression vector pSV2-neo [77]. The cells provide homogenous, rapid proliferation and can be a model for studying cell differentiation and osteoblast functions [77]. The hFOB 1.19 cell was purchased from American Type Cell Culture (ATCC CRL-11372<sup>TM</sup>). Cells were cultured with a 1:1 mixture of Ham's F12 Medium and Dulbecco's Modified Eagle's Medium, with 2.5 mM L-glutamine (without phenol red), supplemented with 10% (v/v) foetal bovine serum (FBS), 5,000 units/ml of penicillin, and 5000  $\mu$ g/ml of streptomycin (Gibco®). For culture conditions, the hFOB 1.19 cells were cultured at 37°C with 5% carbon dioxide (CO<sub>2</sub>) and 95% air.

The cells were subculturing or trypsinisation when they reached 70% confluency or over. For subculture, the cultured media was discarded and washed with sterile phosphate

buffer saline (PBS). Then, 0.25% (w/v) pre-warm trypsin-0.53 mM EDTA (Gibco®) was added and incubated until the cell detached from the culture surface and floated in the culture medium. After that, a complete medium was added to neutralise trypsin activity. The cell suspension was transferred to a sterilised centrifuge tube and centrifuged at 125 x g at 25°C for 5 min. Then the supernatant was discarded, and the cell pellet was resuspended with 1 ml of complete medium. Finally, the suspension cells were transferred to a new tissue culture flask [77].

### **3.3. Preparation of recombinant human secretory leukocyte protease inhibitor encapsulated liposome nanoparticles (rhSLPI-LNPs)**

The fabrication of rhSLPI-liposome nanoparticles (rhSLPI-LNPs) was performed according to the previous report by Aileen M. Gibbons *et al.* [59]. The rhSLPI-LNPs were prepared by the conventional thin film hydration method (Figure 11). To prepare 2 mL of rhSLPI-LNPs, the mixture of 7:3 DOPS and Chol, which is 2,800  $\mu\text{L}$  of 5.67 mg/mL DOPS and 1,200  $\mu\text{L}$  of 1.145 mg/mL Chol by volume, was dissolved in 2:1 by volume chloroform and methanol. Then the solvent was removed by a rotary evaporator into a thin film on the flask. Rehydration was performed by adding 1,340  $\mu\text{L}$  of ultrapure water and 660  $\mu\text{L}$  of 0.33  $\mu\text{g}/\text{ml}$  of rhSLPI [60]. While LNPs rehydration buffer was performed by 2,000  $\mu\text{L}$ . Next, DPOS: Chol thin film was rehydrated with rehydrating buffer.

Homogenization of fabricated LNPs and rhSLPI-LNPs to obtain smaller size liposomes was extruded through a mini-extruder with a 100 nm polycarbonate membrane filter for 11 times; during this step, the temperature must be kept at 60-80°C. Non-encapsulated rhSLPI was removed by centrifugation at 15,000 rpm for 3 h at 4°C. After that, the pellet was resuspended with 2 mL of ultrapure water. Finally, the concentration of LNPs was measured by weighing the power obtained after freeze-drying. The weight of the LNPs or rhSLPI-LNPs can be calculated by first weighing the cortical tube, then 200  $\mu\text{L}$  of LNPs or rhSLPI-LNPs were added to the cortical tube and freezing it at -80°C overnight.

Then the cortical tube was put in a freeze-drying machine until the sample was dry. Finally, the cortical tube was weighed and calculated in milligrammes per millilitre (mg/mL).



ลิขสิทธิ์มหาวิทยาลัยเชียงใหม่  
Copyright© by Chiang Mai University  
All rights reserved

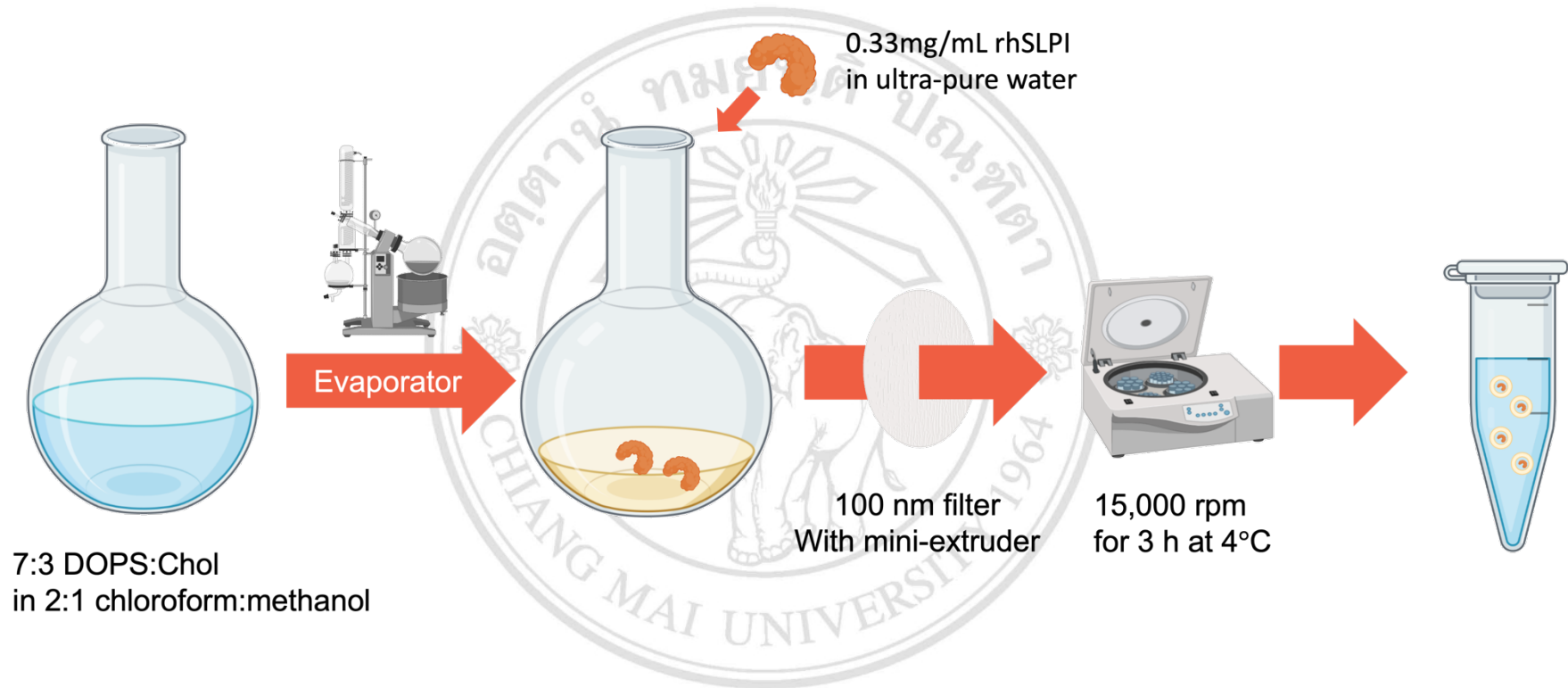


Figure 11. Schematic diagram demonstrating the fabrication of liposome nanoparticles by thin film hydration method [59].

ลิขสิทธิ์มหาวิทยาลัยเชียงใหม่  
Copyright © by Chiang Mai University  
All rights reserved

### **3.4. Determination of physical characteristics of rhSLPI-LNPs**

#### **3.4.1. Determination of morphology by field emission scanning electron microscopy (FE-SEM) and transmission electron microscopy (TEM)**

The morphology of nanoparticles was observed by FE-SEM. Firstly, the LNPs in ultrapure water were dropped on the copper tape and air-dried. The LNPs were put in a desiccator overnight to remove the solution residue. Then, the blank-LNPs were coated with gold for 30 sec under a vacuum. Finally, blank-LNPs were observed under an acceleration voltage of 15.0 kV by FE-SEM (JSM-6700F, JEOL, Japan) at the Faculty of Science, Chiang Mai University. The rhSLPI-LNPs were coated with platinum to a thickness of 3 nm. Finally, rhSLPI-LNPs were observed under an acceleration voltage of 15.0 kV by FE-SEM (CLARA, TESCAN) at Maejo University. It is noted that the morphological assessment of blank-LNPs and rhSLPI-LNPs was performed using different FE-SEM facilities due to the availability of the instrument.

A shell of LNPs was observed by TEM (JEM-2100 Plus, JEOL, Japan). LNPs were dropped on the copper grid and air-dried. Then, the copper grid was put in a desiccator overnight. After that, LNPs were stained with 3% (w/v) uranyl acetate for 15 sec. After incubation, the stain was removed with filter paper and incubated until dry in the dark. Finally, LNPs were observed under an acceleration voltage of 100 kV.

#### **3.4.2. Determination of nanoparticle size and polydispersity Index (PDI)**

The particle size and polydispersity index (PDI) of LNPs were determined by Zetasizer (Malvern, England) (Figure 12a). The LNPs were poured into a disposable cuvette (ZEN004) (Figure 12b) and measured for size and PDI using a Zetasizer (Malvern, England) at the Faculty of Pharmacy, Chiang Mai University.

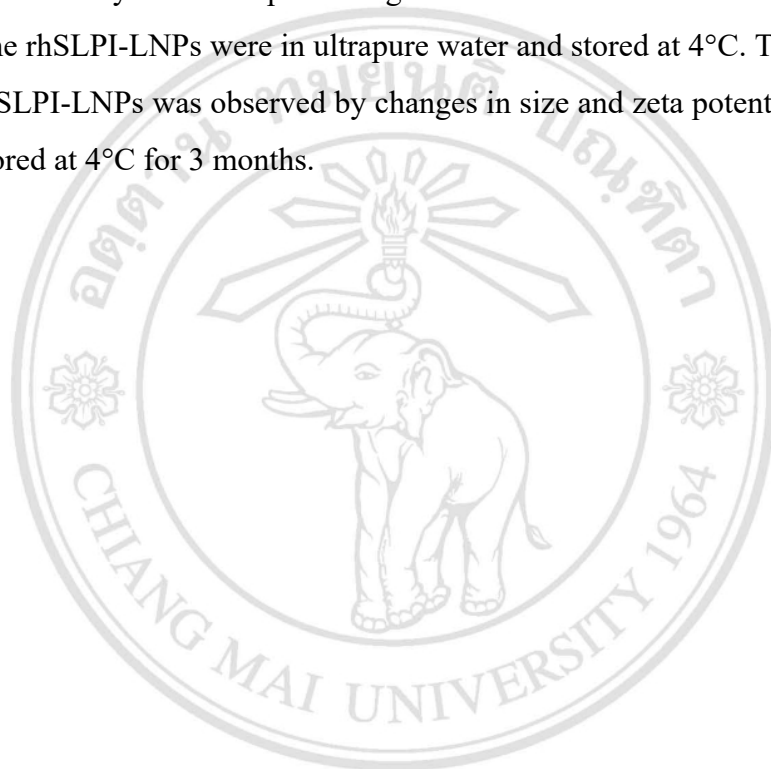


### 3.4.3. Determination of zeta potential of nanoparticles

The zeta potential of LNPs was measured using a Zetasizer (Malvern, England) at the Faculty of Pharmacy, Chiang Mai University. The LNPs were poured into the folded capillary cuvette (DTS1070) (Figure 12c).

### 3.4.4. The stability of LNPs upon storage

The rhSLPI-LNPs were in ultrapure water and stored at 4°C. The stability of rhSLPI-LNPs was observed by changes in size and zeta potential after being stored at 4°C for 3 months.



ลิขสิทธิ์มหาวิทยาลัยเชียงใหม่  
Copyright© by Chiang Mai University  
All rights reserved



Figure 12. The equipment of Zetasizer. a) a Zetasizer analyser (Malvern), b) a disposable cuvette (ZEN004) for size and PDI measurement, and c) a folded capillary cuvette (DTS1070) for zeta potential measurement.

Copyright© by Chiang Mai University  
All rights reserved

### 3.5. Determination of rhSLPI by enzyme-linked immunosorbent assay (ELISA)

The quantitative analysis of rhSLPI peptide concentration was performed by using an enzyme-linked immunosorbent assay (ELISA) commercial kit (Sandwich ELISA) (The SimpleStep ELISA<sup>®</sup>, Abcam, England), which was pre-coated with a specific monoclonal for SLPI. Initially, 50 µl/well of samples were added to the well. Then, 50 µl of cocktail antibody (capture and detector antibodies diluted in Antibody Diluent 4BI) was added to the microplate. After incubation for 1 h at room temperature, the solution was discarded, and the microplate was washed with 350 µl of 1X Wash Buffer three times. Then, 100 µl of TMB Development Solution was added to each well and incubated at room temperature for 10 min. After incubation, 100 µl of Stop Solution was added to each well. The absorbance was determined by the spectrophotometric method at O.D. 450 nm. The concentration was calculated from the standard curve.

### 3.6. Determination of encapsulated rhSLPI concentration

The 100 µL of LNPs were broken with 100 µL of 70% ethanol and vortexed for 15 sec. Then 0.1 µL of the mixture was diluted with 999.9 µL of ultrapure water, for a final ratio of 1:10,000 by volume.

The concentration of encapsulated rhSLPI was measured by an enzyme-linked immunosorbent assay (ELISA) commercial kit (Sandwich ELISA) (The SimpleStep ELISA<sup>®</sup>, Abcam, England). The absorbance was determined by the spectrophotometric method at 450 nm, and the rhSLPI concentration was calculated. The rhSLPI concentration was calculated as the percentage of encapsulation efficiency (%EE).

The encapsulation efficiency was calculated using the following formula [78] :

$$\% \text{ Encapsulation efficiency} = \frac{\text{Amount of drug encapsulated}}{\text{Total of initial drug}} \times 100$$

### **3.7. Drug releasing assay**

The determination of released rhSLPI was measured by ELISA. In the first step, 100 µg/mL of rhSLPI-LNPs were obtained by diluting 14 µL of 11 mg/mL rhSLPI-LNPs with 1,486 µL of phosphate buffered saline (PBS). Next, the releasing step was performed by incubating the LNPs mixture at 37 °C for 10, 30, 60, 120, 240, and 360 min with shaking at 400 rpm. At the end of each incubation time, rhSLPI-LNPs were centrifuged at 15,000 rpm for 3 h. Then, the supernatant was collected, and the rhSLPI concentration was measured by ELISA. The concentration of rhSLPI was calculated as a percentage of the cumulative release. The concentration and percentage of release were compared with the control group, which is lysed rhSLPI-LNPs.

### **3.8. Determination of anti-protease inhibition activity**

The anti-protease inhibition property of rhSLPI-LNPs was determined by a casein protease inhibition assay, which is against the casein digestion of trypsin [79]. Trypsin is a protease enzyme, and one of its substrates is casein, which is a protein that was extracted from mammalian milk. When the proteolysis of the enzyme occurs, the casein is digested into small peptides that cannot be spun down at 12,000 rpm, and when measuring the absorbance at 280 nm, a certain level of protein concentration was observed. But when incubated with rhSLPI, which has the property of being a protease enzyme inhibitor, if rhSLPI could inhibit the digestion of casein after spinning down at 12,000 rpm, the protein concentration in the supernatant should be reduced.

First, the rhSLPI-LNPs were broken by mixing a ratio of 1:2 with 70% ethanol. Then, co-incubation of 50 µl of rhSLPI-LNPs and 50 µl of 1000 U/mg trypsin at 37°C for 1 h. After incubation, 200 µl of 1% (w/v) casein was added and incubated at 37°C for another 30 min. Finally, 250 µl of 5% trichloroacetic acid (TCA) was added and centrifuged at 12,000 rpm for 15 min. Then, the supernatant was collected and the absorbance measured at O.D.280 nm. The inhibition was compared with the control group, which has no rhSLPI-LNPs, and calculated as a percentage of inhibition.

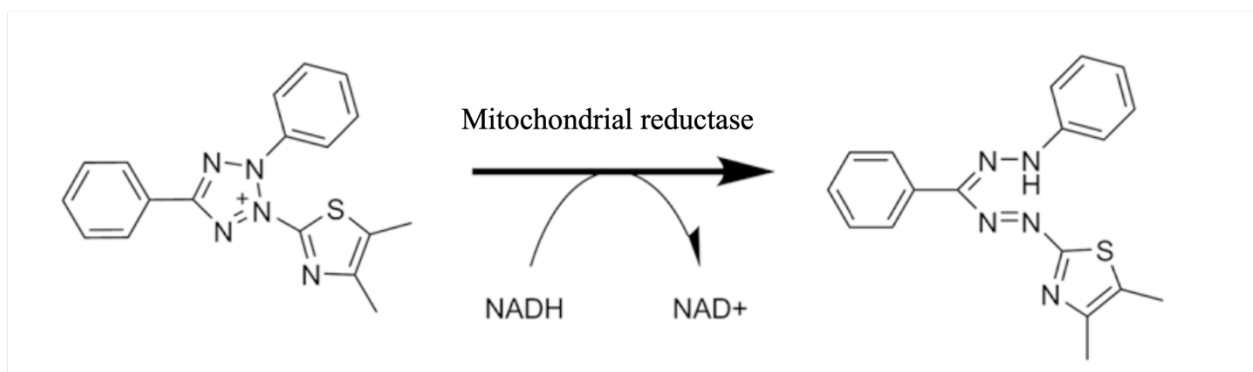
### 3.9. MTT cell viability assay

#### 3.9.1. The principle of MTT cell viability assay

The 3-[4,5-dimethylthiazol-2-yl]-2,5 diphenyl tetrazolium bromide (MTT) assay is based on the cellular reduction of MTT to purple-coloured formazan crystals by viable cells. So, the concentration of formazan crystal is related to the concentration of the living cell [80]. The MTT was converted by mitochondrial or cellular plasma enzymes like mitochondrial dehydrogenase, oxidase, and peroxidase using NADH or NADPH as an electron donor to convert MTT to water-insoluble formazan (Figure 13) [81]. The water-insoluble formazan crystal could be dissolved by a variety of solvents, including acidified isopropanol, dimethyl sulfoxide (DMSO), or organic solvents. The soluble formazan was measured by spectrophotometry at O.D. 570 nm [82].

#### 3.9.2. Determination of cell viability

The hFOB 1.19 cells were seeded into a well plate and incubated at 37 °C with 5% carbon dioxide (CO<sub>2</sub>) and 95% air overnight. After incubation, cells were treated with drugs or agents. After stimulation, culture media or agents were removed, and 150 μL of 0.5 mg/mL MTT solution was added to each well and incubated at 37 °C in the dark for 2 h. Then the MTT solution was discarded, and 150 μL of DMSO was added to solubilize formazan. The absorbance of formazan was measured by spectrophotometry at a wavelength λ570 nm. Finally, the relative percentage of cell viability was calculated as the difference in viable cells compared to the negative control.



3-[4,5-dimethylthiazol-2-yl]-2,5 diphenyl  
tetrazolium bromide (MTT)

**Purple colored formazan**

Figure 13. The conversion of MTT into purple-coloured formazan crystals by mitochondrial enzymatic activity [81].

  
**ลิขสิทธิ์มหาวิทยาลัยเชียงใหม่**  
 Copyright© by Chiang Mai University  
 All rights reserved

### **3.10. Determination of cytotoxicity of LNPs**

The cytotoxicity of LNPs was determined by the MTT cell viability assay. The hFOB 1.19 cells were seeded into a 96-well plate at a concentration of  $2.5 \times 10^5$  cells/mL in 200  $\mu$ l and incubated at 37 °C with 5% carbon dioxide (CO<sub>2</sub>) and 95% air overnight. After incubation, cells were treated with rhSLPI-LNPs and blank-LNPs at concentrations of 0.1, 1, 10, and 100  $\mu$ g/mL in culture media for 24 h at 37 °C with 5% carbon dioxide (CO<sub>2</sub>) and 95% air. Then, after incubation, the culture medium was discarded, and cell viability was measured by the MTT cell viability assay as mentioned in 1.9. The cytotoxicity was calculated as a relative percentage of cell viability.

### **3.11. Cell proliferation**

The effect of rhSLPI-LNPs on osteoblast cell proliferation was determined by the MTT cell viability assay. The hFOB 1.19 cells were seeded into a 96-well plate at  $5.0 \times 10^5$  cells/mL for 200  $\mu$ l and incubated at 37 °C with 5% carbon dioxide (CO<sub>2</sub>) and 95% air overnight. After incubation, cells were treated with rhSLPI-LNPs and blank-LNPs at concentrations of 0.1, 1, 10, and 100  $\mu$ g/mL in culture media for 3 h at 37 °C with 5% carbon dioxide (CO<sub>2</sub>) and 95% air, then replaced with fresh culture media and incubated at 37 °C with 5% carbon dioxide (CO<sub>2</sub>) and 95% air for 3 days. Finally, cell proliferation was measured by MTT assay and calculated as a relative percentage of cell viability.

### **3.12. Cell adhesion**

#### **3.12.1. Optimization of cell adhesion time**

The optimal adhesion time of osteoblast cells was indirectly measured by the number of adhered cells by MTT assay. The hFOB 1.19 cells were seeded into a 96-well plate at  $2.5 \times 10^5$  cells/mL for 200  $\mu$ l and incubated

at 37 °C with 5% CO<sub>2</sub> and 95% air for 10, 20, 30, and 60 min. At the end of the incubation period, the cell suspension was discarded and replaced with fresh media. After adding new culture media, cells were incubated for 2 h at 37 °C with 5% CO<sub>2</sub> and 95% air for stabilisation. Then the number of adhered cells was measured by the MTT cell viability assay. The minimal optimal time, which is a significant difference, was used for the determination of osteoblast cell adhesion.

### 3.12.2. Determination of osteoblast cell adhesion

The osteoblast cell adhesion was performed using the MTT cell viability assay. The hFOB 1.19 cells were seeded into a 24-well plate at  $3.0 \times 10^5$  cells/mL for 500  $\mu$ L/well and incubated at 37 °C with 5% CO<sub>2</sub> and 95% air overnight. Next, cells were treated with rhSLPI-LNPs in culture media at concentrations of 0.1, 1, 10, and 100  $\mu$ g/mL for 1 h. Then the culture medium was discarded, and cells were trypsinized. After the centrifugation step, the media was removed, and cells were resuspended in 1 mL of culture media. Then cells were adjusted to  $2.5 \times 10^5$  cells/mL and seeded in a cell suspension of 200  $\mu$ L/well into a 96-well plate and incubated for 20 min at 37 °C with 5% CO<sub>2</sub> and 95% air. At the end of incubation, the culture medium was removed and replaced with fresh culture medium and incubated at 37 °C with 5% CO<sub>2</sub> and 95% air for 1 h. Finally, the number of adhered cells was measured by the MTT cell viability assay.



### 3.13. Determination of osteoblast cell differentiation

On day 0, the hFOB 1.19 cells at  $1 \times 10^5$  cells/mL concentration were seeded into a 24-well plate and incubated at  $37^\circ\text{C}$  with 5%  $\text{CO}_2$  and 95% air overnight. On day 1, the culture media was removed, and cells were treated with rhSLPI-LNPs in culture media at concentrations of 0.1, 1, 10, and 100  $\mu\text{g}/\text{mL}$  at  $37^\circ\text{C}$  with 5%  $\text{CO}_2$  and 95% air. On day 3, the medium was removed and replaced with new rhSLPI-LNPs with culture media and incubated at  $37^\circ\text{C}$  with 5%  $\text{CO}_2$  and 95% air. The cells were collected on day 7. After that, the cells were extracted for total RNA.

#### 3.13.1. mRNA extraction

The RNA was extracted using a commercial RNA extraction kit (PureLink<sup>®</sup> RNA Mini Kit, Ambion). First, culture media was removed, and cells were lysed with 0.6 mL of Lysis buffer with 1% 2-mercaptoethanol. Cells were homogenised by passing cell lysate through a 21-gauge syringe needle. Then 70% ethanol was added to each well at one volume of the cell lysate. Next, the amount of cell lysate was transferred to the spin cartridge and spun down at  $12,000 \times g$  for 15 sec at room temperature, then discarded the flow-through and reinserted the spin cartridge into the same collection tube. Next, 700  $\mu\text{L}$  of Wash Buffer I was added to the spin cartridge and spun down at  $12,000 \times g$  for 15 sec at room temperature, then discarded the flow-through and reinserted the spin cartridge into a new collection tube. After that, 500  $\mu\text{L}$  of Wash Buffer II was added to the spin cartridge and spun down at  $12,000 \times g$  for 15 sec at room temperature, then discarded the flow-through, and repeated this step once. After repetition, the spin cartridge was centrifuged at  $12,000 \times g$  for 2 min, the collection tube was discarded, and the cartridge was inserted into a recovery tube. The 30  $\mu\text{L}$  RNase-free water was added to the centre of the spin cartridge and incubated for 1 min. Finally, the spin cartridge was centrifuged at  $12,000 \times g$  for 2 min to elute RNA from the membrane into the recovery tube and collect the total RNA. Total RNA was used for

synthesising cDNA. Before converting RNA into cDNA, the concentration and purity of RNA were measured by a spectrophotometer (Nanodrop, Thermo) at wavelengths of 260 nm and 280 nm. The 260/280 ratio was determined to measure the purity of the cDNA.

### 3.13.2. cDNA synthesis

The mRNA was converted to cDNA by using a Tetro™ cDNA Synthesis Kit (Bioline). Firstly, the master mix was prepared, and the components are shown in Table 2. Secondly, the mastermix was incubated at 45°C for 30 min. After incubation, the reaction was terminated at 85°C for 5 min and chilled at 4°C. The cDNA could be stored at 4°C. Quantitative Reverse Transcription Polymerase Chain Reaction (qRT-PCR)

The expression of *Alp*, *Runx2*, *Coll1a1*, and *Ocn* genes was determined by quantitative Reverse Transcription Polymerase Chain Reaction (qRT-PCR) using a SensiFAST™ SYBR® No-ROX kit (Bioline). The PCR-specific primers are shown in Table 3. The PCR results will be normalised to GAPDH, which is an internal control and housekeeping gene based on the  $2^{-\Delta\Delta C_t}$ .

ลิขสิทธิ์มหาวิทยาลัยเชียงใหม่  
Copyright© by Chiang Mai University  
All rights reserved

Table 2 Reagents for cDNA Synthesis

Reagents	Volume
Total RNA (3 µg)	n µL
Oligo (dT) <sub>18</sub>	1 µL
10 mM dNTP mix	1 µL
5x RT Buffer	4 µL
RiboSafe RNase Inhibitor	1 µL
TeTro Reverse Transcriptase (200u/ µL)	1 µL
DEPC-treated water	Up to 20 µL

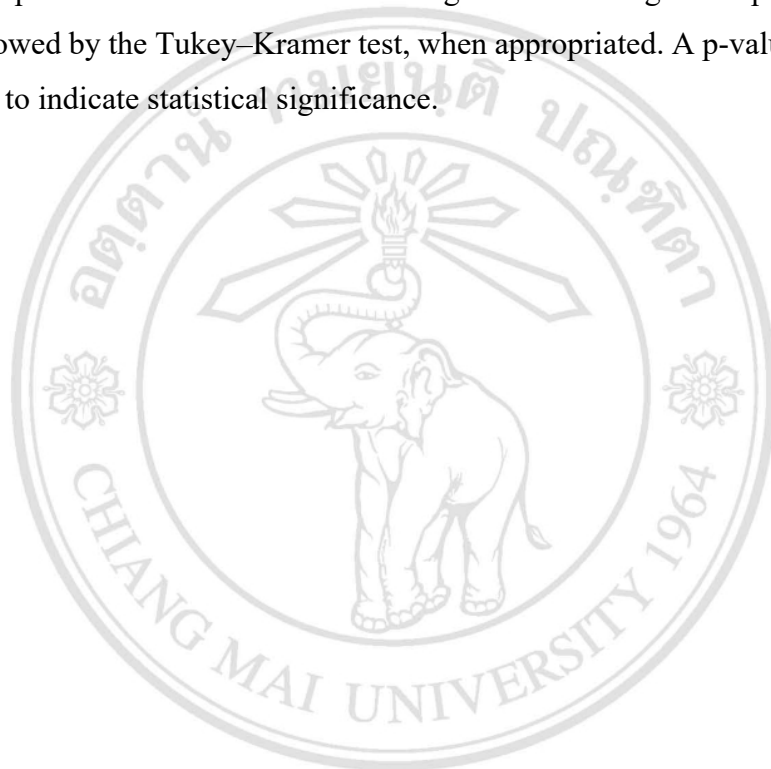
ลิขสิทธิ์มหาวิทยาลัยเชียงใหม่  
 Copyright© by Chiang Mai University  
 All rights reserved

Table 3 Specific primers for detection of mRNA by real-time PCR

Primers	Sequences	T <sub>m</sub> (°C)	Annealing Temp. (°C)
hOCN-F	CTCACACTCCTCGCCCTAT	57	52
hOCN-R	GGTCTCTTCACTACCTCGCTG	58	
hALP-F	CCAAGGACGCTGGGAAATCT	58	53
hALP-R	TATGCATGAGCTGGTAGGCG	58	
hRUNX2-F	GCGCATTCCCATCCCAGTA	58	53
hRUNX2-R	GGCTCAGGTAGGAGGGGTAA	59	
hCOL1A1-F	TCTAGACATTTTCAGCTITGTGGAC	57	52
hCOL1A1-R	TCTGTACGCAGGTGATTGGTG	58	
hGAPDH-F	GCTCTCCAGAACATCATCC	53	48
hGAPDH-R	TGCTTCACCACCTTCTTG	53	

### 3.14. Statistical analysis

In this study, statistical analysis was calculated by using commercially available software (GraphPad Prism version 9, San Diego, CA, USA). All data were expressed as mean  $\pm$  SEM. All comparisons were determined for significance using an unpaired t-test or ANOVA, followed by the Tukey–Kramer test, when appropriated. A p-value of less than 0.05 was used to indicate statistical significance.



ลิขสิทธิ์มหาวิทยาลัยเชียงใหม่  
Copyright© by Chiang Mai University  
All rights reserved

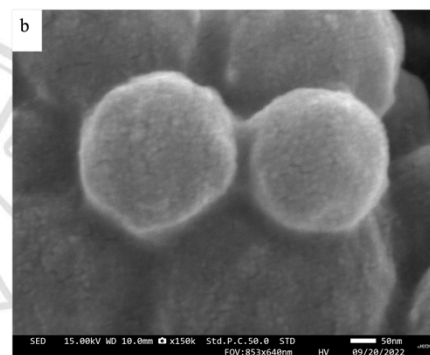
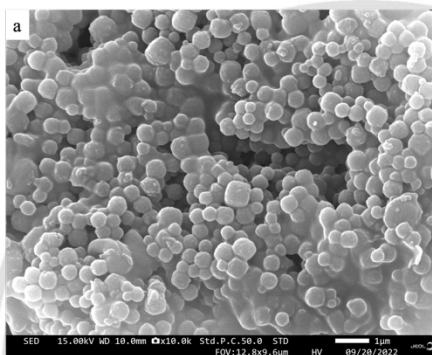
## CHAPTER 4

### Results and Discussion

#### 4.1. Physical characteristics of liposome nanoparticles (LNPs)

The morphology of LNPs was observed under the scanning electron microscope (SEM). The results showed that both blank-LNPs and rhSLPI-LNPs had a spherical shape and a rough surface (Figure 14). Moreover, to directly visualise the inner architecture of particles, the transmission electron microscope (TEM) was used to observe the rhSLPI-LNPs. The result showed that the shell of LNPs was circular in shape and presented an inner lipid bilayer as an onion-like structure (Figure 15). The size, polydispersity index (PDI), and surface zeta potential were measured by Zetasizer (Malvern). The size of blank-LNPs and rhSLPI-LNPs was  $116.8 \pm 0.23$  nm and  $121.5 \pm 0.61$  nm, respectively (Figure 16a). The size of blank-LNPs and rhSLPI-LNPs showed no significant difference. The PDI of blank-LNPs and rhSLPI-LNPs was  $0.08 \pm 0.008$  and  $0.075 \pm 0.006$ , respectively, without significant difference (Figure 16b). The zeta potential of blank-LNPs and rhSLPI-LNPs was  $-64.47 \pm 1.12$  mV and  $-51.98 \pm 0.90$  mV, respectively (Figure 16c). The zeta potential of rhSLPI-LNPs was significantly higher than that of blank-LNPs ( $p < 0.001$ ). In addition, the stability of rhSLPI-LNPs was observed, after storing the nanoparticles in ultrapure water at 4°C for 90 days, by Zetasizer. The size of rhSLPI-LNPs was  $116.2 \pm 0.81$  nm (Figure 16d), while the surface zeta potential was  $-50.4 \pm 1.24$  mV (Figure 16e). Both rhSLPI-LNPs size and zeta potential were not significantly different when compared to the blank LNPs.

**Blank-LNPs**



**rhSLPI-LNPs**

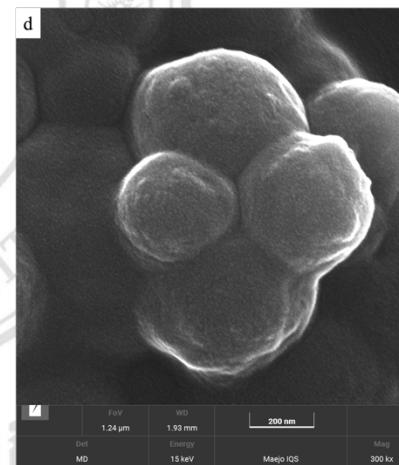
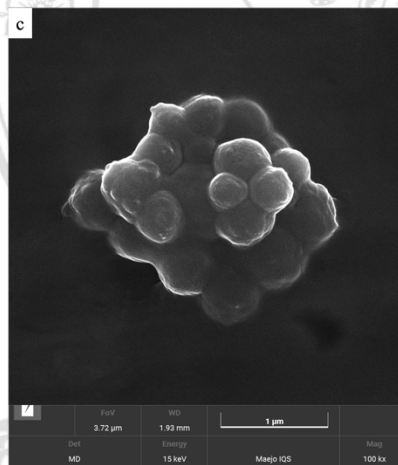


Figure 14. Morphology of nanoparticles by Scanning electron microscope (SEM) a,b) blank-LNPs; c,d) rhSLPI-LNPs.

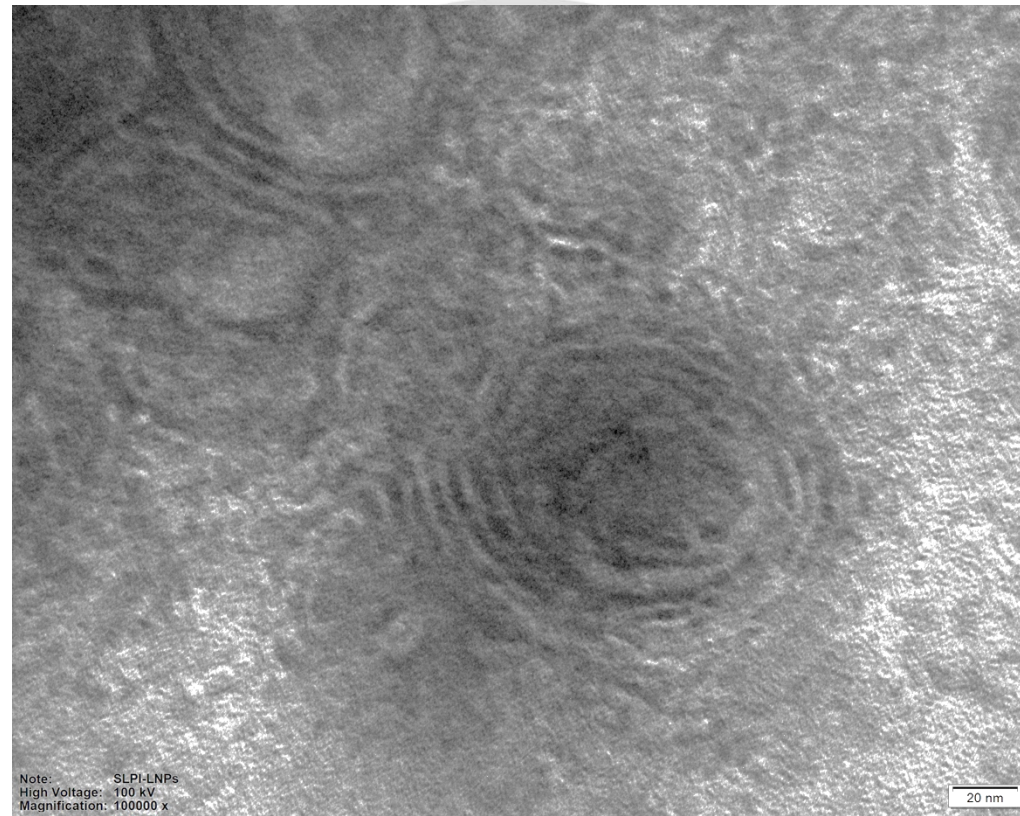


Figure 15. Morphology of the nanoparticles shell was observed by transmission electron microscope (TEM).



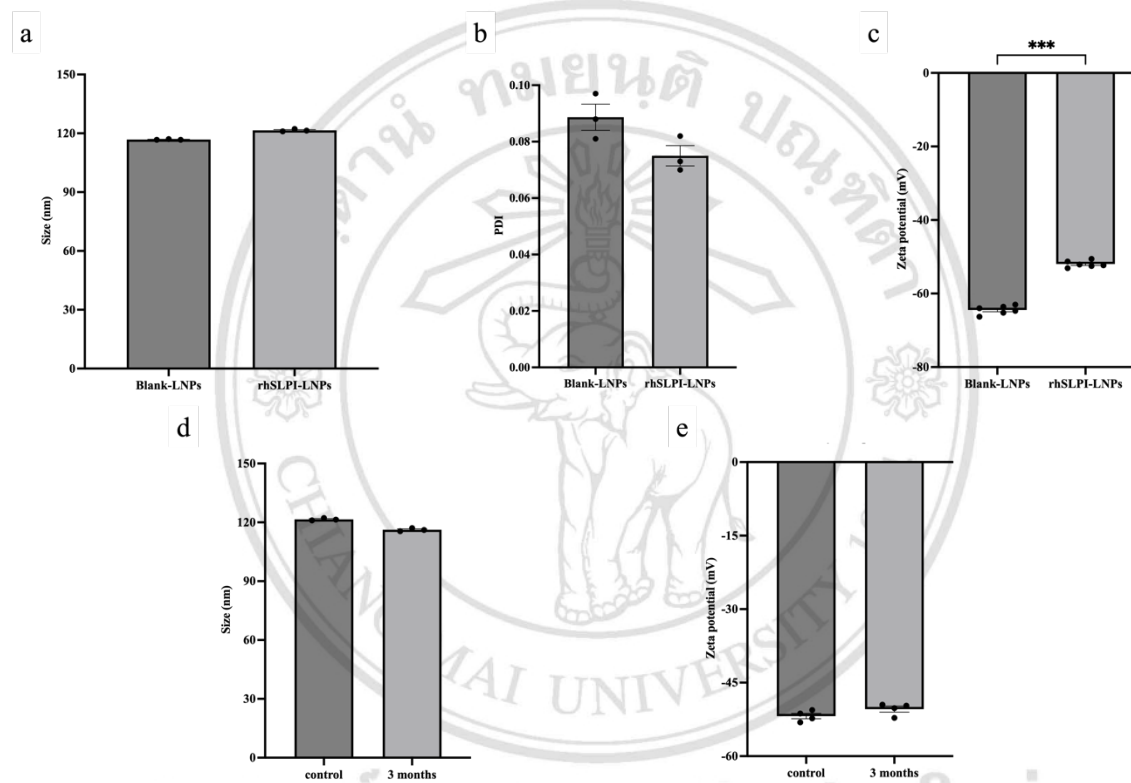


Figure 16. Characterizations of nanoparticles. a) size; b) PDI; c) zeta potential, The stability of rhSLPI-LNPs. c) size; d) zeta potential. \*\*\*  $p < 0.001$  (t-test)

In this current study, a recombinant human secretory leukocyte protease inhibitor (rhSLPI) was the candidate therapeutic protein for improving osteoblast cell differentiation. Previous studies showed that SLPI is capable of enhancing MC3T3 osteoblast cell adhesion on titanium surfaces through the focal adhesion kinase/paxillin signalling pathway [11]. However, SLPI has a short half-life and can be excreted by the kidneys or digested by blood circulation protease [13]. Therefore, protecting the SLPI protein by using nanoparticle encapsulation could be one of the most challenging issues. The liposome nanoparticle is one of well-known nanoparticles for drug delivery, that has been shown to be able to encapsulate peptides [60], offer biocompatibility, and prevent the digestion of protease enzymes [59]. Therefore, liposomes were selected as the peptide carrier to encapsulate recombinant human SLPI (rhSLPI) protein for enhancing osteoblast differentiation. This study is the first study to examine of rhSLPI liposome nanoparticle encapsulation to enhance human osteoblast cell differentiation.

The physical characterization of the LNPs was observed by SEM, TEM, and Zetasizer after the fabrication. SEM was used to characterise the morphology of the LNPs. The morphology of both blank-LNPs and rhSLPI-LNPs showed a spherical shape and a rough surface (Figure 14). The shell of rhSLPI showed a circular shape of the lipid bilayer (Figure 15). From the results, the rhSLPI-LNPs appeared as vesicles, which might be capable of encapsulating drugs or proteins for delivery.

The size of LNPs was determined by Zetasizer. The size of both LNPs was approximately 120 nm, which was no different in size due to both LNPs being filtered by a mini extruder. However, the size of rhSLPI-LNPs was smaller than in the previous study ( $153.6 \pm 2.47$  nm), which is due to the pore size of the filter in the extrude step [59]. In this study, 100 nm of filter pore size was used, whereas the previous study used a 200 nm pore size filter. Thus, this is the reason that the size of LNPs in this study was smaller than reported in the previous study. However, the size of the particles in the current study was still larger than the size of the filter pore. Nanoparticle size reduction does not eliminate particles larger than the filter pore. Rather, it reduces the size and homogeneity of large particles by forcing them through the filter. Moreover, there was reported that the suitable size of

LNPs for drug delivery ranges between 50 and 200 nm, depending on the route of administration [71]. In addition, it was mentioned that LNPs smaller than 50 nm are rapidly excreted by renal clearance, whereas larger than 200 nm of LNPs are strongly opsonized and removed from the blood circulation via the macrophages of the reticuloendothelial system (RE system) [83]. The rapid elimination of the particle results in the activity or fusion of LNPs with the cell, which may not be sufficient to stimulate cell differentiation. The polydispersity index (PDI) of nanoparticles is used to indicate the heterogeneity of nanoparticles based on their size. The international standard organizations (ISOs) reported that PDI values near 0.00 are considered monodisperse nanoparticle samples, whereas PDI values greater than 0.7 are considered polydisperse nanoparticle samples [67]. Thus, the PDI of blank-LNPs ( $0.08 \pm 0.008$ ) and rhSLPI-LNPs ( $0.075 \pm 0.006$ ) values were lower than 0.7, suggesting that both blank-LNPs and rhSLPI-LNPs are homogenous [84]. The zeta potential of rhSLPI-LNPs was  $-51.98 \pm 0.90$  mV (Figure 16c), similar to the previous study, where the SLPI encapsulated liposome nanoparticles ( $-58.80 \pm 1.1458$  mV) [59]. The negative charge of the LNPs is generated from the phosphate group of dioleoyl phosphatidylserine (DOPS) [85], which is the major component of LNPs. It has been known that the zeta potential is used to predict the stability of the nanoparticles; the optimal range of the zeta potential value is higher or equal to  $-35$  mV or lower or equal to  $+35$  mV, which represents less ability for particle aggregation [15]. In the current study, the stability of rhSLPI-LNPs was observed by measuring their size and zeta potential after storing them at  $4^{\circ}\text{C}$  for 90 days in DI water. The result showed that rhSLPI-LNPs could be able to retain their stability for 3 months, which is consistent with a previous study that showed particles stored at  $4^{\circ}\text{C}$  were stable for at least 5 months in a PBS solution [86]. For clinical applications, typically, the preservative agent for therapeutic agents, drugs, or vaccines encapsulated in liposome nanoparticles is not utilised in clinical settings. However, it must be kept in lyophilized form and dissolved prior to use [87].

#### 4.2. Determination of rhSLPI encapsulated concentration

The rhSLPI-LNPs were disrupted by 70% ethanol for the absolute release of the encapsulated molecules. The released-rhSLPI level from LNPs was determined by Enzyme-linked immunosorbent assay (ELISA). The result showed that the rhSLPI concentration of rhSLPI-LNPs was  $61.23 \pm 0.8 \mu\text{g/mL}$ , which was significantly higher than that of blank-LNPs ( $0.00 \pm 0.00 \mu\text{g/mL}$ ;  $p < 0.001$ ) (Figure 17). From the result, the encapsulated concentration was calculated into the percentage of encapsulation efficiency (%EE) of  $18.313 \pm 0.24\%$  as shown below. In addition, the concentration of rhSLPI in LNPs was calculated. The concentration of rhSLPI encapsulated by 0.1, 1, 10, and 100  $\mu\text{g/mL}$  rhSLPI-LNPs was calculated to be 0.6, 5.6, 55.7, and 556.6  $\text{ng/mL}$ , respectively.

$$\% \text{Encapsulation efficiency} = \frac{\text{Amount of drug encapsulated}}{\text{Total of initial drug}} \times 100$$

$$\% \text{Encapsulation efficiency} = \frac{61.23 \mu\text{g/mL}}{330 \mu\text{g/mL}} \times 100 = 18.313\%$$

ลิขสิทธิ์มหาวิทยาลัยเชียงใหม่  
Copyright© by Chiang Mai University  
All rights reserved

### SLPI encapsulation

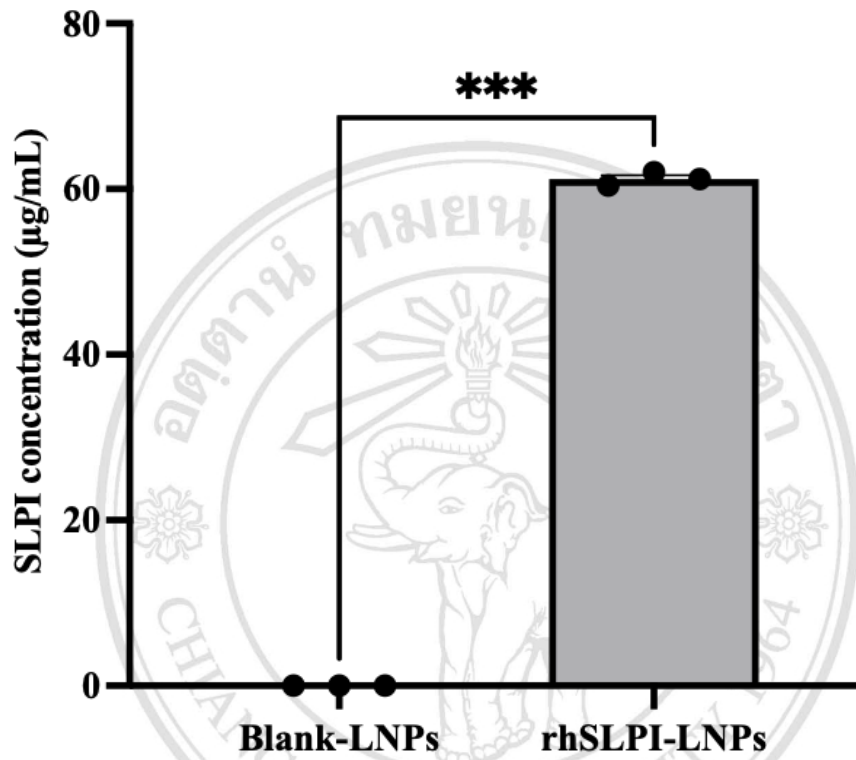


Figure 17. The concentration of encapsulated rhSLPI. \*\*\*  $p < 0.001$  (Unpaired t-test)

ลิขสิทธิ์มหาวิทยาลัยเชียงใหม่  
Copyright© by Chiang Mai University  
All rights reserved

The result of LPNs encapsulation confirms that rhSLPI was successfully encapsulated by LNPs. It was suggested from the previous study that the rhSLPI could be encapsulated in the middle part or internal aqueous core of the LNPs, due to the properties of hydrophilic proteins [67]. Since the protein is located in the core of LNPs the protein might reduce excretion by the kidneys and digestion by blood circulation proteases [15]. Although rhSLPI-LNPs could encapsulate rhSLPI, the percentage of encapsulation efficiency was lower than in the previous study, which used a similar experimental design (%EE  $74.1 \pm 2.97\%$ ) [59]. The explanation for this discrepancy could be due to the method of SLPI measurement. The previous study determined SLPI in samples using reverse-phase High-Performance Liquid Chromatography (RP-HPLC), which used water and acetonitrile with 0.1% trifluoroacetic acid as a mobile phase, whereas in our current study, the immunological technique (ELISA) was used to determine rhSLPI concentration. From this point, it might be the reason why %EE is significantly different compared with this study. The measurement of SLPI concentration by HPLC is suggested as an indirect measurement of protein concentration, which uses the principle of movement of substances based on hydrophobicity into the analyzer, which might interfere with interferences [88]. One of the limitations of the HPLC technique for measuring protein concentration in biological samples is that high concentrations of lipids could interfere with protein measurement and influence the specificity of the technique [89]. However, ELISA, which is an immunological technique based on the interaction of specific antibodies with target molecules, is considered a method to directly measure SLPI concentration with high specificity for rhSLPI protein, and there was no interference from the nanoparticle solution. In addition, the fabrication of particles of different sizes from previous studies might have an effect on the particles' capacity to contain rhSLPI. Moreover, previous studies have demonstrated that the synthesis of particles by the thin film hydration method might give slightly different %EE value [67, 90]. In addition, the encapsulation capacity of the LNPs could be improved by decreasing the concentration of rhSLPI at the fabrication step since the capacity of LNPs might be sufficient for low concentration. From this point, it is necessary to investigate the optimal concentration of protein incorporation into nanoparticles.

### 4.3. Drug releasing

The drug-releasing study was performed with 100 mg/mL of rhSLPI in PBS and incubated for 10, 30, 60, 120, 240, and 360 min at 37°C. The concentration of released-rhSLPI was measured by ELISA. The results showed that the concentration of released-rhSLPI at 10, 30, 60, 120, 240, and 360 min was  $0.0093 \pm 0.008$ ,  $0.0058 \pm 0.005$ ,  $0.021 \pm 0.017$ ,  $0.026 \pm 0.013$ ,  $0.027 \pm 0.008$ , and  $0.051 \pm 0.035$   $\mu\text{g/mL}$ , respectively. These rhSLPI concentrations were significantly lower than those of the control group, which was completely ruptured by 70% ethanol to release entire amounts of encapsulated rhSLPI ( $61.23 \pm 0.8$   $\mu\text{g/mL}$ ) (Figure 18a) ( $p < 0.001$ ). The released-rhSLPI concentration was calculated as a percentage of accumulative releasing. The results showed that after incubation at 10, 30, 60, 120, 240, and 360 min, the releasing is  $0.015 \pm 0.01\%$ ,  $0.0095 \pm 0.008\%$ ,  $0.034 \pm 0.027\%$ ,  $0.043 \pm 0.022\%$ ,  $0.045 \pm 0.013\%$ , and  $0.083 \pm 0.06\%$ , respectively (Figure 18b), which is less than 1%.

The percent release of rhSLPI-LNPs in this study was less than 1% after incubation for 360 min, which is inconsistent with the previous study (73% within 4 h) [60]. The difference between the previous study and our current study might be due to the different methods to assess the release of the protein. The previous study used the dialysis method and immersed the dialysis bag into PBS and stirred it with a magnetic stirrer at 100 rpm at 37°C. whereas in this study, the rhSLPI-LNPs were stirred on an orbital shaker at 100 rpm at 37°C, with no effect of the force from the magnetic bar on the nanoparticles. From this point, it might be the reason for the different abilities to release of rhSLPI. Moreover, Due to the reason that the protein is positively charged though the LNPs are negatively charged, the protein attached to the surface of the LNPs might be unable to be released from the LNPs.

Since rhSLPI is limited in blood circulation, which has a short half-life and can be digested by circulation protease enzymes [13]. For this reason, the inability of the protein

to be secreted from the LNPs may be able to reduce the above limitation of the rhSLPI and increase the chances of the rhSLPI reaching the target cell.

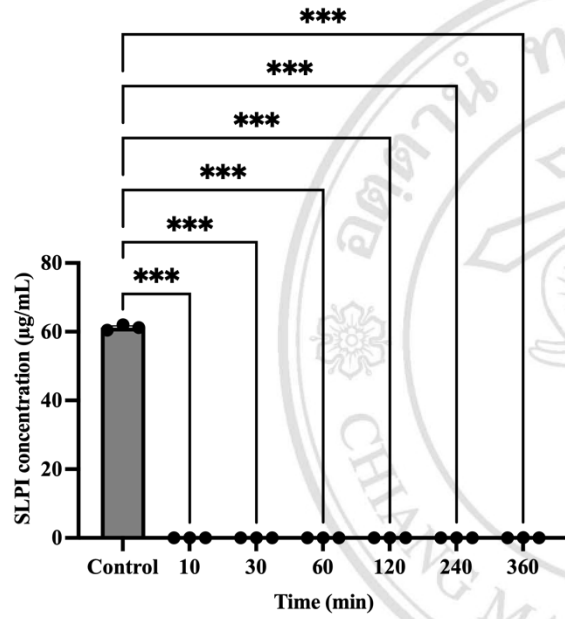
Although the rhSLPI-LNPs could less release of rhSLPI protein, the biological effects might still be able to proceed. This might be due to the biological effects of rhSLPI, which could activate intracellular mechanistic pathways. The mechanism of liposome nanoparticle-cell interaction mainly occurs by fusion with the plasma membrane, which is liposomal lipid merged into the cell membrane, and the content or drug being delivered into the cytoplasm [91]. The liposome nanoparticles may bind to the surface of the cell membrane and cause a locally high concentration of liposomal contents, resulting in decreased liposome stability and leakage of liposomal contents to the cell surface. Under the influence of passive diffusion or transport, these substances are then transported across the cell membrane and taken up by the cell [92]. The LNPs could be uptaken by endocytosis, including pinocytosis, phagocytosis, clathrin-mediated endocytosis, and non-clathrin-mediated endocytosis [93].

In addition to its ability to inhibit proteases, it has been reported that SLPI has a direct effect that can reduce injury and apoptosis independently of its anti-protease activity [94]. Additionally, SLPI might have a direct beneficial effect on bones. However, it must be proven with the recombinant anti-protease-deficient mutant SLPI in order to demonstrate that its properties on bone cells might not require the ability to inhibit the enzyme.

Delivery of rhSLPI by LPNs might rather fuse to cell membrane and release the rhSLPI into the intracellular compartment. Therefore, the less releasing of rhSLPI might not matter when it could provide sufficient intracellular deliverly of rhSLPI.



a



b

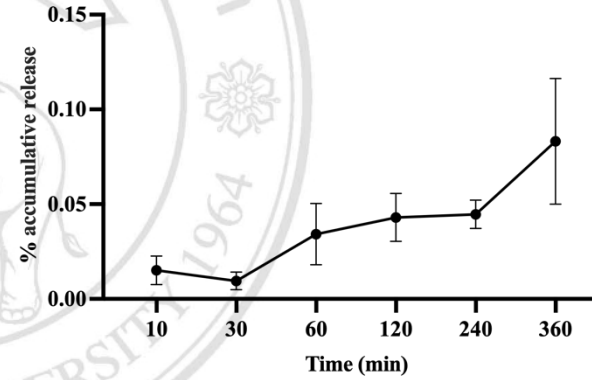


Figure 18. Release profile of rhSLPI-LNPs. a) the concentration of rhSLPI compared with control. \*\*\*  $p < 0.001$  (ANOVA); b) the percentage of accumulative released-rhSLPI.

ลิขสิทธิ์มหาวิทยาลัยเชียงใหม่  
Copyright © by Chiang Mai University  
All rights reserved

#### 4.4. Anti-protease inhibition activity

Anti-protease inhibition activity was performed by a casein protease inhibition assay. The results showed that rhSLPI-LNPs significantly reduced the percentage of protease activity compared to blank-LNPs ( $65.63 \pm 1.86$  % of rhSLPI-LNPs vs.  $100 \pm 3.90$  % of blank-LNPs;  $p < 0.001$ ) (Figure 19).

According to the results, the rhSLPI protein retains its proteolytic inhibitory properties after the fabrication process. The existence of the anti-protease property might increase the efficiency of rhSLPI-LNPs for clinical applications such as reducing tissue destruction from protease enzyme [27]. In this study, the anti-protease activity of rhSLPI was observed from encapsulated rhSLPI molecules to verify the intact anti-protease activity of SLPI. The results showed that rhSLPI from encapsulated LPNs was still able to inhibit the protease activity of serine protease Trypsin, which contradicts the findings of previous experiments in this study indicating that very little rhSLPI is secreted. Before measuring the rhSLPI ability in this experiment, the rhSLPI-LNPs were broken by 70% alcohol, allowing the protein to completely flee into the solution.

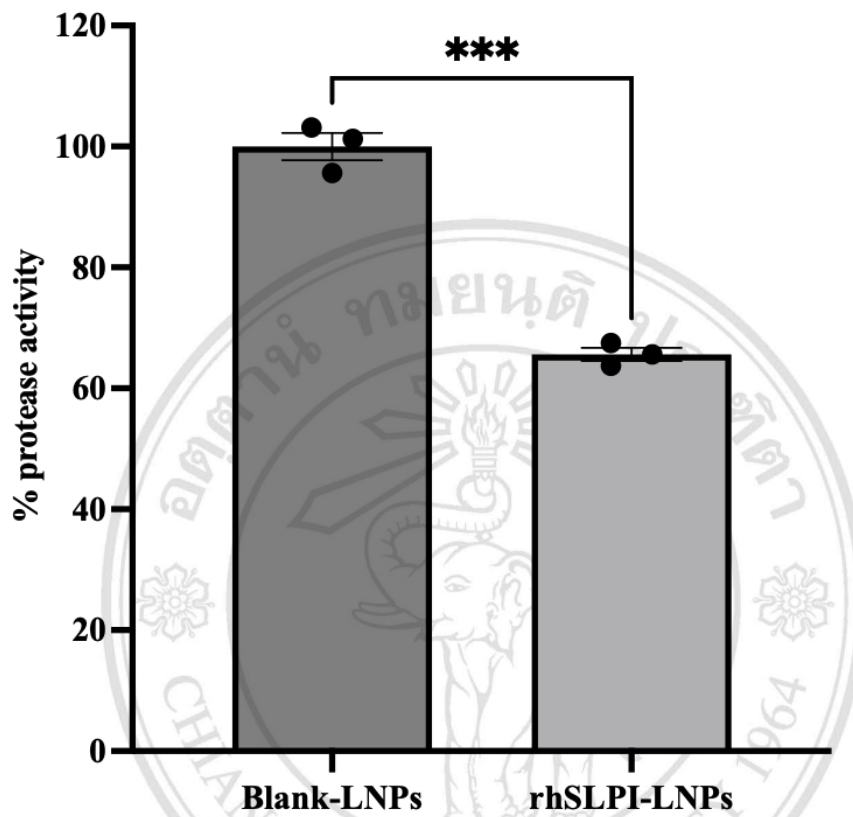


Figure 19. The protease inhibition activity of rhSLPI-LNPs. \*\*\*  $p < 0.001$  (Unpaired t-test)

ลิขสิทธิ์มหาวิทยาลัยเชียงใหม่  
 Copyright© by Chiang Mai University  
 All rights reserved

#### 4.5. The cytotoxicity of LNPs

The cytotoxicity of LNPs was determined by incubating human osteoblast hFOB 1.19 cells with blank-LNPs or rhSLPI-LNPs for 24 h. After incubation, the cytotoxicity was determined by the MTT cell viability assay. The results showed that all concentrations (0.1, 1, 10, and 100  $\mu\text{g}/\text{mL}$ ) of both blank-LNPs ( $98.58 \pm 8.62\%$ ,  $104.20 \pm 10.10\%$ ,  $100.70 \pm 5.76\%$ , and  $90.58 \pm 8.30\%$ , respectively) and rhSLPI-LNPs ( $100.90 \pm 5.24\%$ ,  $103.20 \pm 12.98\%$ ,  $109.00 \pm 12.06\%$ , and  $91.96 \pm 7.15\%$ , respectively) were not significantly reduced in cell viability compared with the control (untreated) groups ( $100.00 \pm 10.96\%$ ). However, treatment with 100  $\mu\text{g}/\text{mL}$  of blank-LNPs and rhSLPI-LNPs reduced the relative percentage of cell viability to less than 95% ( $90.58 \pm 8.3\%$ , and  $91.96 \pm 7.2\%$ , respectively).

After the successful encapsulation of rhSLPI into LNPs, the cytotoxicity was investigated by the MTT cell viability assay. The results showed that both blank-LNPs and rhSLPI-LNPs are non-toxic to osteoblast cells, which is consistent with previous studies [59]. According to the experimental results, the rhSLPI-LNPs might be safe in real clinical usage. Although both blank-LNPs and rhSLPI-LNPs had no statistical significance to the control group but 100  $\mu\text{g}/\text{mL}$  of blank-LNPs and rhSLPI-LNPs caused less than 95% cell survival (Lethal dose 5, LD5) since under typical conditions, approximately 5% of cells per day die. There has been reported that high concentrations of LNPs slightly affect cell survival. The excessive lipid content increases LNPs fusing to cells, resulting in decreased cell membrane stability and cell death [95].

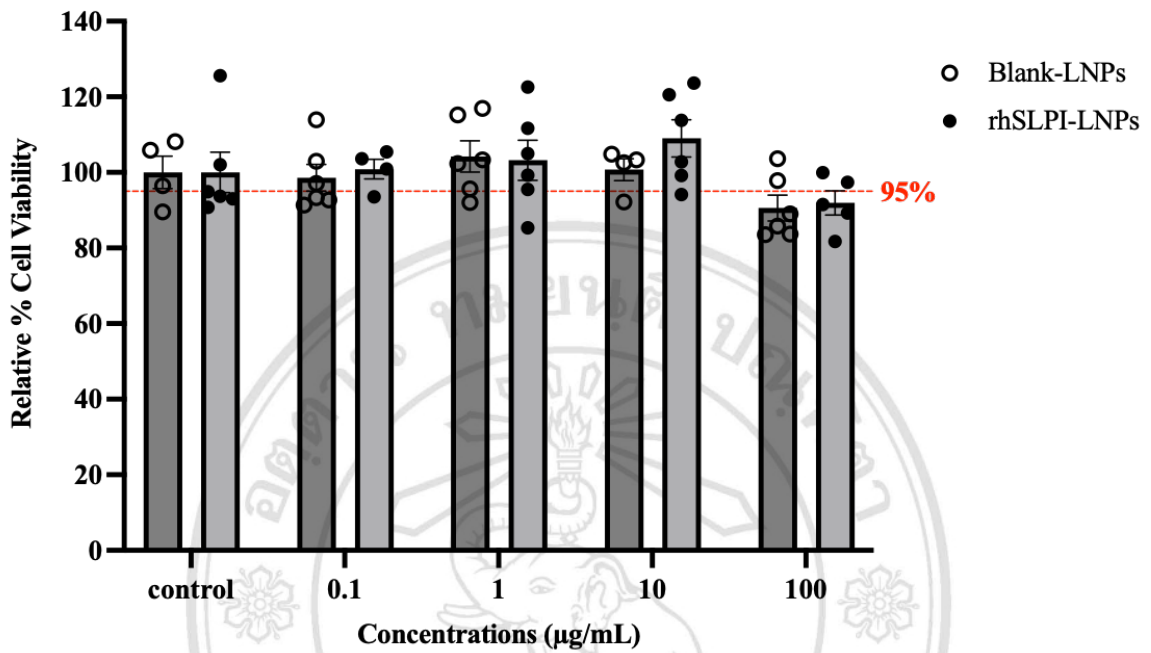


Figure 20. The cytotoxicity assay by the relative percentage of cell viability (ANOVA).

#### 4.6. Cell proliferation

The cell proliferation effect of rhSLPI-LNPs was determined by the MTT cell viability assay. The results showed that 1 and 10  $\mu\text{g/mL}$  of rhSLPI-LNPs ( $126.70 \pm 21.75\%$ , and  $123.4 \pm 15.95\%$ , respectively) were significantly higher compared with blank-LNPs ( $99.54 \pm 13.11\%$ , and  $97.43 \pm 8.90\%$ , respectively) (Figure 21). However, 0.1 and 100  $\mu\text{g/mL}$  of both blank-LNPs ( $106.3 \pm 10.33\%$ , and  $91.45 \pm 7.37\%$ , respectively) and rhSLPI-LNPs ( $126.2 \pm 13.72\%$ , and  $105.50 \pm 10.04\%$ , respectively) showed no significant difference.

Although rhSLPI-LNPs at concentrations of 0.1 and 100  $\mu\text{g/mL}$  increased cell proliferation higher than the control. However, it was found that all concentrations of rhSLPI-LNPs had a higher effect on cell proliferation than the control, but there were no statistically significant differences. Less than 1  $\mu\text{g/mL}$  of rhSLPI-LNPs might not contain enough rhSLPI to promote cell proliferation. On the other hand, rhSLPI-LNPs at a concentration of 100  $\mu\text{g/mL}$ , which did not show a statistically significant difference, may be due to an excessive concentration of LNPs causing cytotoxicity and cell death [95]. Previous studies reported that SLPI promotes cell proliferation via stimulating the Ras/MAPK signalling pathway, which is a cell survival pathway to increase the phosphorylation of ERK1/2 in ovarian cancer cells [11, 96]. In addition, SLPI is involved in promoting the phosphorylation AKT signalling pathway, which is an intracellular signalling pathway that promotes cell growth, cell survival, and cell proliferation, there has been reported that phosphorylation AKT was decreased after the knockdown of SLPI gene [26]. In 2015, Soon-Jeong Jeong *et al.* reported that SLPI could stimulate osteoblast cell proliferation through FAK/Grb2/Ras/ERK1/2 signalling pathway related to mitosis [11]. The previous results indicated that rhSLPI-LNP might be a candidate molecule to increase osteoblast cell proliferation. Osteoblast cell proliferation plays a vital role in bone healing processes. Osteoblasts are the cells responsible for bone formation, and their proliferation is essential for synthesis of new bone tissue and facilitating the repair of fractures [97]. The proliferation of osteoblast cell is critical for bone healing as it drives the synthesis of bone matrix, callus formation, mineralization, remodelling, and the

production of growth factors [98]. Osteopathic rehabilitation is more difficult for the elderly than for adults [99]. The ability of rhSLPI to increase osteoblast cell proliferation might be useful in the treatment of bone fractures in elderly patients.



ลิขสิทธิ์มหาวิทยาลัยเชียงใหม่  
Copyright© by Chiang Mai University  
All rights reserved

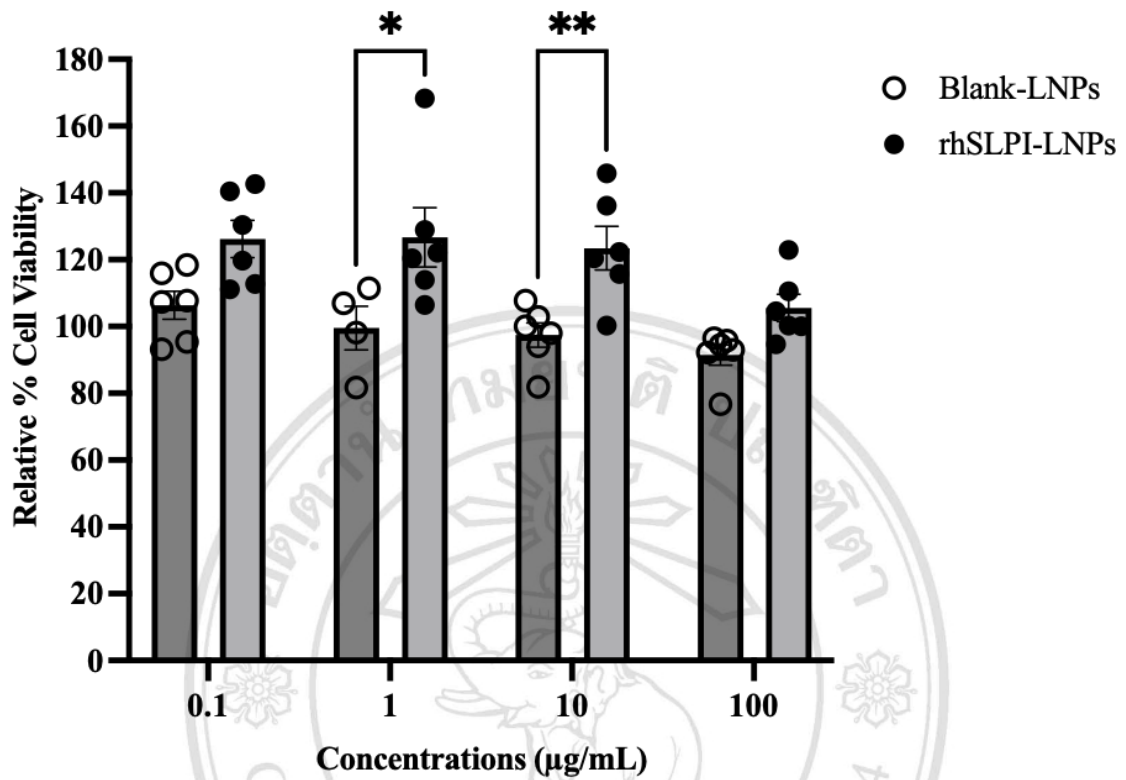


Figure 21. Osteoblast cell proliferation after being treated with blank-LNPs and rhSLPI-LNPs was determined by MTT cell viability assay. \*  $p < 0.05$ , \*\*\*  $p < 0.01$  (ANOVA).



#### 4.7. Cell adhesion

The osteoblast cell adhesion time was optimised by the MTT assay (Figure 22a). The results showed that 10 min was significantly different compared with 20, 30, and 60 min. There was no significant difference between the 20, 30, and 60 min when compared among themselves. Twenty minutes were selected for the osteoblast cell adhesion experiment.

After optimisation, the effect of rhSLPI-LNPs on enhancing osteoblast adhesion was performed on hFOB 1.19 cells after exposure to rhSLPI-LNPs for 24 h. The results showed that hFOB 1.19 cells after exposed to rhSLPI-LNPs at a concentration of 10  $\mu\text{g}/\text{mL}$  were significantly enhanced osteoblast adhesion when compared to control untreated cells ( $0.1004 \pm 0.0098$  vs.  $0.0559 \pm 0.0161$ , respectively) ( $p < 0.001$ ) (Figure 22b). However, increasing the concentration to 100  $\mu\text{g}/\text{mL}$  of rhSLPI-LNPs ( $0.05441 \pm 0.0146$ ) could not significantly increase osteoblast adhesion.

The adhesion of osteoblast cells plays an important role in bone fracture regeneration. It permits callus formation, deposition of new bone matrix, communication and signalling, osteoblast migration and recruitment, integration with existing bone, and bone remodelling. Enhancing osteoblast adhesion and optimising adhesion-related signalling pathways can enhance bone fracture healing [11, 100]. Moreover, the adhesion of osteoblast cells is able to enhance the signalling pathways related to survival, such as increased cell proliferation and decreased cell apoptosis [11, 101].

To assess the properties of rhSLPI-LNPs, the adhesion assay was investigated. The results showed that 10  $\mu\text{g}/\text{mL}$  of rhSLPI-LNPs could enhance osteoblast cell adhesion compared with the control group (Figure 22b). In addition, a greater concentration of rhSLPI-LNPs further improves cell adhesion. However, 100  $\mu\text{g}/\text{mL}$  of rhSLPI-LNPs demonstrated decreased osteoblast cell adhesion, so there might be competition when there is an over-concentration of rhSLPI, and the signal involved in adhesion might be decreased. In addition, excessive concentrations of LNPs can result in cytotoxicity and cell death. ,

Nevertheless, experimental findings revealed that 10  $\mu\text{g/mL}$  of rhSLPI-LNPs was sufficient to increase the adhesion of osteoblast cells.

Previous studies reported that SLPI could promote MC3T3-E1 osteoblast cell adhesion via stimulating the focal adhesion kinase (FAK) and paxillin signalling pathways, which are involved in cytoskeleton modification, cell migration [27], and cell adhesion [11]. Therefore, SLPI might be the candidate molecule to enhance osteoblast cell adhesion.



ลิขสิทธิ์มหาวิทยาลัยเชียงใหม่  
Copyright© by Chiang Mai University  
All rights reserved

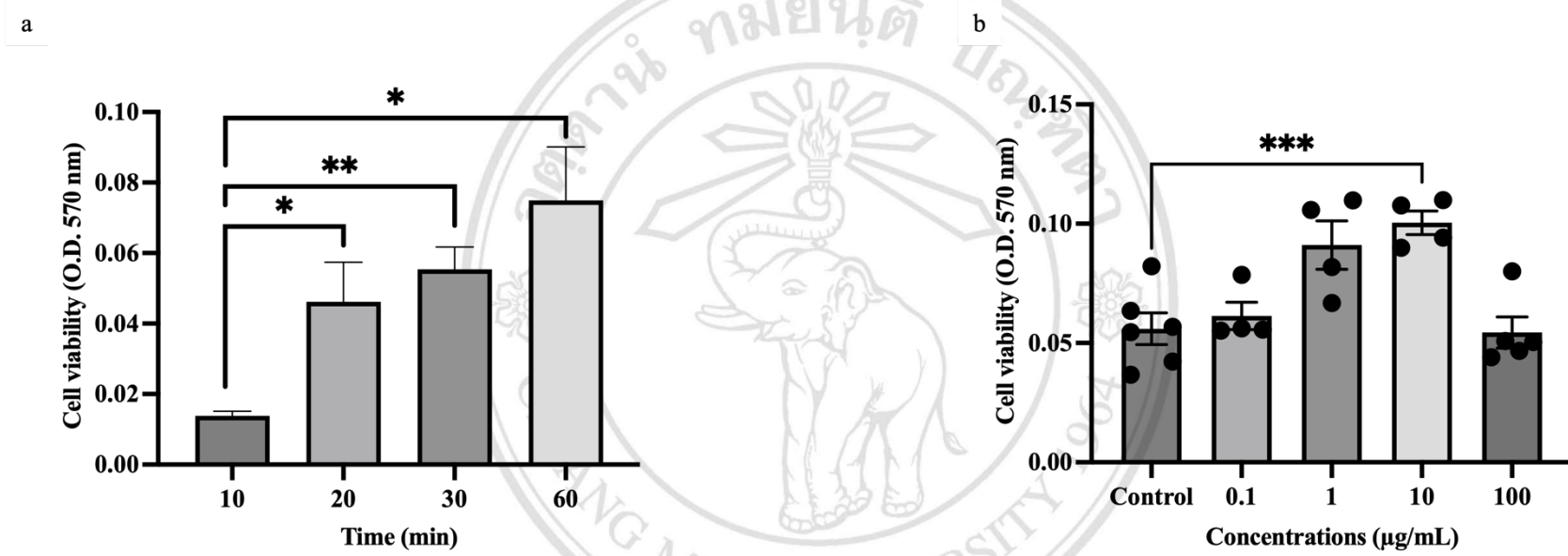


Figure 22. Cell adhesion assay was performed by MTT assay. a) The optimization adhesion time for osteoblast cells. \*  $p < 0.05$ , \*\*  $p < 0.01$  (Unpaired t-test); b) Osteoblast cell adhesion of rhSLPI-LNPs. \*\*\*  $p < 0.001$  (ANOVA).

ลิขสิทธิ์มหาวิทยาลัยเชียงใหม่  
 Copyright© by Chiang Mai University  
 All rights reserved

#### 4.8. Osteoblast cell differentiation

The expression of genes that involved in osteoblast differentiation was determined by qRT-PCR. The hFOB 1.19 cells were treated with 0.1, 1, 10, and 100 µg/mL of rhSLPI-LNPs for 7 days and the expression of *Runx2*, *Alp*, *Colla1*, and *Ocn* gene was determined compared with the control group (blank-LNPs). The results showed that 1 µg/mL of rhSLPI-LNPs significantly enhanced the expression of *Runx2* compared with blank-LNPs ( $4.86 \pm 2.60$  vs.  $2.19 \pm 0.81$ , respectively;  $p < 0.05$ ) while 10 and 100 µg/mL of rhSLPI-LNPs ( $3.23 \pm 0.91$  and  $1.68 \pm 1.33$ , respectively) showed no significant difference compared with blank-LNPs ( $3.78 \pm 2.26$  and  $1.23 \pm 0.18$ , respectively) (Figure 23a). In term of *Alp* expression, there was no significant difference in *Alp* expression in cells treated with all concentrations of rhSLPI-LNPs (Figure 23b). For *Colla1* expression, treatment with 1, 10, and 100 µg/mL of rhSLPI-LNPs ( $5.84 \pm 1.65$ ,  $4.48 \pm 0.45$ , and  $6.56 \pm 2.81$ , respectively) could significantly enhance *Colla1* gene expression in hFOB1.19 greater than blank-LNPs ( $1.84 \pm 0.82$ ,  $1.23 \pm 1.31$ , and  $3.64 \pm 0.84$ , respectively) (\* $p < 0.05$ , \*\* $p < 0.01$ ) (Figure 23c). For *Ocn* expression, treatment with 100 µg/mL of rhSLPI-LNPs could significantly enhance *Ocn* expression greater than blank-LNPs ( $5.36 \pm 1.63$  vs.  $2.92 \pm 0.44$ , respectively;  $p < 0.05$ ), whereas there were no significant difference at 1 and 10 µg/mL of LNPs.

When mesenchymal stem cells (MSCs) are exposed to specific signalling molecules and growth factors that promote osteogenic differentiation, bone differentiation initiates [20]. Following the stimulation, MSCs differentiate into osteoblast, a process governed by the *Runx2* gene, the master regulator of the bone differentiation [102]. In addition, *Runx2* can activate the expression of multiple genes implicated in osteoblast development and function, such as collagen type I (*Coll*), osteocalcin (*Ocn*), and alkaline phosphatase (*Alp*). Collagen is the primary structural protein in bone, encoding the structural proteins *Colla1* and *Col2* that provide tensile strength and stability. The *Ocn* is a non-collagenous protein produced by osteoblasts and is regarded as an indicator of osteoblast maturation. *Alp* is an osteoblast-produced enzyme that is essential for bone mineralization [103, 104].

As a result, the rhSLPI-LNPs could enhance the expression of *Runx2*, *Colla1*, and *Ocn* mRNA at the varying concentrations (Figure 23). The osteoblast cells were stimulated for only 7 days, which might be the reason that *Alp* expression was not significantly differentiated. This study dispersed rhSLPI-LNPs in a complete medium, not an osteogenic differentiation medium. Therefore, the enhancement of osteogenic gene expression found in this study could be due to the direct effect of SLPI. From the results, the rhSLPI-LNPS might be effective in enhancing osteoblast cell differentiation.

According to a previous study performed by Baik-Dong Choi *et al.* [12], mouse preosteoblasts MC3T3-E1 were treated with rhSLPI before being cultured on titanium discs and then stimulated with an osteogenic differentiation medium to differentiate. On days 4, 7, and 10, gene expression was evaluated. *Alp*, *Dspp*, *Dmp1*, *Bsp*, and *Col I* mRNA, which are differentiation markers of bone differentiation were observed. The results showed that SLPI increased the expression of *Alp*, *Dspp*, *Dmp1*, *Bsp*, and *Col I* mRNA expression in MC3T3-E1 cells compared with the untreated group. The mRNA expression of *Alp*, *Dspp*, and *Col I* had significantly increased levels on day 4, while *Dmp-1* and *Bsp* mRNA expression was significantly higher on day 7 compared with the untreated group. According to the results of the previous study, seven days to evaluate mRNA expression after SLPI treatment is sufficient for determining a statistically significant difference. However, other studies investigated the differentiation of osteoblast cells with an osteogenic differentiation medium and determined at 7, 14, and 21 days. Although in our study, the osteogenic differentiation medium was not used to stimulate osteoblast differentiation since we desired to establish the effect of SLPI on differentiation without differentiating stimulating factors from the osteogenic differentiation medium.

The advantages of rhSLPI treatment could improve bone proliferation, adhesion, and differentiation. In addition, rhSLPI also provides several beneficial effects, including anti-inflammation, anti-microorganism, reduction of cell death, and improved wound healing [10, 27, 105-107]. Using rhSLPI for enhancing bone healing by improving bone adhesion and differentiation not only benefit bone cells but also has other benefit such as

reducing inflammation, preventing infection, and a shortened time for wound healing. Moreover, it also helps to reduce inflammation from the immune response or reduce the chance of infection due to the properties of the SLPI protein.

### **Limitations of study and suggestions**

In this current study, there are several limitations. The encapsulation of rhSLPI showed that only  $61.23 \pm 0.8$   $\mu\text{g/mL}$  of rhSLPI was encapsulated. This concentration of rhSLPI seems very low when compared with the protein concentration used in the preparation method (0.33 mg/mL), which is only 18.313% of the loaded protein concentration. This concentration was much lower than the concentration of rhSLPI shown to enhance mouse osteoblast cell (MC3T3-E1) adhesion and differentiation, which was 1  $\mu\text{g/mL}$  rhSLPI [11, 108]. However, our results showed that although the concentration found in the LPNs was much lower, it could efficiently enhance human osteoblast cell adhesion and differentiation.

In stability examinations, nanoparticles' physical properties were measured by Zetasizer. However, the ability of rhSLPI to inhibit protease after 3 months of storage at 4°C in DI water was not evaluated.

In this study, the cytotoxicity of LNPs was determined by the MTT assay. However, in the investigation of the toxicity of medical devices according to ISO 10993-5:2009, in addition to measuring cell death with MTT, changes in cell morphological characteristics such as size must be observed under a microscope.

Due to the limitation of facility availability, blank-LNPs and rhSLPI were determined for their morphology using different devices. Moreover, the shell of blank-LNPs was not observed by TEM. From this point, it might cause unclearly defined characteristics of the LNPs.

In this study, we did not perform the intracellular uptake of LNPs since this study requires the use of fluorescein-labelled SLPI peptides. This substance cannot be synthesised in our

lab and could be a time-consuming process. A previous study reported that rSLPI-fluorescein encapsulated liposomes were determined by fluorescence microscopy [59]. Therefore, this point could be considered a suggestion for further study.

In addition, this study showed the *in vitro* effects of rhSLPI-LNPs, which might lack clinical impact. For future studies, *ex vivo* and *in vivo* models should be performed to observe the real physiological effect of rhSLPI-LNPs.

### **Future perspective of the study**

It is inevitable to accept that an *in vitro* model of the determination of rhSLPI-LNPs in the hFOB 1.19 cell is not represent a model that closely related to real physiological conditions of bone adhesion and bone differentiation, as well as assessment of the clinical applications of rhSLPI-LNPs in bone fracture treatment. Future studies concerning the *in vivo* effect of rhSLPI-LNPs on bone healing, particularly in an experimental animal model, should be performed. Moreover, the *ex vivo* and *in vivo* effects of rhSLPI-LNPs on bone healing in comorbidity models such as the ageing model, diabetic model, or osteoporosis model should also be performed, which will provide more information on the clinical usefulness of rhSLPI-LNPs. An *in vivo* study on rhSLPI has not previously been reported this matter. However, it was discovered that there was a comparative study by Xue Feng *et al.* [109], who investigated the effect of Water-Soluble Matrix Protein (WSMP) from specific oyster shells on *in vitro* and *in vivo* proliferation, differentiation, and mineralization of osteoblast cells and its activity against osteoporosis. In an *in vitro* model, MC3T3-E1 has investigated the proliferation effect, differentiation markers including *Alp*, *Ocn*, and *Bmp-2*, and mineralization activity after being treated with WSMP. In addition, an *in vivo* study was observed in osteoporosis rats, which investigated tartrate-resistant acid phosphatase (TRAP), which is an indicator of osteoclast activity, and Bone alkaline phosphatase (BALP). The *OCN* expression indicates osteoblast differentiation was determined. Moreover, Bone mineral density (BMD) and bone mineral content (BMC) of bone recovery were also observed.

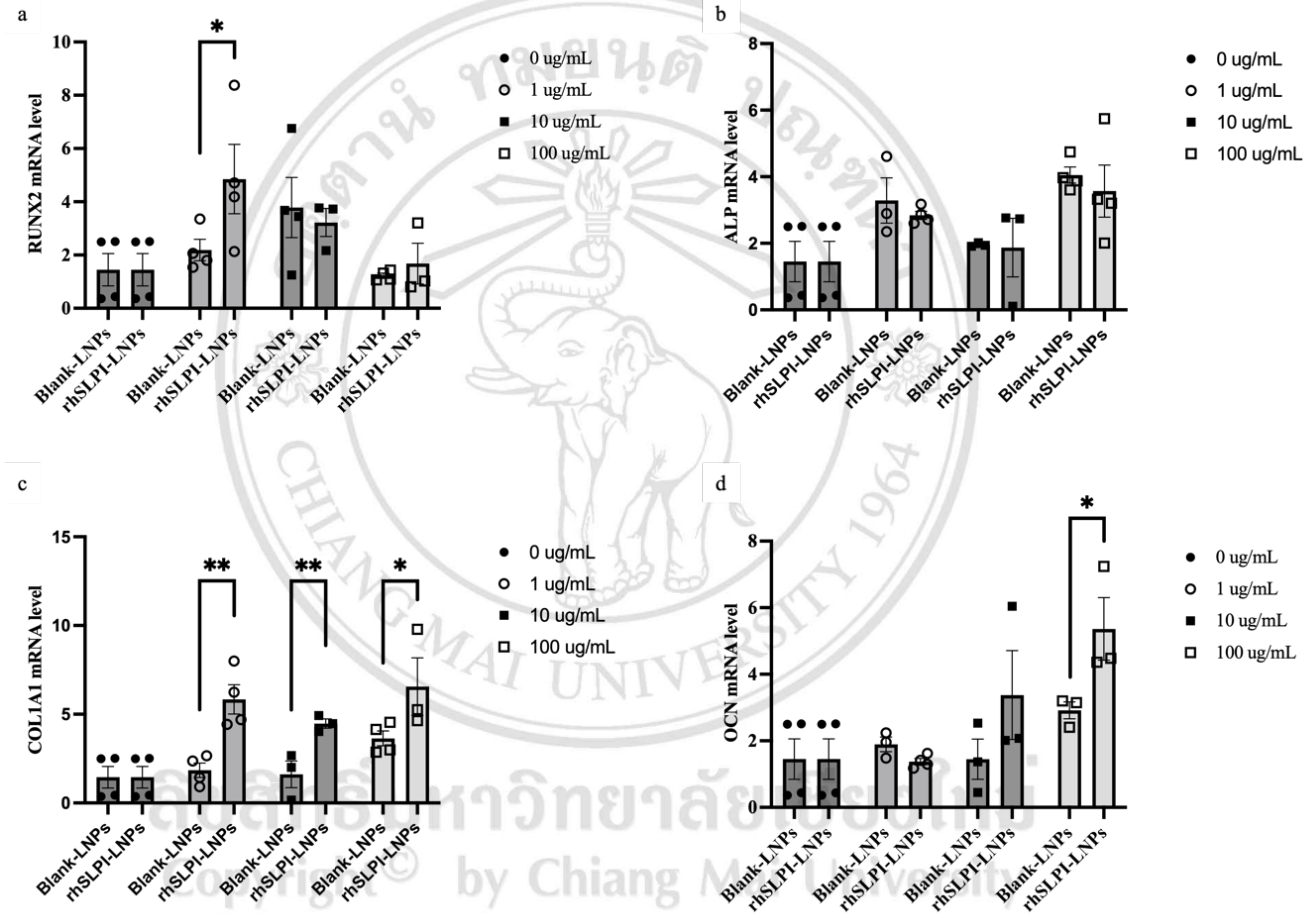


Figure 23. The mRNA expression of cell differentiation. a) *Runx2*; b) *Alp*; c) *Col1a1*; d) *Ocn*. \*  $p < 0.05$ , \*\*  $p < 0.01$  (ANOVA).



## CHAPTER 5

### Conclusion

The previous studies showed that rhSLPI-encapsulated liposome nanoparticles have been reported in asthma models and prevention of protease digestion models. In addition, rhSLPI has been reported to be encapsulated in other types of nanoparticles, including liposome alginate/chitosan, and human serum albumin. However, there are no reports of liposome nanoparticles encapsulating rhSLPI that enhance bone proliferation, adhesion, and differentiation. Thus, this is the first study to show that rhSLPI-encapsulated liposome nanoparticles (rhSLPI-LNPs) are biocompatible with human osteoblast cells. This could improve an *in vitro* human osteoblast cell proliferation, adhesion, and differentiation. In this current study, 10 µg/mL of rhSLPI-LNPs was found to represent the optimal concentration for enhancing osteoblast cell proliferation and adhesion. Meanwhile, the optimal concentration for enhancing osteoblast differentiation could not be concluded. However, it could be concluded that rhSLPI-LNPs have the ability to enhance osteoblast cell differentiation. For applications in real clinical use, rhSLPI-LNPs could be a candidate for use in orthopaedic surgery, such as coating the nanoparticles on metal for metal implantation or dental implantation in dentistry. In addition, the rhSLPI-LNPs might be combined with calcium phosphate cement (bone cement), which has been used to repair the fractures or replenish bone tissue after surgery, which might increase healing efficacy.

## REFERENCES

- [1] Nations U. World Population Ageing 2020 Highlight 2020 [Available from: [https://www.un.org/development/desa/pd/sites/www.un.org.development.desa.pd/files/files/documents/2020/Sep/un\\_pop\\_2020\\_pf\\_ageing\\_10\\_key\\_messages.pdf](https://www.un.org/development/desa/pd/sites/www.un.org.development.desa.pd/files/files/documents/2020/Sep/un_pop_2020_pf_ageing_10_key_messages.pdf)].
- [2] Buck DW, 2nd, Dumanian GA. Bone biology and physiology: Part I. The fundamentals. *Plast Reconstr Surg*. 2012;129(6):1314-20.
- [3] Fuller GF. Falls in Elderly: American Family Physician; 2000 [Available from: <https://www.aafp.org/afp/2000/0401/p2159.html>].
- [4] center NioHOaRBDNR. Preventing falls and related fractures: National Institutes of health; 2018 [Available from: <https://www.bones.nih.gov/health-info/bone/osteoporosis/fracture/preventing-falls-and-related-fractures>].
- [5] Williamson S, Landeiro F, McConnell T, Fulford-Smith L, Javaid MK, Judge A, et al. Costs of fragility hip fractures globally: a systematic review and meta-regression analysis. *Osteoporos Int*. 2017;28(10):2791-800.
- [6] Aspray TJ, Hill TR. Osteoporosis and the Ageing Skeleton. *Subcell Biochem*. 2019;91:453-76.
- [7] channel B. Bone fractures 2014 [cited 2022 May, 10]. Available from: <https://www.betterhealth.vic.gov.au/health/conditionsandtreatments/bone-fractures>.
- [8] Buck DW, 2nd, Dumanian GA. Bone biology and physiology: Part II. Clinical correlates. *Plast Reconstr Surg*. 2012;129(6):950e-6e.

- [9] Fracture Healing Overview [Internet]. StatPearls. 2021. Available from: <https://www.ncbi.nlm.nih.gov/books/NBK55167>.
- [10] Majchrzak-Gorecka M, Majewski P, Grygier B, Murzyn K, Cichy J. Secretory leukocyte protease inhibitor (SLPI), a multifunctional protein in the host defense response. *Cytokine Growth Factor Rev.* 2016;28:79-93.
- [11] Jeong SJ, Wang G, Choi BD, Hwang YH, Kim BH, Ko YM, et al. Secretory Leukocyte Protease Inhibitor (SLPI) Increases Focal Adhesion in MC3T3 Osteoblast on Titanium Surface. *J Nanosci Nanotechnol.* 2015;15(1):200-4.
- [12] Choi BD, Lee SY, Jeong SJ, Lim DS, Cha HJ, Chung WG, et al. Secretory leukocyte protease inhibitor promotes differentiation and mineralization of MC3T3-E1 preosteoblasts on a titanium surface. *Mol Med Rep.* 2016;14(2):1241-6.
- [13] Bergenfeldt M, Björk P, Ohlsson K. The elimination of secretory leukocyte protease inhibitor (SLPI) after intravenous injection in dog and man. *Scand J Clin Lab Invest.* 1990;50(7):729-37.
- [14] Yusuf A, Almotairy ARZ, Henidi H, Alshehri OY, Aldughaim MS. Nanoparticles as Drug Delivery Systems: A Review of the Implication of Nanoparticles's Physicochemical Properties on Responses in Biological Systems. *Polymers.* 2023;15(7):1596.
- [15] Guimarães D, Cavaco-Paulo A, Nogueira E. Design of liposomes as drug delivery system for therapeutic applications. *International Journal of Pharmaceutics.* 2021;601:120571.
- [16] Datta HK, Ng WF, Walker JA, Tuck SP, Varanasi SS. The cell biology of bone metabolism. *J Clin Pathol.* 2008;61(5):577-87.

- [17] hero C. Bone classification and Structure 2022 [cited 2022 May, 19]. Available from: <https://www.coursehero.com/study-guides/nemcc-ap/bone-classification/>.
- [18] Coveney S. Osteogenesis Imperfecta (OI) NEWS MEDICAL LIFE SCIENCES2021 [cited 2022 may 21]. Available from: [https://www.news-medical.net/health/Osteogenesis-imperfecta-\(OI\).aspx](https://www.news-medical.net/health/Osteogenesis-imperfecta-(OI).aspx).
- [19] Harbawi BA. Osteogenesis imperfecta [May, 22 2022]. Radiopaedia2021 [cited 2022 May, 22].
- [20] Raggatt LJ, Partridge NC. Cellular and molecular mechanisms of bone remodeling. *J Biol Chem*. 2010;285(33):25103-8.
- [21] Komori T. Regulation of osteoblast differentiation by transcription factors. *J Cell Biochem*. 2006;99(5):1233-9.
- [22] Teitelbaum SL. Bone Resorption by Osteoclasts. *Science*. 2000;289(5484):1504-8.
- [23] Hadjidakis D, Androulakis I. Bone Remodeling. *Annals of the New York Academy of Sciences*. 2007;1092:385-96.
- [24] Kini U, Nandeesh BN. Physiology of Bone Formation, Remodeling, and Metabolism. In: Fogelman I, Gnanasegaran G, van der Wall H, editors. *Radionuclide and Hybrid Bone Imaging*. Berlin, Heidelberg: Springer Berlin Heidelberg; 2012. p. 29-57.
- [25] Britannica TEOE. bone remodeling [May, 22 2022]. 2016 [cited 2022 May, 22]. Available from: <https://www.britannica.com/science/bone-remodeling>.
- [26] Wei Z, Liu G, Jia R, Zhang W, Li L, Zhang Y, et al. Targeting secretory leukocyte protease inhibitor (SLPI) inhibits colorectal cancer cell growth, migration and invasion via downregulation of AKT. *PeerJ*. 2020;8:e9400.

- [27] Nugteren S, Samsom JN. Secretory Leukocyte Protease Inhibitor (SLPI) in mucosal tissues: Protects against inflammation, but promotes cancer. *Cytokine Growth Factor Rev.* 2021;59:22-35.
- [28] Sallenave JM, Si Tahar M, Cox G, Chignard M, Gauldie J. Secretory leukocyte proteinase inhibitor is a major leukocyte elastase inhibitor in human neutrophils. *J Leukoc Biol.* 1997;61(6):695-702.
- [29] Grütter MG, Fendrich G, Huber R, Bode W. The 2.5 Å X-ray crystal structure of the acid-stable proteinase inhibitor from human mucous secretions analysed in its complex with bovine alpha-chymotrypsin. *EMBO J.* 1988;7(2):345-51.
- [30] Menckeberg CL, Hol J, Simons-Oosterhuis Y, Raatgeep HC, de Ruiter LF, Lindenberg-Kortleve DJ, et al. Human buccal epithelium acquires microbial hyporesponsiveness at birth, a role for secretory leukocyte protease inhibitor. *Gut.* 2015;64(6):884.
- [31] Samsom JN, van der Marel AP, van Berkel LA, van Helvoort JM, Simons-Oosterhuis Y, Jansen W, et al. Secretory leukoprotease inhibitor in mucosal lymph node dendritic cells regulates the threshold for mucosal tolerance. *J Immunol.* 2007;179(10):6588-95.
- [32] Xu W, He B, Chiu A, Chadburn A, Shan M, Buldys M, et al. Epithelial cells trigger frontline immunoglobulin class switching through a pathway regulated by the inhibitor SLPI. *Nature Immunology.* 2007;8(3):294-303.
- [33] Fernie-King BA, Seilly DJ, Davies A, Lachmann PJ. Streptococcal inhibitor of complement inhibits two additional components of the mucosal innate immune system: secretory leukocyte proteinase inhibitor and lysozyme. *Infect Immun.* 2002;70(9):4908-16.

- [34] Wiedow O, Harder J, Bartels J, Streit V, Christophers E. Antileukoprotease in Human Skin: An Antibiotic Peptide Constitutively Produced by Keratinocytes. *Biochemical and Biophysical Research Communications*. 1998;248(3):904-9.
- [35] Sallenave JM. The role of secretory leukocyte proteinase inhibitor and elafin (elastase-specific inhibitor/skin-derived antileukoprotease) as alarm antiproteinases in inflammatory lung disease. *Respir Res*. 2000;1(2):87-92.
- [36] Baranger K, Zani M-L, Labas V, Dallet-Choisy S, Moreau T. Secretory Leukocyte Protease Inhibitor (SLPI) Is, like Its Homologue Trappin-2 (Pre-Elafin), a Transglutaminase Substrate. *PLOS ONE*. 2011;6(6):e20976.
- [37] Zhang Y, DeWitt DL, McNeely TB, Wahl SM, Wahl LM. Secretory leukocyte protease inhibitor suppresses the production of monocyte prostaglandin H synthase-2, prostaglandin E2, and matrix metalloproteinases. *J Clin Invest*. 1997;99(5):894-900.
- [38] Zabieglo K, Majewski P, Majchrzak-Gorecka M, Wlodarczyk A, Grygier B, Zegar A, et al. The inhibitory effect of secretory leukocyte protease inhibitor (SLPI) on formation of neutrophil extracellular traps. *J Leukoc Biol*. 2015;98(1):99-106.
- [39] Zhu J, Nathan C, Jin W, Sim D, Ashcroft GS, Wahl SM, et al. Conversion of proepithelin to epithelins: roles of SLPI and elastase in host defense and wound repair. *Cell*. 2002;111(6):867-78.
- [40] Mihaila A, Tremblay GM. Human alveolar macrophages express elafin and secretory leukocyte protease inhibitor. *Z Naturforsch C J Biosci*. 2001;56(3-4):291-7.
- [41] Si-Tahar M, Merlin D, Sitaraman S, Madara JL. Constitutive and regulated secretion of secretory leukocyte proteinase inhibitor by human intestinal epithelial cells. *Gastroenterology*. 2000;118(6):1061-71.

- [42] Prompant E, Sanit J, Barrère-Lemaire S, Nargeot J, Noordali H, Madhani M, et al. The cardioprotective effects of secretory leukocyte protease inhibitor against myocardial ischemia/reperfusion injury. *Exp Ther Med*. 2018;15(6):5231-42.
- [43] The Recombinant Human Secretory Leukocyte Protease Inhibitor (SLPI) protects cardiac fibroblasts injury against an in vitro ischemia/reperfusion injury. *Journal of Applied Pharmaceutical Science*. 2018;8(6):156-62.
- [44] Taggart CC, Lowe GJ, Greene CM, Mulgrew AT, O'Neill SJ, Levine RL, et al. Cathepsin B, L, and S cleave and inactivate secretory leucoprotease inhibitor. *J Biol Chem*. 2001;276(36):33345-52.
- [45] Wilczewska AZ, Niemirowicz K, Markiewicz KH, Car H. Nanoparticles as drug delivery systems. *Pharmacological Reports*. 2012;64(5):1020-37.
- [46] Yusuf A, Almotairy ARZ, Henidi H, Alshehri OY, Aldughaim MS. Nanoparticles as Drug Delivery Systems: A Review of the Implication of Nanoparticles's Physicochemical Properties on Responses in Biological Systems. *Polymers [Internet]*. 2023; 15(7).
- [47] Brown SB, Wang L, Jungels RR, Sharma B. Effects of cartilage-targeting moieties on nanoparticle biodistribution in healthy and osteoarthritic joints. *Acta Biomater*. 2020;101:469-83.
- [48] Zhang C-x, Cheng Y, Liu D-z, Liu M, Cui H, Zhang B-l, et al. Mitochondria-targeted cyclosporin A delivery system to treat myocardial ischemia reperfusion injury of rats. *Journal of Nanobiotechnology*. 2019;17(1):18.
- [49] He C, Yue H, Xu L, Liu Y, Song Y, Tang C, et al. siRNA release kinetics from polymeric nanoparticles correlate with RNAi efficiency and inflammation therapy via oral delivery. *Acta Biomater*. 2020;103:213-22.

- [50] Zhang L, Beatty A, Lu L, Abdalrahman A, Makris TM, Wang G, et al. Microfluidic-assisted polymer-protein assembly to fabricate homogeneous functionalnanoparticles. *Mater Sci Eng C Mater Biol Appl*. 2020;111:110768.
- [51] Afsharzadeh M, Hashemi M, Mokhtarzadeh A, Abnous K, Ramezani M. Recent advances in co-delivery systems based on polymeric nanoparticle for cancer treatment. *Artif Cells Nanomed Biotechnol*. 2018;46(6):1095-110.
- [52] Jose S, A CT, Sebastian R, H SM, A AN, Durazzo A, et al. Transferrin-Conjugated Docetaxel-PLGA Nanoparticles for Tumor Targeting: Influence on MCF-7 Cell Cycle. *Polymers (Basel)*. 2019;11(11).
- [53] Wang T, Rong F, Tang Y, Li M, Feng T, Zhou Q, et al. Targeted polymer-based antibiotic delivery system: A promising option for treating bacterial infections via macromolecular approaches. *Progress in Polymer Science*. 2021;116:101389.
- [54] Yang W, Liang H, Ma S, Wang D, Huang J. Gold nanoparticle based photothermal therapy: Development and application for effective cancer treatment. *Sustainable Materials and Technologies*. 2019;22:e00109.
- [55] Tarhini M, Pizzoccaro A, Benlyamani I, Rebaud C, Greige-Gerges H, Fessi H, et al. Human serum albumin nanoparticles as nanovector carriers for proteins: Application to the antibacterial proteins "neutrophil elastase" and "secretory leukocyte protease inhibitor". *Int J Pharm*. 2020;579:119150.
- [56] Lomis N, Westfall S, Farahdel L, Malhotra M, Shum-Tim D, Prakash S. Human Serum Albumin Nanoparticles for Use in Cancer Drug Delivery: Process Optimization and In Vitro Characterization. *Nanomaterials*. 2016;6:116.
- [57] Mitchell MJ, Billingsley MM, Haley RM, Wechsler ME, Peppas NA, Langer R. Engineering precision nanoparticles for drug delivery. *Nature Reviews Drug Discovery*. 2021;20(2):101-24.



- [58] Sercombe L, Veerati T, Moheimani F, Wu SY, Sood AK, Hua S. Advances and Challenges of Liposome Assisted Drug Delivery. *Front Pharmacol.* 2015;6:286.
- [59] Gibbons AM, McElvaney NG, Taggart CC, Cryan SA. Delivery of rSLPI in a liposomal carrier for inhalation provides protection against cathepsin L degradation. *J Microencapsul.* 2009;26(6):513-22.
- [60] Gibbons A, Padilla-Carlin D, Kelly C, Hickey AJ, Taggart C, McElvaney NG, et al. The effect of liposome encapsulation on the pharmacokinetics of recombinant secretory leukocyte protease inhibitor (rSLPI) therapy after local delivery to a guinea pig asthma model. *Pharm Res.* 2011;28(9):2233-45.
- [61] Hill M, Twigg M, Sheridan EA, Hardy JG, Elborn JS, Taggart CC, et al. Alginate/Chitosan Particle-Based Drug Delivery Systems for Pulmonary Applications. *Pharmaceutics.* 2019;11(8):379.
- [62] Tarhini M, Pizzoccaro A, Benlyamani I, Rebaud C, Greige-Gerges H, Fessi H, et al. Human serum albumin nanoparticles as nanovector carriers for proteins: Application to the antibacterial proteins "neutrophil elastase" and "secretory leukocyte protease inhibitor". *International journal of pharmaceutics.* 2020;579:119150.
- [63] Hill M, Twigg M, Sheridan EA, Hardy JG, Elborn JS, Taggart CC, et al. Alginate/Chitosan Particle-Based Drug Delivery Systems for Pulmonary Applications. *Pharmaceutics.* 2019;11(8).
- [64] Mathiyazhakan M, Wiraja C, Xu C. A Concise Review of Gold Nanoparticles-Based Photo-Responsive Liposomes for Controlled Drug Delivery. *Nano-Micro Letters.* 2017;10(1):10.
- [65] Maherani B, Arab-Tehrany E, R. Mozafari M, Gaiani C, Linder M. Liposomes: A Review of Manufacturing Techniques and Targeting Strategies. *Current Nanoscience.* 2011;7(3):436-52.

- [66] Bangham AD, Standish MM, Watkins JC, Weissmann G. The diffusion of ions from a phospholipid model membrane system. *Protoplasma*. 1967;63(1):183-7.
- [67] Laouini A, Jaafar-Maalej C, Blouza I, Sfar S, Charcosset C, Fessi H. Preparation, Characterization and Applications of Liposomes: State of the Art. *Journal of Colloid Science and Biotechnology*. 2012;1:147-68.
- [68] Pattni BS, Chupin VV, Torchilin VP. New Developments in Liposomal Drug Delivery. *Chemical Reviews*. 2015;115(19):10938-66.
- [69] Akbarzadeh A, Rezaei-Sadabady R, Davaran S, Joo SW, Zarghami N, Hanifehpour Y, et al. Liposome: classification, preparation, and applications. *Nanoscale Research Letters*. 2013;8(1):102.
- [70] Antimisariis SG, Kallinteri P, Fatouros DG. Liposomes and Drug Delivery. *Pharmaceutical Manufacturing Handbook 2008*. p. 443-533.
- [71] William B, Noémie P, Brigitte E, Géraldine P. Supercritical fluid methods: An alternative to conventional methods to prepare liposomes. *Chemical Engineering Journal*. 2020;383:123106.
- [72] Schubert R. Liposome Preparation by Detergent Removal. *Methods in Enzymology*. 367: Academic Press; 2003. p. 46-70.
- [73] Yen THT, Nho Dan L, Duc HL, Tung TB, Hue TMP. Preparation and Characterization of Freeze-dried Liposomes Loaded with Amphotericin B. *Current Drug Therapy*. 2019;14(1):65-73.
- [74] Andra V, Pammi SVN, Bhatraju L, Ruddaraju LK. A Comprehensive Review on Novel Liposomal Methodologies, Commercial Formulations, Clinical Trials and Patents. *Bionanoscience*. 2022;12(1):274-91.
- [75] Pasquali I, Bettini R. Are pharmaceuticals really going supercritical? *Int J Pharm*. 2008;364(2):176-87.

- [76] Zhao L, Temelli F. Preparation of anthocyanin-loaded liposomes using an improved supercritical carbon dioxide method. *Innovative Food Science & Emerging Technologies*. 2017;39:119-28.
- [77] Culture ATC. hFOB 1.19: ATCC; 2021 [Available from: <https://www.atcc.org/products/crl-11372>].
- [78] Kumaraswamy P, Sethuraman S, Krishnan UM. Development of a dual nanocarrier system as a potential stratagem against amyloid-induced toxicity. *Expert Opin Drug Deliv*. 2014;11(8):1131-47.
- [79] Bacha AB, Jemel I, Moubayed NMS, Abdelmalek IB. Purification and characterization of a newly serine protease inhibitor from *Rhamnus frangula* with potential for use as therapeutic drug. *3 Biotech*. 2017;7(2):148.
- [80] van Meerloo J, Kaspers GJL, Cloos J. Cell Sensitivity Assays: The MTT Assay. In: Cree IA, editor. *Cancer Cell Culture: Methods and Protocols*. Totowa, NJ: Humana Press; 2011. p. 237-45.
- [81] Präbst K, Engelhardt H, Ringgeler S, Hübner H. Basic Colorimetric Proliferation Assays: MTT, WST, and Resazurin. *Methods Mol Biol*. 2017;1601:1-17.
- [82] Berridge MV, Tan AS. Characterization of the cellular reduction of 3-(4,5-dimethylthiazol-2-yl)-2,5-diphenyltetrazolium bromide (MTT): subcellular localization, substrate dependence, and involvement of mitochondrial electron transport in MTT reduction. *Arch Biochem Biophys*. 1993;303(2):474-82.
- [83] Cole AJ, Yang VC, David AE. Cancer theranostics: the rise of targeted magnetic nanoparticles. *Trends Biotechnol*. 2011;29(7):323-32.
- [84] Danaei M, Dehghankhold M, Ataei S, Hasanzadeh Davarani F, Javanmard R, Dokhani A, et al. Impact of Particle Size and Polydispersity Index on the Clinical Applications of Lipidic Nanocarrier Systems. *Pharmaceutics*. 2018;10(2).

- [85] Lütgebaucks C, Macias-Romero C, Roke S. Characterization of the interface of binary mixed DOPC:DOPS liposomes in water: The impact of charge condensation. *J Chem Phys*. 2017;146(4):044701.
- [86] Yohannes G, Pystynen K-H, Riekkola M-L, Wiedmer SK. Stability of phospholipid vesicles studied by asymmetrical flow field-flow fractionation and capillary electrophoresis. *Analytica Chimica Acta*. 2006;560(1):50-6.
- [87] Bulbake U, Doppalapudi S, Kommineni N, Khan W. Liposomal Formulations in Clinical Use: An Updated Review. *Pharmaceutics*. 2017;9(2).
- [88] Kattla JJ, Struwe WB, Doherty M, Adamczyk B, Saldova R, Rudd PM, et al. 3.41 - Protein Glycosylation. In: Moo-Young M, editor. *Comprehensive Biotechnology (Second Edition)*. Burlington: Academic Press; 2011. p. 467-86.
- [89] Hussain MT, Forbes N, Perrie Y. Comparative Analysis of Protein Quantification Methods for the Rapid Determination of Protein Loading in Liposomal Formulations. *Pharmaceutics* [Internet]. 2019; 11(1).
- [90] Meure LA, Foster NR, Dehghani F. Conventional and dense gas techniques for the production of liposomes: a review. *AAPS PharmSciTech*. 2008;9(3):798-809.
- [91] Knoll G, Burger KN, Bron R, van Meer G, Verkleij AJ. Fusion of liposomes with the plasma membrane of epithelial cells: fate of incorporated lipids as followed by freeze fracture and autoradiography of plastic sections. *Journal of Cell Biology*. 1988;107(6):2511-21.
- [92] Allen TM, McAllister L, Mausolf S, Gyorffy E. Liposome-cell interactions A study of the interactions of liposomes containing entrapped anti-cancer drugs with the EMT6, S49 and AE1 (transport-deficient) cell lines. *Biochimica et Biophysica Acta (BBA) - Biomembranes*. 1981;643(2):346-62.

- [93] Liu W, Hou Y, Jin Y, Wang Y, Xu X, Han J. Research progress on liposomes: Application in food, digestion behavior and absorption mechanism. *Trends in Food Science & Technology*. 2020;104:177-89.
- [94] Mongkolpathumrat P, Kijawornrat A, Prompant E, Panya A, Chattipakorn N, Barrère-Lemaire S, et al. Post-Ischemic Treatment of Recombinant Human Secretory Leukocyte Protease Inhibitor (rhSLPI) Reduced Myocardial Ischemia/Reperfusion Injury. *Biomedicines*. 2021;9(4):422.
- [95] Inglut CT, Sorrin AJ, Kuruppu T, Vig S, Cicalo J, Ahmad H, et al. Immunological and Toxicological Considerations for the Design of Liposomes. *Nanomaterials* [Internet]. 2020; 10(2).
- [96] Haglund K, Rusten T, Stenmark H. Aberrant Receptor Signaling and Trafficking as Mechanisms in Oncogenesis. *Critical reviews in oncogenesis*. 2007;13:39-74.
- [97] Feng X, McDonald JM. Disorders of bone remodeling. *Annu Rev Pathol*. 2011;6:121-45.
- [98] Clark D, Nakamura M, Miclau T, Marcucio R. Effects of Aging on Fracture Healing. *Curr Osteoporos Rep*. 2017;15(6):601-8.
- [99] Khosla S, Riggs BL. Pathophysiology of age-related bone loss and osteoporosis. *Endocrinol Metab Clin North Am*. 2005;34(4):1015-30, xi.
- [100] Gruber R, Koch H, Doll BA, Tegmeier F, Einhorn TA, Hollinger JO. Fracture healing in the elderly patient. *Exp Gerontol*. 2006;41(11):1080-93.
- [101] Aamodt KI, Powers AC. Signals in the pancreatic islet microenvironment influence  $\beta$ -cell proliferation. *Diabetes Obes Metab*. 2017;19 Suppl 1(Suppl 1):124-36.

- [102] Florencio-Silva R, Sasso GRdS, Sasso-Cerri E, Simões MJ, Cerri PS. Biology of Bone Tissue: Structure, Function, and Factors That Influence Bone Cells. *BioMed Research International*. 2015;2015:421746.
- [103] Jensen ED, Gopalakrishnan R, Westendorf JJ. Regulation of gene expression in osteoblasts. *Biofactors*. 2010;36(1):25-32.
- [104] Amarasekara DS, Kim S, Rho J. Regulation of Osteoblast Differentiation by Cytokine Networks. *Int J Mol Sci*. 2021;22(6).
- [105] McNeely TB, Dealy M, Dripps DJ, Orenstein JM, Eisenberg SP, Wahl SM. Secretory leukocyte protease inhibitor: a human saliva protein exhibiting anti-human immunodeficiency virus 1 activity in vitro. *J Clin Invest*. 1995;96(1):456-64.
- [106] Tehrani FA, Modaresifar K, Azizian S, Niknejad H. Induction of antimicrobial peptides secretion by IL-1 $\beta$  enhances human amniotic membrane for regenerative medicine. *Sci Rep*. 2017;7(1):17022.
- [107] Yang J, Zhu J, Sun D, Ding A. Suppression of macrophage responses to bacterial lipopolysaccharide (LPS) by secretory leukocyte protease inhibitor (SLPI) is independent of its anti-protease function. *Biochim Biophys Acta*. 2005;1745(3):310-7.
- [108] Choi BD, Lee SY, Jeong SJ, Lim DS, Cha HJ, Chung WG, et al. Secretory leukocyte protease inhibitor promotes differentiation and mineralization of MC3T3-E1 preosteoblasts on a titanium surface. *Mol Med Rep*. 2016;14(2):1241-6.
- [109] Feng X, Jiang S, Zhang F, Wang R, Zhao Y, Mingyong Z. Shell Water-Soluble Matrix Protein from Oyster Shells Promoted Proliferation, Differentiation and Mineralization of Osteoblasts in Vitro and Vivo. *International Journal of Biological Macromolecules*. 2022;201.

## CURRICULUM VITAE

Author's Name	Mr. Wannapat Chouyratchakarn
Place of Birth	Kamphaeng Phet, Thailand
Education	2015 High School Certificate, Watcharawittaya school, Kamphaeng Phet 2020 Bachelor of Science Program in Medical Technology (Second class honor), Naresuan University, Phitsanulok
Scholarship	TA&RA Scholarship 2021 from Graduate school, Chiang Mai University, Chiang Mai Biomedical Engineering Institute (BMEI), Chiang Mai University and ACADEMIC ACTIVITIES SCHOLARSHIP- Graduate school, Chiang Mai University for travel grant to attend International Conference and Exhibition on Science, Technology and Engineering of Materials (Istem2022). November 29- December 3, 2022. Pattaya, Cholburi, Thailand.
Presentation	<b>Wannapat Chouyratchakarn,</b> Chayanisa Phutiyothin, Fraprathan Pikwong, Tanpong Chaiwarit, Phornsawat Baipaywad, Sarawut Kumphune. Development of nanoparticles for delivering recombinant human secretory leukocyte protease inhibitor (rhSLPI) for enhancing human osteoblast differentiation. The International Conference and Exhibition on Science, Technology and Engineering of Materials (Istem 2022). 29 November -2 December 2022, Pattaya, Thailand

## Publications

1. **Chouvratchakarn W.**, Phutiyothin C., Pikwong F., Chaiwarit T., Baipaywad P., Kumphune S.. Development of nanoparticles for delivering recombinant human secretory leukocyte protease inhibitor (rhSLPI) for enhancing human osteoblast differentiation. *Materials Today: Proceedings*. 2023 (In press) DOI: 10.1016/j.matpr.2023.04.074
2. Pikwong F., **Chouyachakarn W.**, Phutiyothin C., Chanabodeehalermrung B., Baipaywad P., Kumphune S. Development of gelatin-silicon dioxide nanoparticles (GSNPs) for delivering recombinant human secretory leukocyte protease inhibitor (rhSLPI) for reducing myocardial ischemia/reperfusion injury. *Materials Today: Proceedings*. 2023 (In press) DOI: 10.1016/j.matpr.2023.04.101
3. Phutiyothin C., **Chouvratchakarn W.**, Pikwong F., Jantrawut P., Baipaywad P., Kumphune S. Development of nanoparticles for delivering recombinant human secretory leukocytes protease inhibitor (rhSLPI) for reducing vascular endothelial cell injury and death. *Materials Today: Proceedings*. 2023 (In press) DOI: 10.1016/j.matpr.2023.04.095
4. Pikwong F., Phutiyothin C., **Chouvratchakarn W.**, Baipaywad P., Kumphune S. Gelatin coated -Silicon oxide nanoparticles encapsulated recombinant human secretory leukocyte protease inhibitor (rhSLPI) reduced cardiac cell death against an in vitro simulated ischemia/reperfusion injury. *Heliyon*. 2023.
5. Mongkolpathumrat P., **Chouvratchakarn W.**, Pikwong F., Phutiyothin C., Kumphune S. Roles of secretory leukocyte



protease inhibitor (SLPI) in non-communicable diseases and study models. 2023 (*Manuscript in submission*).

6. Leelasukseree R., Trikasemsak L., Theerawanon P., Phutiyothin C., **Chouyratchakarn W.**, Pikwong F., Baipaywad P., Udomsom S., Supanchart C., Kumphune S. Recombinant human secretory leukocyte protease inhibitor (rhSLPI) coated Titanium material enhanced osteoblast adhesion and differentiation. 2023 (*In revision*).

7. Phutiyothin C., Pikwong F., **Chouyratchakarn W.**, Baipaywad P., Kumphune S. An in vitro vasculo-protective effect of human serum albumin nanoparticle carrier of recombinant human secretory leukocyte protease inhibitor (rhSLPI) against ischemia/reperfusion injury in vascular endothelial cells. 2023 (*Manuscript in preparation*).

8. **Chouyratchakarn W.**, Pikwong F., Phutiyothin C., Baipaywad P., Kumphune S. Liposome carrier of recombinant human secretory leukocyte protease inhibitor (rhSLPI) enhancing human osteoblast differentiation. 2023 (*Manuscript in preparation*).

ลิขสิทธิ์ © by Chiang Mai University  
All rights reserved